REPUBLIC OF CAMEROON
****
Peace – Work – Fatherland
****

****
DEPARTMENT OF ENVIRONMENTAL ENGINEERING
****

REPUBLIQUE DU CAMEROON
****
Paix – Travail – Patrie
****

****
DEPARTMENT OF CIVIL, ARCHITECTURAL AND ENVIRONMENTAL ENGINEERING
****

OPTIMIZATION OF BIOGAS YIELDS FROM ANAEROBIC CO-DIGESTION WITH COW DUNG VIA RESPONSE SURFACE METHODOLOGY

Case study of substrates: pineapple, banana and/or watermelon waste.

An end-of-year thesis submitted in fulfilment of the requirements for the award of the degree

Masters of Engineering (MEng) *option* ***Environmental Engineering***

Presented by:

DJOUFACK LEKE Stéphane

Matriculation number: 16TP21094

Supervised by:

Pr. NKENG George ELAMBO **Pr. NDE Divine BUP** **Pr. Eng. Maria Christina LAVAGNOLO**

Academic Year: **2020/2021**

DEDICATION

I dedicate this work to my parents

LEKEALEM Joseph *and* ***LEKEALEM Sidonie***

who have always loved me unconditionally and whose good examples have taught me to work hard for the things that I aspire to achieve.

ACKNOWLEDGEMENTS

This project would not have been possible without the support of many people.

First, I will express my gratitude towards my supervisor **Pr. NDE Divine** as well as **Pr. NKENG George ELAMBO** for their guidance and immense knowledge in drilling me throughout this work. They have been ideal teachers, mentors, and thesis supervisors, offering advice. I'm grateful for my time working with them.

I would equally like to express my gratitude to my co-supervisor, **Pr. Maria Cristina LAVAGNOLO** for her guidance and motivation while working throughout this work.

Then, I would like to thank the Director of the National Advanced School of Public Works, **Prof. NKENG George ELAMBO**; my Head of Department, **Prof. TALLA André** and the entire institution's administration for providing a conducive working environment throughout my stay in this institution.

I thank the examiner, **Prof. TALLA André** and the president, **Prof. Roberto RAGA** as they were the members of the Jury during my defence.

I thank **Prof. ESOH ELAME**, who allowed us to acquire shared knowledge from other countries through the partnership with the University of Padova.

In addition, I will like to thank **Eng. Gerard**, **Eng. Patrice**, **Eng Charles** and **Eng Sylvain** of the National Laboratory for Diagnosis and Analysis of Agricultural Products and Inputs of the Ministry of Agriculture and Rural Development (MINADER) for their guidance and encouragement throughout the experimental phase of my work.

Special thanks to my colleagues **DOUAYA Laurent**, **ATEAFAC Marie**, **ARRAH Samuel** and friends **DONGMO KAZE Leticia**, **DONGMO Sandrine**, **DOUANLA Jonathan, Eng. DONGMO Jeff** and **NDEMEFFO Emmanuel** for their support and encouragement throughout this work.

Finally, my **entire family** for the moral, academic and financial support provided during all these years.

ABSTRACT

In the urgency of transitioning from non-renewable to renewable energy sources, the anaerobic digestion of food waste is one of the most important technologies for waste recovery. The main objective of this work was the production and quantification of biogas from various food wastes. More specifically, determining the optimal conditions for the biogas production from pineapple, watermelon and banana waste in co-digestion with cow dung and determining mixtures of substrate that produce high biogas yields. An experimental design, sampling pre-treatment and biochemical methane potential (BMP) tests were conducted. Analytical methods (proximate and ultimate analysis), kinetic modelling (first order and modified Gompertz model) and the face-centred central composite design was applied to the samples and BMP assays respectively to predict responses (biogas yields). The optimal Inoculum (I) to Substrate (S) to Water (W) (I:S:W) ratio for co-digestion of pineapple peelings (PP) with cow dung (CD) was 1 : 2.09 : 4.06 and the corresponding biogas yield was 73.78 ml/g on volatile solids (VS) basis. For watermelon rind (WR), the I:S:W ratio equalled 3 : 1 : 5.8 and the corresponding biogas yield was 100.45 ml/g VS. Finally, for banana peelings (BP), the I:S:W ratio equalled 3 : 1 : 5.3 and the corresponding biogas yield was 98.75 ml/g VS. The digestion in mixtures of substrates produced lesser biogas yield than the co-digestion set ; PP – BP (25.5 ml/g VS), PP – WR (11.3 ml/g VS), WR - BP (5.1 ml/g VS) and WR – BP – PP (18.7 ml/g VS).

Keywords: Anaerobic digestion, cow dung, food waste, biogas production, optimisation, response surface methodology.

RESUME

Dans l'urgence de la transition des sources d'énergie non renouvelables aux sources d'énergie renouvelables, la digestion anaérobie des déchets alimentaires est l'une des technologies les plus importantes pour la valorisation des déchets. L'objectif principal de ce travail était la production et la quantification de biogaz provenant de divers déchets alimentaires. Plus spécifiquement, déterminer les conditions optimales pour la production de biogaz à partir de déchets d'ananas, de pastèques et de bananes en codigestion avec la bouse de vache et déterminer les mélanges de substrats qui produisent des rendements élevés de biogaz. Un plan expérimental, un échantillonnage et un prétraitement ainsi que des essais de méthane biochimique ont été réalisés. Les méthodes analytiques (analyse immédiate et analyse ultime), la modélisation cinétique (modèle de Gompertz modifié et de premier ordre) et le plan composite central centré sur la face ont été appliqués aux échantillons et aux essais de BMP respectivement pour prédire les réponses (rendement des biogaz). Le rapport optimal entre l'inoculum (I) et le substrat (S) par rapport à l'eau (W) (I:S:W) pour la codigestion des épluchures d'ananas (PP) avec la bouse de vache (CD) était de 1 : 2,09 : 4,06 et le rendement en biogaz correspondant était de 73,78 ml/g sur la base des solides volatils (VS). Pour les déchets de pastèque (WR), le rapport I:S:W était égal à 3 : 1 : 5,8 et le rendement en biogaz correspondant était de 100,45 ml/g VS. Enfin, pour les épluchures de bananes (BP), le rapport I:S:W était égal à 3 : 1 : 5,3 et le rendement en biogaz correspondant était de 98,75 ml/g VS. La digestion dans des mélanges de substrats a produit un rendement de biogaz moindre que l'ensemble des essais en codigestion : PP – BP (25,5 ml/g VS), PP – WR (11,3 ml/g VS), WR - BP (5,1 ml/g VS) et WR – BP – PP (18,7 ml/g VS).

Mots-clés : Digestion anaérobie, bouse de vache, déchets alimentaires, production de biogaz, optimisation, méthodologie de surface de réponse.

SUMMARY

Dedication ii
Acknowledgements iii
Abstract iv
Résumé v
Summary 115
List of abbreviations and symbols vii
List of Figures ix
List of Tables xii
List of Appendixes xiii
General Introduction 1
CHAPTER 1 . LITERATURE REVIEW 3
1.1. Concepts and definitions 3
1.2. Food waste generation 5
1.3. Food waste recovery technologies and circular economy 14
1.4. Anaerobic digestion technology 19
1.5. Response surface methodology 36
CHAPTER 2 . MATERIAL AND METHODS 39
2.1. Software used 39
2.2. Materials 40
2.3. Design of experiment (DOE) 43
2.4. Sample collection 51
2.5. Preparation of samples and pretreatment 54
2.6. Experimental setup 57
2.7. Analytical methods 64
2.8. Theoretical biochemical methane potential 69
2.9. Kinetic modelling 70
CHAPTER 3 . RESULTS AND DISCUSSION 73
3.1. Physical and chemical characteristics of the substrates and inoculum 73
3.2. Theoretical biogas potential estimation 75
3.3. Anaerobic digestion - blank assays 75
3.4. Anaerobic co-digestion with cow dung 79
3.5. Anaerobic digestion of mixtures of substrates 96
3.6. Biogas yield to energy classification 99
General conclusion and perspectives 101
References 103
Appendix 108
Table of content vi

LIST OF ABBREVIATIONS AND SYMBOLS

AD	Anaerobic Digestion
ANOVA	Analysis of Variance
BMP	Biochemical methane potential
BOD	Biological Oxygen Demand
BP	Banana Peelings
BUCREP	Bureau Central du Recensement et des Etudes de Population
C	Center level of a central composite design
C/N	Carbon to Nitrogen ratio
CCD	Central Composite Design
CD	Cow Dung
CDC	Cameroon Development Corporation
CH_4	Methane
CO_2	Carbon dioxide
COD	Chemical Oxygen Demand
DOE	Design Of Experiment
EPA	Environmental Protection Agency of the United States
FAO	Food and Agricultural Organization of the United Nations
FCCD	Face-centered Central Composite Design
FL	Food Loss
FRH	Food Recovery Hierarchy
FSC	Food Supply Chain
FW	Food Waste
H	High level of a central composite design
HTR	Hydraulic Retention Time
L	Low level of a central composite design
MATLAB	Matrix Laboratory
MINADER	Ministry of Agriculture and Rural Development
MSW	Municipal Solid Waste
NIS	National Institute of Statistics
OC	Organic Carbon

OLR Organic Loading Rate

OLR Organic Loading Rate

PHP Plantation de Haut Penja

PP Pineapple Peelings

RMSE Root Mean Squared Error

RSM Response Surface Methodology

RSS Residual Sum of Squares

SDG Sustainable Development Goals

SIE Système d'Information Energétique du Cameroun

SRT Solid Retention Time

TBMP Theoretical Biochemical Methane Potential

TS Total Solids

UN United Nations

VFA Volatile Fatty Acids

VS Volatile Solids

WR Watermelon Rind

λ Lag phase of the anaerobic digestion process (in days)

g gram

ρ density

G_0 Biogas potential of a substrate (in cubic meter per ton, on volatile solids basis)

ml milliliter

k Biogas production rate constant (in per day)

R^2 Correlation coefficient

R_{max} Maximum biogas production rate (in in cubic meter per ton, on volatile solids basis per day)

LIST OF FIGURES

Figure 1.1: Production volumes of groups of commodities, per region (million tons).....6
Figure 1.2: Per capita food losses and waste, at consumption and pre-consumptions stages, in different regions 7
Figure 1.3: Part of the initial production lost or wasted at different stages of the FSC for fruits and vegetables in different regions 8
Figure 1.4: Municipal waste composition in sub-Saharan Africa and globally.....9
Figure 1.5: Variation of total postharvest losses between 1994 and 2013 in Cameroon. 10
Figure 1.6: Pineapple production in Awae.....11
Figure 1.7: PHP plantations banana conditioning factory, Loum, Cameroon. 12
Figure 1.8: A food waste dump, South Africa (2018). 13
Figure 1.9: Composting at the Municipal Agency of Waste Management (AMGED), Dschang, Cameroon 15
Figure 1.10: Vermicompost beds with beds sold in India.....15
Figure 1.11: A simplified diagram of organic waste to bio-energy using anaerobic digestion 16
Figure 1.12: Food Recovery Hierarchy provided by the Environmental Protection Agency of the United States 18
Figure 1.13: Circular economy approach's model. 19
Figure 1.14: Utilization of individual substrate components during anaerobic digestion. 20
Figure 1.15: Simplified schematic diagram of different reactions involved in anaerobic digestion of complex organic matter.....23
Figure 1.16: Relationship between the rate of degradation and retention time for various types of organic compounds.....25
Figure 1.17: Temperature ranges for anaerobic treatment processes.....27
Figure 1.18: Effect of pH on hydrogen sulphide–sulphide equilibrium (10−3 molar solution, 32 mg H_2S/l) 31
Figure 1.19: Effect of pH on ammonia–ammonium equilibrium 32
Figure 1.20: Biogas digester types considered for developing countries 33
Figure 1.21: Illustration of a fixed-dome digester 34
Figure 1.22: Scheme of the floating-drum digester (left), floating-drum digester for market waste in India (right). 35
Figure 1.23: Scheme of balloon digester 36

Figure 1.24: Example of a central composite with face-centered points 38
Figure 2.1: Experimental design flowchart 44
Figure 2.2: Independent and dependent variables of an anaerobic digestion process 45
Figure 2.3: Pineapple and watermelon fruit market and waste (A) and cow slaughterhouse at Etoudi (B) 51
Figure 2.4: Fresh fruit waste at pineapple and watermelon selling points in the Mendong market 52
Figure 2.5: Map of important sites visited for waste collection and research study activities 53
Figure 2.6: Waste samples prepared for proximate analysis 54
Figure 2.7: Cutting up of substrates for air-drying 55
Figure 2.8: Samples after being air-dried, pounded and sieved 55
Figure 2.9: The knife drilling machine (a), cut waste in preparation for milling (b) and milled waste (c) 56
Figure 2.10: Cross section of a bioreactor setup for biochemical methane potential testing . 57
Figure 2.11: Steps of BMP assay formation 58
Figure 2.12: Steps of BMP assay formation 59
Figure 2.13: Steps of BMP assay formation 59
Figure 2.14: Steps of BMP assay formation 59
Figure 2.15: BMP assays setup 60
Figure 2.16: Sealing equipment and areas sealed for all batch experimentations 61
Figure 2.17: Batch experiment identification for mixed substrates 62
Figure 2.18: Syringe plugged into the infusion set's end 62
Figure 2.19: Oven (capacity 120 °C) (A), muffle furnace (capacity 600 °C) (B) and desiccator (C) 64
Figure 2.20: Addition of diphenylamine droplets to the test solutions (A) and Titration of solution with $FeSO_4$ (B) 66
Figure 3.1: Cumulative biogas yield for BMP batch experimentations of the blank assays .. 77
Figure 3.2: First-order model for blanks 78
Figure 3.3: Gompertz model for blanks 78
Figure 3.4: Cumulative biogas yield from pineapple peelings 80
Figure 3.5: Cumulative biogas yield from watermelon rind 81
Figure 3.6: Cumulative biogas yield from banana peelings 81
Figure 3.7: Comparison of batch experiments in co-digestion against the blanks. 82
Figure 3.8: First-order model fitting curves for pineapple peelings 84

Figure 3.9: Gompertz model fitting curves for pineapple peelings 84
Figure 3.10: First-order model fitting curves for watermelon rind.....85
Figure 3.11: Modified Gompertz model fitting curves for watermelon rind 85
Figure 3.12: First-order model fitting curves for banana peelings 86
Figure 3.13: Modified Gompertz model fitting curves for banana peelings.....87
Figure 3.14: Response optimization; PP (top-left), WR (top-right) and BP (bottom-center).90
Figure 3.15: Contour and surface plots of Pineapple peelings' (PP) anaerobic digestion.....92
Figure 3.16: Contour and surface plots of Watermelon rind's (WR) anaerobic digestion 92
Figure 3.17: Contour and surface plots of Banana peelings' (BP) anaerobic digestion.....93
Figure 3.18: The plot of predicted vs actual yield (left) and the Pareto chart of standardized effects (right) of PP's co-digestion 94
Figure 3.19: The plot of predicted vs actual yield (left) and the Pareto chart of standardized effects (right) of WR's co-digestion 95
Figure 3.20: The plot of predicted vs actual yield (left) and the Pareto chart of standardized effects (right) of BP's co-digestion.....95
Figure 3.21: Cumulative biogas yield from BMP batch experimentations of mixtures of substrates.....97
Figure 3.22: First-order kinetics model fitted curves for mixtures of substrates.....98
Figure 3.23: Modified Gompertz model curves fittings for mixtures of substrates.....98

LIST OF TABLES

Table 1.1: IPCC classification of municipal solid waste 8
Table 1.2: Decomposition results of food losses in Cameroon 1994 - 2013 (unit tons) 10
Table 1.3: Typical Composition of Functional Anaerobic Treatment Process 23
Table 1.4: Average Time of Regeneration of Some Microbial Groups 28
Table 1.5: Biogas plants in Africa 36
Table 2.1: Walkley and Black Method materials and reagents 41
Table 2.2: Kjeldahl Method materials and reagents 42
Table 2.3: Factor level values 48
Table 2.4: Central composite design table for digestion of pineapple peelings (PP), watermelon rind (WR) and banana peelings (BP) 49
Table 2.5: Fit options in MATLAB's curve fitting tool 72
Table 3.1: Results of the proximate analysis of the substrates 73
Table 3.2: Density of substrates and cow dung 74
Table 3.3: Partly performed ultimate analysis' results 74
Table 3.4: Theoretical Biochemical Methane Potential (TBMP) of substrates and inoculum 75
Table 3.5: BMP results of blank assays 76
Table 3.6: Kinetic model of the blank assays 77
Table 3.7: Kinetic modelling of pineapple peelings batch experimentations 83
Table 3.8: Kinetic modelling of watermelon rind batch experimentations 84
Table 3.9: Kinetic modelling of banana peelings batch experimentations 86
Table 3.10: Model fitness parameters 88
Table 3.11: ANOVA results for co-digestion of PP with cow dung 88
Table 3.12: ANOVA results for the co-digestion of WR with cow dung 88
Table 3.13: ANOVA results for the co-digestion of BP with cow dung 89
Table 3.14: Initial parameters for co-digestion batch experiments 91
Table 3.15: Optimum parameters of C/N and TS (%) for all the substrates 91
Table 3.16: BMP results of the mixture set 96
Table 3.17: Kinetic model of the mixture of substrates assays 97
Table 3.18: Biogas yield to energy classification table 99

LIST OF APPENDIXES

Appendix 1: Updated IPCC classification of MSW, 2019 108
Appendix 2: Continuation of the updated IPCC classification of MSW, 2019 108
Appendix 3: Dumping site for pineapple waste at one of the processing facilities in Kangulmumira, Uganda. 109
Appendix 4: Automatic Methane Potential Test System (AMPTS) II. 109
Appendix 5: Anaerobic digestion plant in Kenya 109
Appendix 6: Central composite design 2D diagram for the anaerobic digestion of pineapple peelings, watermelon rind and banana peelings 110
Appendix 7: Results of the analysis of the density of substrates 110
Appendix 8: FCCD table of pineapple peelings 111
Appendix 9: FCCD table of watermelon rind 111
Appendix 10: FCCD table of banana peelings 112
Appendix 11: Proximate analysis of the substrates 112
Appendix 12: Laboratory substrate analyses' estimates 113
Appendix 13: Laboratory analyses of substrates' results 114

GENERAL INTRODUCTION

Background

Of recent, because of the fear of exhaustion of fossil fuels and the environmental problems it poses, much attention is being turned to the production and use of renewable energies such as bio-diesel, bio-gas and more. Anaerobic digestion (AD) is a microbiological process whereby organic matter (substrate) is decomposed in the absence of oxygen. All over the years, the process has been engineered and controlled, as such, nowadays, the anaerobic process is being used to treat the organic biodegradable waste matter in airproofed reactor tanks, commonly named digesters, resulting to an energy-rich biogas and a nutritious digestate. Municipal Solid Waste (MSW), food industry waste agricultural waste and plant residues are the major waste categories that serve as substrates in anaerobic digestion plants due to their high organic matter content and therefore high potential for biogas production (Mata-Alvarez, 2003).

Furthermore, this activity provides benefits like generating renewable energy, reducing greenhouse gases, reducing dependency on fossil fuels, job creation, and closing the nutrient cycle. It improves the energy balance of a country but also contributes to the preservation of natural resources by reducing deforestation, and protecting the environment by reducing pollution from waste and fossil fuels (Al Seadi et al., 2008).

In Cameroon, nowadays, millions of people lack access to electricity. Although access to electricity is beneficial for lighting, communication, healthcare, and education providing benefits for communities and households. The World Bank (2020) reported that in 2020 only 65% of the nation's population had access to electricity. According to Mboumboue & Njomo (2018), in Cameroon, about 19% of electricity comes from the combustion of fossil fuels in thermal power plants and more than 80% of the population still relies on traditional biomass. This combustion pollutes the atmosphere and emits Greenhouse gases (GHG). In addition, domestic cooking gas is very expensive and cannot be afforded by most families regularly.

Problem statement, research questions and objectives

The quantity and quality of a specific bio-gas is most often dependent on the substrate and the processing conditions under which it is produced. Some food products that generate large quantities of waste in Cameroon include pineapple, mango, rice, banana and watermelon. A combination of different feedstocks in different proportions may equally have a significant

effect on the quality and quantity of the gas produced. To study the situation presented above and propose adequate solutions, our research will try to answer the questions:

- What substrate or substrate combination from the available substrates should be used to obtain a desired and yet, good biogas yield?
- Under what suitable anaerobic operational conditions should these substrates be subjected?

The general objective of this work is to produce and quantify biogas from different food waste. Specifically, the work aims to;

1. **Determine the optimum conditions for biogas production from pineapple, banana and watermelon peelings.**
2. **Determine mixtures of the substrates that give high yields of good quality biogas.**

Thesis Structure

This work is composed of three (03) chapters preceded by the general introduction and followed by a general conclusion. The three (03) chapters are presented as thus:

Chapter 1: Literature review;

Chapter 2: Material and methods;

Chapter 3: Results and discussion.

CHAPTER 1 . LITERATURE REVIEW

The objective of this chapter is to present different concepts and terminologies related to our topic: anaerobic digestion, biogas potential and yield, substrate, co-digestion, optimization, food waste and renewable energy, and the literature review run through some keywords like circular economy, response surface methodology (RSM) and others. It is divided into five (05) parts namely: concepts and definitions, food waste generation, food waste recovery technologies, anaerobic digestion technology and response surface methodology.

1.1. CONCEPTS AND DEFINITIONS

1.1.1. Anaerobic digestion

Anaerobic digestion (AD) is a unique process where different microbial species (bacteria and fungi) decompose organic materials in the absence of oxygen. AD has been widely practised in full-scale facilities all over the world. Several AD techniques have been applied to convert livestock manure, wastewaters, and solid lignocellulosic waste into biogas (Singh et al., 2020). Anaerobic digestion for biogas production takes place in a sealed vessel called a reactor, which is designed and constructed in various shapes and sizes specific to the site and feedstock conditions. This concept is further elaborated in section 1.4.

1.1.2. Biogas potential and biogas yield

The biogas potential of a specific substrate defines the maximum amount of biogas that can potentially be produced during anaerobic digestion. While the biogas yield describes the achieved fraction of the biogas potential under practical conditions during an experimental or technical digestion process (Weinrich et al., 2018).

1.1.3. Substrate

"Supporting surface" on which an organism grows. The substrate may simply provide structural support or may provide water and nutrients. A substrate may be inorganic, such as rock or soil, or it may be organic, such as wood, (UCMP, 2009). When mixed with a fluid (water) or inoculum, it may also be referred to as feedstock or simply feed.

1.1.4. Co-digestion

Co-digestion refers to the simultaneous anaerobic digestion of multiple organic wastes in one digester. Co-digestion is used to increase methane production from low-yielding or difficult-

to-digest materials. For the co-digestion process, care must be taken to select compatible co-digestion feedstocks that enhance methane production (and to avoid materials that may inhibit methane generation), (EPA, 2012).

1.1.5. Optimization

Optimization is one of the most powerful tools in process integration. Optimization involves the selection of the "best" solution from among the set of candidate solutions, (Mahmoud & El-Halwagi, 2006). In other words, optimisation is the process carried out when we have a range of parameters that can be controlled and a single variable that we want to maximise or minimise: in the case of AD for energy production this might be the biogas yield or, in the case of AD for waste management, the quantity of residual waste solids for disposal (Wellinger Arthur et al., 2013). The degree of goodness of the solution is quantified using an objective function (for example, a second order equation) which is to be minimized or maximized.

1.1.6. Food loss, food waste and the food supply chain

A Food Supply Chain (FSC) or food system refers to the processes that describe how food from a farm ends up on our tables. The processes include production, transportation, processing, distribution, consumption and disposal.

Generally, waste is defined as a leftover, redundant product or material of no or marginal value for the owner and that the owner wants to discard. According to the Food and Agricultural Organization of the United Nations (FAO), Food Loss (FL) is defined as any change in the availability, edibility, wholesomeness or quality of edible material that prevents it from being consumed by people (FAO, 1981). Afterwards, this definition evolved over decades up to a recent publication (Gustavsson et al., 2011) which recognised food losses as the decrease in edible food mass throughout the part of the FSC that specifically leads to edible food for human consumption. Furthermore, Food losses take place during the production, postharvest and processing stages in the food supply chain (Parfitt et al., 2010). Food losses occurring at the end of the food chain (retail and final consumption) are rather called food waste, which relates to retailers' and consumers' behaviour (Parfitt et al., 2010).

Other researchers come to the same conclusion FL and FW overlap and these terms are used for material discharged at both the manufacturing and retail stages and the consumption or household levels (Girotto et al., 2015).

1.1.7. Renewable energy

Renewable energies are sun, wind, water, biomass, tidal and geothermal energies. These energy sources are important members of the earth's biogeochemical cycles, explaining why they are called renewable. They are also known as sustainable energy sources because their utilisation does not affect the ability of future generations to cope with their energy needs. Sunlight, wind, and other renewable resources are increasingly being converted into useful forms of energy with ever-greater efficiency. As such, as time goes on and technology improves, renewable energy has been more and more considered a better alternative to the finite, non-renewable and less environmentally friendly fossil fuels.

- **Energy transition**

A renewables-based energy transition promises to deliver vast socio-economic benefits to countries across Africa, improving energy access, creating jobs and boosting energy security. The Sustainable Development Goals (SDGs), set by the United Nations General Assembly in 2015, are a collection of 17 goals designed to be a blueprint to achieve a better and more sustainable future for all. These goals are part of the UN 2030 Agenda for Sustainable Development, and the intent is to achieve them by 2030.

The following goals are particularly relevant: SDG 7 – Affordable and Clean Energy, SDG 8 – Decent Work and Economic Growth, SDG 9 – Industry, Innovation and Infrastructure, and SDG 13 – Climate Action. SDG 7 is particularly well aligned with the objectives of this research work, as it calls for universal access to sustainable energy by 2030. Biomass as a renewable energy source exists as biofuels. Biomethane (refined biogas) as fuel, among the biofuels, has the highest energy efficiency (Smyth et al. 2009).

1.2. FOOD WASTE GENERATION

As earlier defined in section 1.1, food waste refers to the masses of food wasted on the part of the food chain. Therefore, food that was originally meant for human consumption but which fortuity gets out of the human food chain is considered as food loss or waste even if it is then directed to a non-food use (feed or bioenergy).

1.2.1. Sources of food loss (FL) and food waste (FW)

Food is wasted throughout the FSC, from initial agricultural production down to final household consumption. Significant FL and FW occur early in the FSC. In low-income

countries food is mainly lost during the early and middle stages of the food supply chain; much less food is wasted at the consumer level (Gustavsson et al., 2011). Food waste (FW) is mainly discharged from households, restaurants, canteens, local shops, processing industries as well as mass-market systems (Li, et al., 2020; Pham et al., 2015). FL and FW occur at every level of the FSC;

- Agricultural production (during harvesting),
- Transportation,
- Industrial or domestic processing,
- Distribution (wholesale markets, supermarkets and retailers),
- Consumption and disposal (household).

1.2.2. Food waste statistics

Figure 1.1 shows that industrialized Asia is the highest in production of fruits and vegetables, roughly 630 million tons per year, followed by south and southeast Asia with around 300 million tons per year. Meanwhile, Sub-Saharan Africa's production level reaches around 100 million tons per year. That are enormous quantities of food produced per year. In the subsequent sections, we are going to see which parts of this production go to waste.

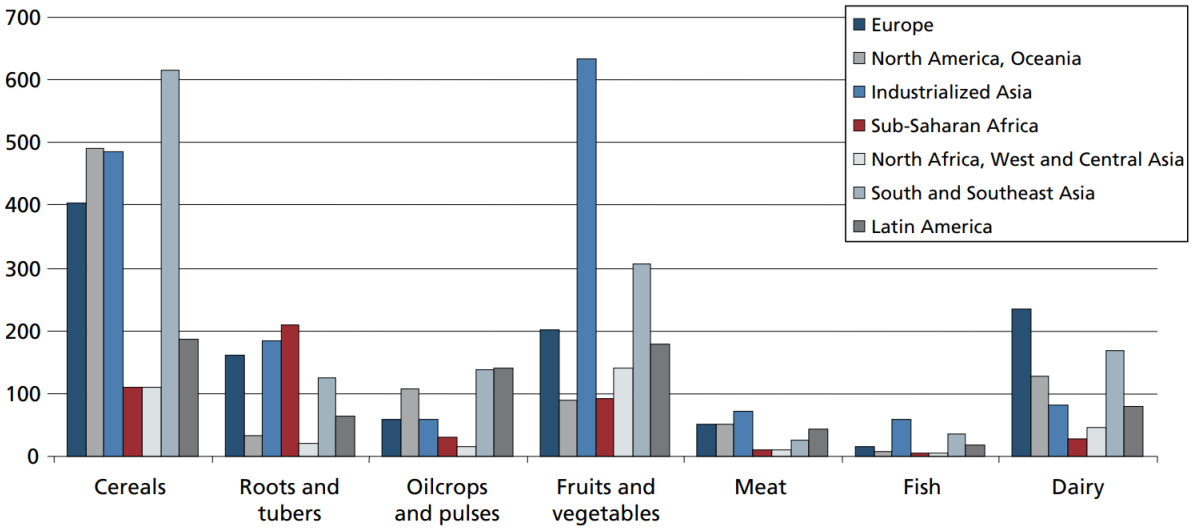

Figure 1.1: Production volumes of groups of commodities, per region (million tons) (Gustavsson, 2011).

1.2.2.1. Worldwide

Globally, approximately 30% of edible parts of food produced for human consumption get lost or wasted, which is about 1.3 billion tons per year (Kojima & Ishikawa, 2013).

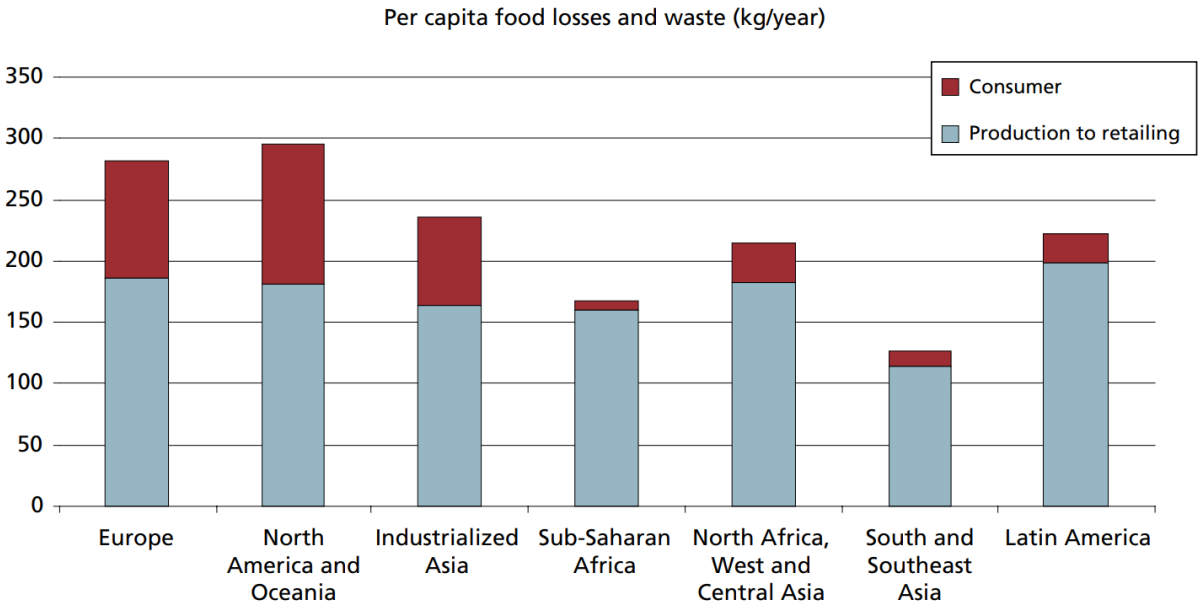

Figure 1.2: Per capita food losses and waste, at consumption and pre-consumptions stages, in different regions (Gustavsson, 2011).

Gustavsson et al. (2011) equally give equivalent proportions of food that goes into waste (**Figure 1.2**) at the household and from production to retail under the same categories as in **Figure 1.1**. We can observe that globally most of the food wasted occurs between the production and the retail end of the FSC. The per capita food loss in Europe and North America is 280-300 kg/year. In Sub-Saharan Africa and South/Southeast Asia, it is 120-170 kg/year. Per capita food wasted by consumers in Europe and North America is 95-115 kg/year, while this figure in sub-Saharan Africa and South/Southeast Asia is only 6-11 kg/year.

A better representation of fruits and vegetables per stage of the FSC is elaborated in Gustavsson et al., **Figure 1.3**. Food is wasted at every stage. For both Industrialized and developing countries, agricultural production dominates total losses throughout the FSC. But in Europe, North America and Industrialized Asia, a great number of fruits and vegetables are also wasted at the consumer stage with 15-30 % by mass of purchases discarded by consumers. While in the other categories especially in Sub-Saharan Africa and south and southeast Asia, more food is wasted at the agricultural and processing stages and less at the consumer stage. Losses during post-harvest and distribution stages are also severe, explained by the deterioration of perishable

crops in the warm and humid climate of many developing countries as well as by seasonality that leads to unsaleable gluts.

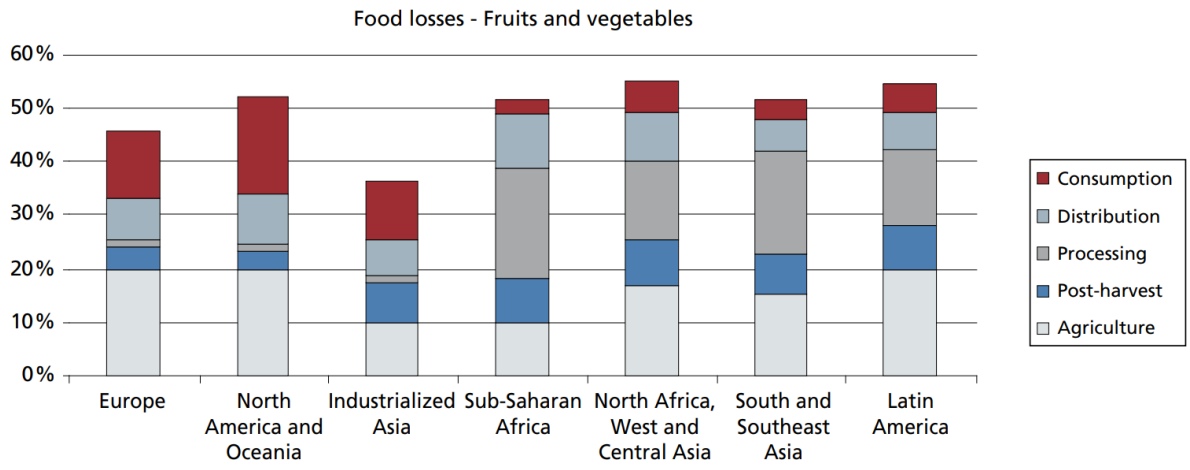

Figure 1.3: Part of the initial production lost or wasted at different stages of the FSC for fruits and vegetables in different regions (Gustavsson, 2011).

The Intergovernmental Panel on Climate Change (IPCC) classified the municipal solid waste (MSW) composition by continent, **Table 1.1**. The column concerning food waste shows that Africa's highest percentage of MSW goes to food waste.

Table 1.1: IPCC classification of municipal solid waste (Bhada-Tata & Hoornweg, 2012).

Region	Food Waste	Paper/ Card-board	Wood	Textiles	Rubber/ Leather	Plastic	Metal	Glass	Other
Asia									
Eastern Asia	26.2	18.8	3.5	3.5	1	14.3	2.7	3.1	7.4
South-Central Asia	40.3	11.3	7.9	2.5	0.8	6.4	3.8	3.5	21.9
South-Eastern Asia	43.5	12.9	9.9	2.7	0.9	7.2	3.3	4	16.3
Western Asia & Middle East	41.1	18	9.8	2.9	0.6	6.3	1.3	2.2	5.4
Africa									
Eastern Africa	53.9	7.7	7	1.7	1.1	5.5	1.8	2.3	11.6
Middle Africa	43.4	16.8	6.5	2.5		4.5	3.5	2	1.5
Northern Africa	51.1	16.5	2	2.5		4.5	3.5	2	1.5
Southern Africa	23	25	15						
Western Africa	40.4	9.8	4.4	1		3	1		
Europe									
Eastern Europe	30.1	21.8	7.5	4.7	1.4	6.2	3.6	10	14.6
Northern Europe	23.8	30.6	10	2		13	7	8	
Southern Europe	36.9	17	10.6						
Western Europe	24.2	27.5	11						
Oceania									
Australia & New Zealand	36	30	24						
Rest of Oceania	67.5	6	2.5						
America									
North America	33.9	23.2	6.2	3.9	1.4	8.5	4.6	6.5	9.8
Central America	43.8	13.7	13.5	2.6	1.8	6.7	2.6	3.7	12.3
South America	44.9	17.1	4.7	2.6	0.7	10.8	2.9	3.3	13
Caribbean	46.9	17	2.4	5.1	1.9	9.9	5	5.7	3.5

1.2.2.2. Africa

Food losses and waste in Africa are significant occurring primarily at the early stage of the FSC as seen in **Figure 1.3**. Roughly 37 % of all food produced is lost or wasted. For a continent with high levels of poverty, hunger and malnutrition, the loss and wastage of more than a third of all food produced, is unacceptable. **Figure 1.4** shows the fraction of waste generated in sub-Saharan Africa. **Appendix 1** and **Appendix 2** show that great amounts of MSW (around 50%) are constituted of food waste in Africa. Compared to **Figure 1.4**, approximately 50% of the 57% organic for sub-Saharan Africa.

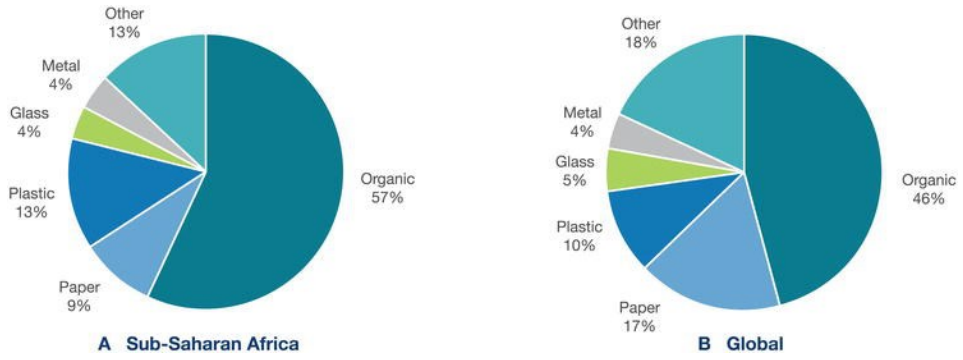

Figure 1.4: Municipal waste composition in sub-Saharan Africa and globally (Zaman & Reynolds, 2015)

1.2.2.3. Cameroon

A recent study analysed FL in Cameroon using available data from the National Institute of Statistics (NIS) and the Central Bureau of the Census and Population Studies (BUCREP). These agencies are the main national agencies in Cameroon responsible to provide data in all sectors of the country. During 1994 - 2013, FL experienced a significantly increased trend in Cameroon, rising from $0.43 * 10^6$ tons to $2.25 * 10^6$ tons, a little more than a 4-fold increase, (Feukam Nzudie et al., 2021).

FL changes may be divided into two distinct periods: between 1994 and 2004, FL was relatively stable with 34.43% increases based on 1994 levels. In contrast, between 2004 and 2013 there was a significant rise in FL amounting to 282.46% of that 2004 levels. **Figure 1.5** and **Table 1.2** show postharvest losses for the 9 selected crops in the 1994 - 2013 range. The magnitude of FL in descending order was: cassava, maize, banana, sorghum, yams, beans, groundnut, pineapple, and rice.

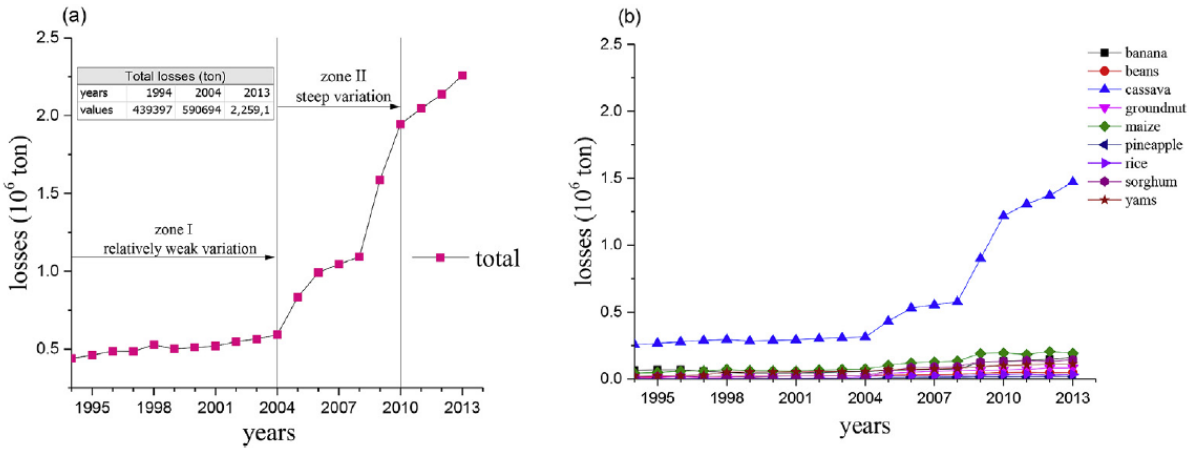

Figure 1.5: Variation of total postharvest losses between 1994 and 2013 in Cameroon (Feukam Nzudie et al., 2021)

Table 1.2: Decomposition results of food losses in Cameroon 1994 - 2013 (unit tons) (Feukam Nzudie et al., 2021).

years	ΔS	ΔI	ΔE	ΔSc	ΔP	total
1995	−8993	−4621	16,370	6023	11,888	20,667
1996	829	−712	4228	9443	12,184	25,971
1997	14,162	2928	−1122	−28753	12,239	−546
1998	6595	5688	1582	15,933	12,620	42,417
1999	21,923	−7661	−35818	−18304	12,860	−27000
2000	−8902	1793	10,658	−6078	12,822	10,294
2001	−5529	−356	5395	−4929	13,237	7818
2002	−8200	1773	−1796	22,680	13,863	28,321
2003	−4007	−980	6804	1049	14,633	17,499
2004	−4088	6279	−7041	15,345	15,361	25,856
2005	−999	129,743	−7490	101,845	18,880	241,979
2006	524	62,884	7477	64,030	24,663	159,579
2007	−2185	2549	−5873	30,931	27,832	53,254
2008	−741	−569	−10141	29,448	29,324	47,321
2009	9304	293,340	21,841	133,005	36,266	493,755
2010	28,519	179,930	8998	92,954	47,994	358,395
2011	28,446	−1524	−28769	48,038	54,182	100,374
2012	1755	−8193	−10872	52,659	56,476	91,826
2013	24,018	8682	−33120	63,477	58,956	122,014
T*	92,431	670,975	−58687	628,794	486,281	1,819,794

ΔS = structure, ΔI = intensity, ΔE = self-sufficiency, ΔSc = supply scale, and ΔP = population. T* is the total change in FL during 1994–2013 for the five drivers.

1.2.2.4. Pineapple, banana and watermelon plantations in Cameroon

Pineapple is essentially grown for its fruit. According to Selina W. (2022), on average, more than 300 thousand tons of pineapples are produced annually in Cameroon. In 2010, the production was about 136 thousand tons. *Ananas Comosus* is a plant that grows around tropical zones. The main varieties of pineapple are Cayenne Smooth, Sweet, Sugar Loaf and Queen.

Pineapple is available all year round with peaks from November to April. The main production areas are;

- Bafia and Awae in the central region, **Figure 1.6** is a picture of a pineapple plantation in Awae;
- Njombé in the Littoral region.

Pineapple is also one of the fruits cultivated in the entire region and beyond with relatively cheap labour. However, the system of agriculture is still rudimentary. Following the launch of the Agropoles project, supervised by the Ministry of Economy and meant to boost local production, 118 hectares of pineapple farm was announced in Kumba, in the South West region to boost pineapple production (Crtv, 2018).

Figure 1.6: Pineapple production in Awae (Invest Cameroon, 2013).

There are two major companies producing bananas in Cameroon; Cameroon Development Corporation (CDC) (with 22,000 employees, cultivating 4,525 Ha of bananas) and Plantations du Haut Penja (PHP) (owned by Compagnie Fruitière with 7063 employees, cultivating 5,150 Ha of bananas). The Association of Banana producers of Cameroon (ASSOBACAM) reported Cameroon's average annual production is approximately 300,000 tons (Crtv, 2018). **Figure 1.7** presents one the PHP warehouse.

Figure 1.7: PHP plantations banana conditioning factory, Loum, Cameroon (K., 2020).

Watermelon *Citrullus lanatus* is a fruit vegetable grown predominantly in the North West and West Region, both located in the western highland agricultural zones of Cameroon. This industry has potential in the South West Region, located in the humid rainforest agriculture zone of the country, although yet to be well established (Denis Achiri et al., 2019).

1.2.3. Environmental and social impacts of mismanaged food waste

The major risk associated with poor management of solid waste is the pollution of all the environment's components, that is, the atmosphere, lithosphere, hydrosphere and biosphere. The weak collection systems in Africa combined with uncontrolled and controlled dumping of waste, often associated with open burning and waste leakage causes significant economic, social and environmental impacts.

1.2.3.1. Harm to Biodiversity

Biodiversity simply refers to the different species and organisms that make up an environment's ecosystem. Eutrophication and water pollution deal with the acquiring of a water body to a high concentration of nutrients especially phosphate and nitrate that promote excessive growth of algae. It is a chemical, physical or biological change in the quality of water that harms anything that drinks or uses it. The indiscriminate dumping of waste in urban areas creates risks of disease, including the risk of cholera, malaria, typhoid fever and more.

1.2.3.2. Contribution to climate change

When food is left to rot in our landfills, it subsequently releases methane, a powerful greenhouse gas twenty-five times stronger than carbon dioxide. When methane is released, it lingers for 12 years and traps heat from the sun. It contributes towards 20% of the global

greenhouse gas emissions released. When we factor in the greenhouse gas emissions released from the use of natural resources, the contribution to climate change is astonishing. If a decent food waste treatment system were implemented, it would stop 11% of global greenhouse gas emissions. The level of methane from landfills varies by country, depending on waste composition, climatic conditions (ambient temperature, precipitation) and waste disposal practices.

Apart from landfills, open burning of waste causes air pollution which impacts human health and contributes to changes in climate.

1.2.3.3. Waste of Natural Resources

When we waste food, we waste the natural resources used for producing that food, the three main ones being energy, fuel and water. Water is needed for all stages of the food production process, as well as in all types of food produced. Agriculture accounts for 70% of the water used throughout the world. This includes the irrigation and spraying required for crops, and the water needed for rearing cattle, poultry and fish. By wasting food, we are wasting fresh water.

Figure 1.8 shows a food waste dump in South Africa and **Appendix 3** shows one of the dumping sites closer to a processing facility in Uganda. Both images illustrate improper disposal of food waste.

Figure 1.8: A food waste dump, South Africa (2018) (3SMedia, 2020).

In addition, dumping of waste into river basins streams are one of the contributors to flooding.

1.3. FOOD WASTE RECOVERY TECHNOLOGIES AND CIRCULAR ECONOMY

1.3.1. Composting and vermicomposting

Composting occurs through the activity of microorganisms naturally found in soils. Under natural conditions, earthworms, nematodes and soil insects such as mites, sowbugs, springtails, ants, and beetles do most of the initial mechanical breakdown of organic materials into smaller particles. The result of a successfully composted organic material is a biologically stable humic substance that makes excellent soil amendments. **Figure 1.9** shows an example composting facility. This facility is handled by the municipal agency of solid waste management of Dschang, Cameroon. Carbon dioxide is released during this process.

On the other hand, Vermicomposting is a non-reactor process through which the ecosystem engineers, that is, the epigeic earthworms ingest organic material and subsequently transform it into a nutrient-rich humified organic fertilizer (Yadav and Madan, 2013). During the vermicomposting process, the feedstock substrate is initially ground in the gizzard to form smaller particles, increasing the surface area. The material is further acted upon by earthworm gut microbial flora and digestive enzymes to produce a fine granular product enriched with beneficial nutrients and microflora. Besides these physical and biochemical mechanisms involved, earthworms also facilitate aeration due to their burrowing nature, contributing to uniform mixing of the material (Yadav and Garg, 2011). Vermicomposting is one of the best organic matter recycling options as it offers an environmentally and economically sound strategy to obtain a product of premium value enriched with all sorts of bioactive compounds.

In both composting and vermicomposting, there exist several treatment technologies. For composting:

Figure 1.9: Composting at the Municipal Agency of Waste Management (AMGED), Dschang, Cameroon

Figure 1.10: Vermicompost beds with beds sold in India (IndiaMART InterMESH, n.d.).

1.3.2. Incineration

Incineration treatment is one of three thermal technologies that require high temperatures to alter the chemical structure of waste. Waste to energy plants is used to use the heat produced from the thermal plant for electricity production. In some countries, which have less land available, incineration has become one of the most important MSW treatment methods, alongside other thermal conversion technologies such as gasification and pyrolysis. The high moisture content of up to 80% in FW has led to the need to pre-treat and co-combust with coal

in order to ensure that the incineration is operating efficiently (Lombardi 2015). However, even under optimum conditions, the energy efficiency is only 18-34% depending on the scale and the specific technology used. The final ashes are sent to landfill.

1.3.3. Landfill treatment

A landfill is a site where garbage is layered with dirt and other absorbing material to prevent contamination of the surrounding land or water. It was originally designed to mitigate the problem of waste pollution, but over time it has shown many defects. Research from the World Bank shows that each tonne of organic waste produces 300-1000 kg of CO_2 when sent to landfill (Zaman & Reynolds, 2015). International legislation is clear about the need to gradually reduce the amount of biodegradable waste to landfills, in order to minimize greenhouse gas emissions and to produce a leachate with lower organic load. For that reason, Landfills should receive residual waste after recoverable fractions are collected separately. Biodegradable organic matter should be diverted from waste destined to landfills. Also, solid waste generation is growing exponentially and is set to double in large and medium-sized cities and triple in the poorest countries by 2050. Low-income countries do not have the financial means to build sanitary landfills, consequently, most of their waste is managed improperly, remains untreated, and is disposed of in open dumps (Vergara & Jammi, 2022).

1.3.4. Anaerobic digestion

As discussed in Section 1.1.1, anaerobic digestion (AD) is the degradation of organic matter in an oxygen-deprived environment. AD technologies can help preserve and integrate livestock production within communities and creates renewable energy resources to serve a growing bioeconomy within rural communities. **Figure 1.11** illustrates the benefits of AD.

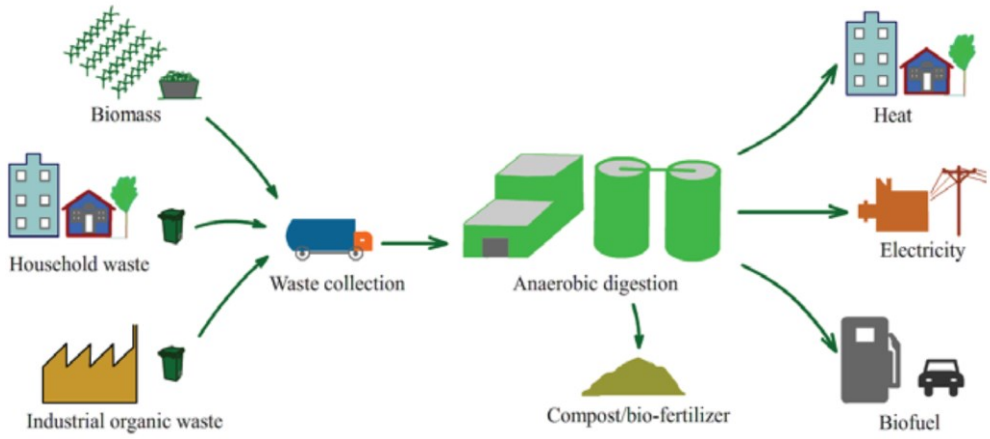

Figure 1.11: A simplified diagram of organic waste to bio-energy using anaerobic digestion (Zaman & Reynolds, 2015).

According to (Ward et al., 2008), the production of biogas through anaerobic digestion offers significant advantages over other forms of waste treatment, including: less biomass sludge produced in comparison to aerobic treatment technologies, successful in treating wet wastes of less than 40% dry matter (Mata-Alvarez, 2002), more effective pathogen removal (Kunte et al., 2004; Sahlstrom, 2003) or if a pasteurisation step is included in the process, high degree of compliance with many national waste strategies implemented to reduce the amount of biodegradable waste entering landfill, the slurry produced (digestate) is an improved fertiliser in terms of both its availability to plants (Tafdrup, 1995) and its rheology (Pain and Hepherd, 1985) and it is a source of carbon neutral energy is produced in the form of biogas. So, it is a more favourable organic waste treatment method than aerobic treatment from the simultaneous perspective of greenhouse gases, food security (sustainable fertiliser), and biofuel.

1.3.5. Food recovery hierarchy and circular economy

1.3.5.1. Food recovery hierarchy

The Food Recovery Hierarchy (FRH) prioritizes actions organizations can take to prevent and divert wasted food. Each tier of the FRH focuses on different management strategies for your wasted food, **Figure 1.12**. The top levels of the hierarchy are the best ways to prevent and divert wasted food because they create the most benefits for the environment, society and the economy (EPA, 2021).

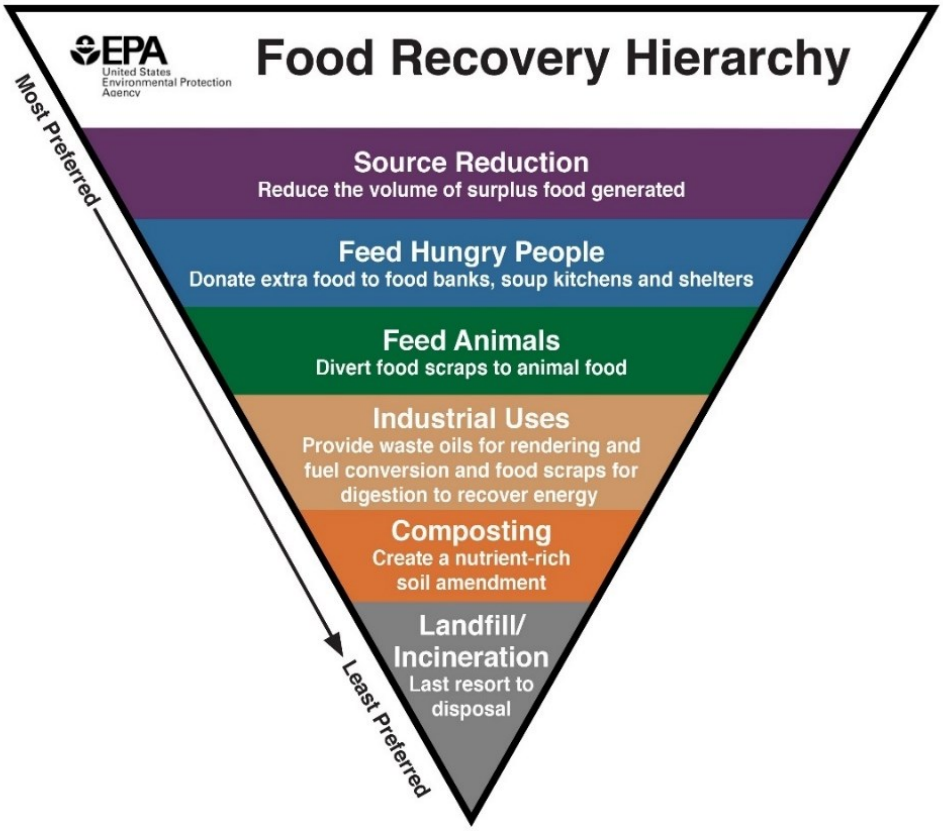

Figure 1.12: Food Recovery Hierarchy provided by the Environmental Protection Agency of the United States (EPA, 2021).

The Food and Agriculture Organization (FAO) focuses a lot its work on the reduction of loss in the supply chain, that is, loss that occurs between harvest and the market. This complies with tier 1 in **Figure 1.12** which is the most preferred food waste recovery measure. The second most preferred measure is feeding people or feeding humans. Then comes the fourth most preferred measure which consists of fuel conversion and digestion to recover energy.

1.3.5.2. Circular economy

The circular economy is an approach particular to the waste management system that stresses on the fact that it is necessary to close the loop described by the linear economy. As seen on **Figure 1.13**, in contrast to the linear economy, the waste produced enters the 3Rs (Reuse, Repair and Recycle) phase and is been recycled so that as to be an input for the production phase again.

Figure 1.13: Circular economy approach's model (Repak, 2019).

Combining **Figure 1.12** and **Figure 1.13**, we can conclude that anaerobic digestion of food waste is a key element to achieving a circular economy approach, achieving tier 4 (Industrial uses) of the FRH and working forward to achieving the SDG 7. And achieving SDG 7 will have a ripple effect on SDG 8, 9 and 13 (Renewable Energy Agency et al., 2021).

1.4. ANAEROBIC DIGESTION TECHNOLOGY

1.4.1. Biodegradability parameters

The degradability of different substrates depends on their dry organic matter content, also called 'Volatile Solids' VS. It is a parameter commonly used to characterise the organic waste for anaerobic digestion and is practically a fraction of the total dry matter of the waste, referred to as Total Solids (TS). It is common for biowaste substrates to be considered suitable for anaerobic digestion if their organic dry matter is greater than 70% of the TS. **Figure 1.14** shows how parts of a substrate are utilized during anaerobic digestion to produce bioenergy.

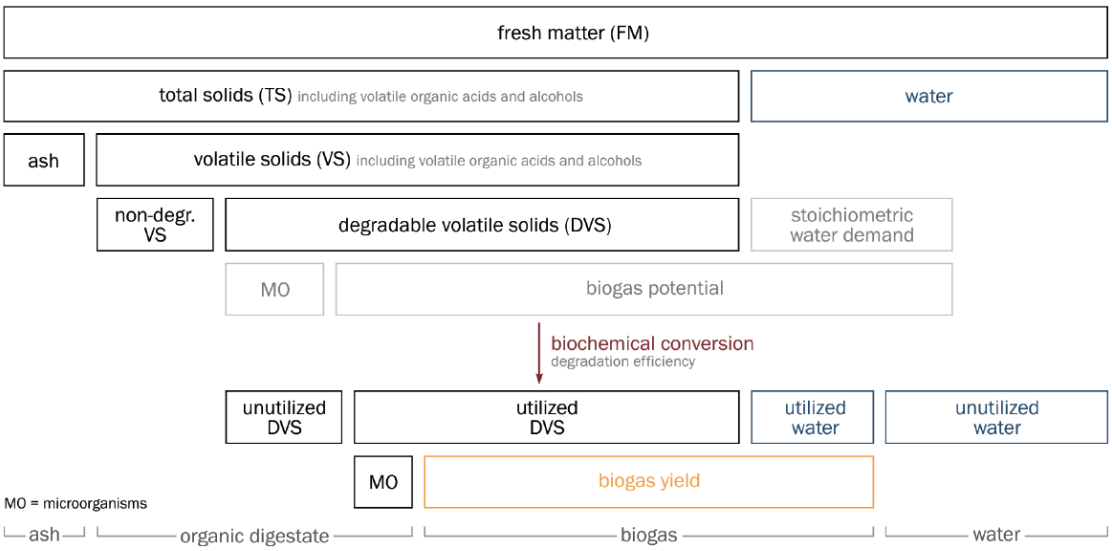

Figure 1.14: Utilization of individual substrate components during anaerobic digestion (Weinrich et al., 2018)

In literature, there is divergent information about TS and VS from different substrate sources, surely because the specific waste composition is different despite identical naming (for example, market waste).

1.4.2. Biochemical reactions in anaerobic digestion

Biological processes in the absence of molecular oxygen, where the electron acceptors are carbon dioxide, organics, and sulphate are generally referred to as anaerobic processes (Akunna, 2018). These processes are similar to those that occur naturally in the stomachs of ruminant animals, marshes, organic sediments from lakes and rivers, and sanitary landfills. The main gaseous by-products are carbon dioxide (CO_2), methane (CH_4), and trace gases such as hydrogen sulphide (H_2S), hydrogen (H_2), and a liquid or semiliquid by-product known as digestate. The digestate consists of microorganisms, nutrients (nitrogen, phosphorus, mainly), metals, undegraded organic matter and inert materials. The biochemical process of anaerobic digestion typically occurs in four (04) steps, namely: Hydrolysis, acidogenesis, acetogenesis and methanogenesis. **Figure 1.15** illustrates the path of organic matter under anaerobic digestion.

1.4.2.1. Hydrolysis

It is the first stage in the digestion process and it is usually the slowest of the four degradation steps. Hydrolysis involves the breakdown of complex polymeric organic substrates such as proteins, carbohydrates, and lipids into smaller monomeric compounds such as amino acids,

sugars (monosaccharides), and fatty acids respectively. Since large particulate organic matter is too large to be directly absorbed as a substrate, this reaction is facilitated by extracellular specific enzymes produced by a consortium of varied hydrolytic bacteria (Akunna, 2018; Arnell & et al, 2007; Mata-Alvarez, 2003).

1.4.2.2. Acidogenesis

In this second stage, the monomers released during hydrolysis are converted by bacterial metabolism of acid-forming bacteria also known as fermentative bacteria into hydrogen or formate, carbon dioxide, pyruvate, ammonia, volatile fatty acids, lactic acid, and alcohols (Mata-Alvarez, 2003). Carbon dioxide and hydrogen gases are also produced during carbohydrate catabolism (Akunna, 2018). The following are the chemical reactions involved during the fermentation process (Lavagnolo, 2020). **Equations 1.1**, **1.2** and **1.3** show the various chemical reactions that undergo in the digester or anaerobic medium during anaerobic digestion.

$$C_6H_{12}O_6 + H_2O \rightarrow 2CH_3COOH + H_2 + 2CO_2 \quad (0.1)$$

$$C_6H_{12}O_6 \rightarrow CH_3C_2H_4COOH + 2H_2 + 2CO_2 \quad (0.2)$$

$$C_6H_{12}O_6 \rightarrow 2CH_3CH_2OH + 2CO_2 \quad (0.3)$$

Where: $\boldsymbol{C_6H_{12}O_6}$– glucose;
CH_3COOH – acetic acid;
$CH_3C_2H_4COOH$ – butyric acid;
CH_3CH_2OH – ethanol.

1.4.2.3. Acetogenesis

In this third stage, both long-chain fatty acids and volatile fatty acids and alcohols are oxidized by the action of obligate hydrogen-producing acetogens to hydrogen, carbon dioxide and acetic acid (acetate) (Voegeli, 2014). During this reaction, the BOD (biological oxygen demand) and the COD (chemical oxygen demand) are both reduced and the pH decreases (Bischofsberger et al., 2005). Hydrogen plays an important intermediary role in this process, as the reaction will only occur if the partial pressure is low enough to thermodynamically allow the conversion of all the acids. Hydrogen scavenging bacteria lead to lower partial pressure. Thus, the hydrogen

concentration in a digester is an indicator of its "health" (Mata-Alvarez, 2003). **Equations 1.4 to 1.7** shows reactions at the acetogenesis' phase.

$$CH_3CH_2COOH + 2H_2O \rightarrow CH_3COOH + CO_2 + 3H_2 \quad (0.4)$$

$$CH_3C_2H_4COOH + 2H_2O \rightarrow 2CH_3COOH + 2H_2 \quad (0.5)$$

$$CH_3CH_2OH + H_2O \rightarrow CH_3COOH + 2H_2 \quad (0.6)$$

$$C_6H_5COOH + 4H_2O \rightarrow 3CH_3COOH + H_2 \quad (0.7)$$

Where: CH_3CH_2COOH – propionic acid;
C_6H_5COOH – benzoic acid;
CO_2 – carbon dioxide;
H_2O – water.

1.4.2.4. Methanogenesis

Methanogenesis leads to the formation of CH_4. During this final stage, methanogenic bacteria use acetic acid, methanol, carbon dioxide, and hydrogen to produce methane gas and carbon dioxide. Seventy percent of the methane produced is from acetic acid by acetoclastic methanogenic bacteria, making it the most important substrate for methane formation (Mata-Alvarez, 2003). Methanogenesis is affected by conditions in the reactor such as temperature, feed composition and organic loading rate (Parawira, 2004). And for biogas to be flammable, the methane content should be greater than 45% (Deublein & Steinhauser, 2011). **Equations 1.8 to 1.11** show reactions at the methanogenesis' phase

$$4H_2 + CO_2 \rightarrow CH_4 + 2H_2O \quad (0.8)$$

$$CH_3COOH \rightarrow CH_4 + CO_2 \quad (0.9)$$

$$HCOOH + 3H_2 \rightarrow CH_4 + 2H_2O \quad (0.10)$$

$$CH_3OH + H_2 \rightarrow CH_4 + H_2O \quad (0.11)$$

Where: $HCOOH$ – formic acid;
CH_3OH – methanol;
CH_4 – methane;

H_2 – hydrogen.

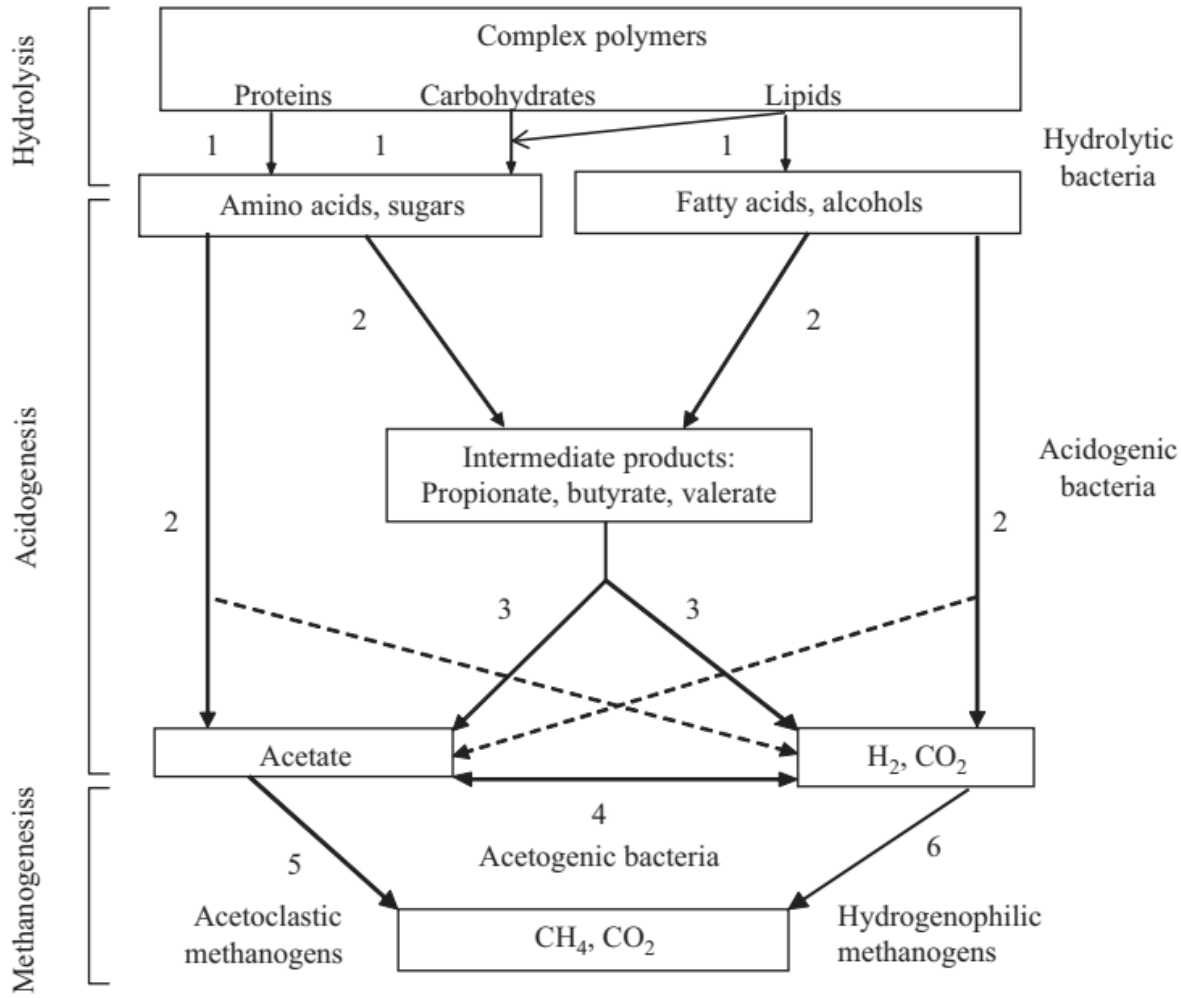

Figure 1.15: Simplified schematic diagram of different reactions involved in anaerobic digestion of complex organic matter (Akunna, 2018)

Table 1.3: Typical Composition of Functional Anaerobic Treatment Process (German Solar Energy Society and Ecofys, 2005; IEA Bioenergy, 2006)

Component	**Typical Range (% Volume)**
Methane (CH_4)	50 – 75
Carbon dioxide (CO_2)	25 – 50
Nitrogen (N_2)	0 – 10
Hydrogen (H_2)	0.01 – 5
Oxygen (O_2)	0.1 – 2

Water vapour	0 – 10
Ammonia (NH_3)	Less than 1%
Hydrogen Sulphide (H_2S)	0.01 – 3
Siloxanes	0 – 0.00002

1.4.3. Factors affecting anaerobic process efficiency

1.4.3.1. Start-up inoculum

Throughout literature, the presence of inoculum at digestion start-up has shown to be of very good help as far as lag-phase and digestion rate are concerned. The performance and stability of anaerobic treatment processes depend on the quantity and quality of active methanogens present in the system. Appropriate inoculum can be obtained from active anaerobic reactors. A low inoculum-to-feed ratio may lead to the dominance of acidogens over methanogens and can result in low pH. When this occurs, recovery may be possible depending on the alkalinity of the system. Where alkalinity is low, a chemical buffer may be added to the feed to avoid system failure (Akunna, 2018).

Some other researcher proposes to dilute the inoculum in a 1:1 ratio with water (Voegeli, 2014). The minimum cow dung required for inoculation amounts to 10% of the total active reactor volume. Furthermore, he discusses the importance of maintaining a balanced microorganism population. Once a bacterial population gets used to a certain amount of feed, overloading presents a risk to the overall failure of the anaerobic process. Overloading results from either feeding too much biodegradable organic matter compared to the active population capable of digesting it, or rapidly changing digesters conditions (for example, abrupt change of temperature, accumulation of toxic substances, flow rate increase). Such disturbances specifically affect methanogenic bacteria, whereas the acidogenic bacteria, which are more tolerant, continue to work, and produce acids. This eventually leads to an acidification of the digester which inhibits the activity of methanogens. Such an imbalance of acidogenic versus methanogenic bacteria can result in digester failure. The addition of manure can avoid this as it increases the buffer capacity, thereby reducing the risk of acidification (Voegeli, 2014).

Following the sequence of anaerobic biochemical processes, in the first weeks after start-up, carbon dioxide (CO_2) is mainly produced. This gas is not flammable and can be released. After a few days the methane content of the gas will have sufficiently increased to a level that can sustain a flame (CH4 > 45 Vol.- %) and lead to high-quality biogas (55 – 70 Vol.- %).

1.4.3.2. Waste Organic content and biodegradability

Anaerobic treatment is most suitable for solid residues, slurries, and wastewaters with COD concentrations in the intermediate to high strength range, that is, from 2,000 COD/L. Organic removal efficiencies tend to increase with increasing influent organic strength. However, up to 80 %–90 % of COD removal is achievable in an efficiently operated system (Voegeli, 2014).

The chemical composition of the waste or wastewater is one of the primary indicators of amenability of the organic constituents to biological treatment. **Figure 1.16** shows the relative biodegradation rates and reaction times of various types of organic compounds. Biodegradability may be limited by the chemical structure of compounds such as lignin, cellulose, and hemicellulose, which are not readily amenable to enzymatic hydrolysis. These compounds may require prior treatment or pretreatment.

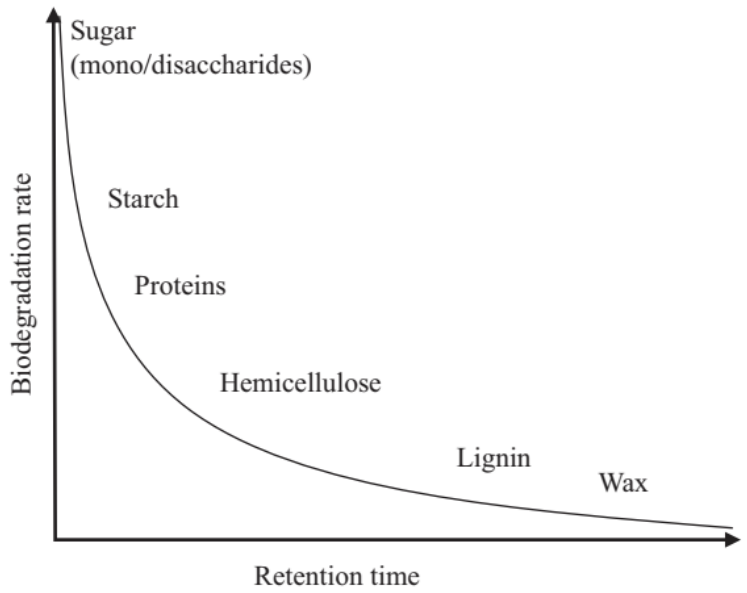

Figure 1.16: Relationship between the rate of degradation and retention time for various types of organic compounds (Voegeli, 2014)

Total solids (TS) are the measure of the solid content of an organic matter. Hydrolysis of particulate biodegradable organic matter is a relatively slow biological reaction for certain types of compounds and may represent the process-limiting step in the treatment of high solids wastes. Such wastes usually require longer retention times to bring about high levels of treatment and biogas production. Conversely, if the organic constituents are primarily soluble in nature, high levels of biodegradation can be achieved at shorter retention times.

Biochemical methane potential (BMP) assays are used for preliminary assessment of the anaerobic biodegradability and possible methane yield of organic residues.

1.4.3.3. Nutrient availability

The ideal feedstock composition ratio for carbon (C), nitrogen (N), phosphorus (P), and sulfur (S) (the C/N/P/S ratio) for hydrolysis and acidogenesis) is considered to be 500/15/5/3, and for methanogenesis, the ratio is theoretically assumed to be 600/15/5/3 (Weiland, 2001).

Sulfur and phosphorous requirements are very low compared to the other macronutrients; carbon, in particular, is naturally abundant in organic wastes. Therefore, the limiting nutrient for the anaerobic digestion process is considered mainly nitrogen. So, to measure the nitrogen sufficiency of waste for the biological process, the Carbon to Nitrogen ratio (C/N) is used. Good ratios for the process have been reported in the literature (Deublein & Steinhauser, 2011; Zareei & Khodaei, 2017) to range from 20 to 30. Higher C/N ratios can lead to decreased bacterial growth due to nitrogen deficiency. The methanogens rapidly consume the nitrogen till nitrogen depletion leading to low gas production. On the other hand, a low ratio may result in a pH increase and ammonia toxicity in the microbial population (Voegeli, 2014). Although methanogenic bacteria can adapt to very high ammonia concentrations this only happens if concentrations are increased gradually allowing time for adaptation. Optimum C/N ratios can be ensured by mixing different feedstock materials, with high (like organic solid waste) and low (like sewage or animal manure) C/N ratios to achieve an ideal C/N ratio level.

Another important anaerobic microbial requirement is trace elements, or micronutrients, notably iron, cobalt, nickel, and zinc. These elements, when available in relatively small amounts, can stimulate methanogenic activities. The exact amount needed may vary for different wastes, and prior laboratory scale trials are needed before they are added to anaerobic treatment systems (Akunna, 2018).

1.4.3.4. pH and alkalinity

The stability of anaerobic treatment processes is highly dependent on pH. While the acidogenic bacteria are more tolerant to pH values below 6.0, optimum pH values for methanogenic bacteria lie between 7 and 8. Therefore, the pH range of 6.5 – 7.8 is suitable for the entire process. Acidic pH can occur in anaerobic treatment systems where a slower methanogenesis rate results in an accumulation of volatile fatty acids. This situation is likely to occur when

there is a sudden or excessive increase of organic matter added to the system. On the other hand, alkaline pH can result where the feed constitutes of high amounts of nitrogenous compounds, such as proteins. Nitrogenous compounds hydrolyze to produce ammonia, which causes alkaline pH. When pH values rise above 8.5, ammonia begins to exert a toxic effect on methanogenic bacteria (Hartmann & Ahring, 2006).

Lime is commonly used to raise the pH of AD systems when the process is too acidic, however frequently leads to precipitation and clogging of pipes when used in large quantities. Alternatively, sodium bicarbonate can also be used for pH adjustment (Voegeli, 2014).

1.4.3.5. Temperature

Like all biological processes, anaerobic processes are affected by temperature, **Figure 1.17**. Anaerobic treatment systems can be operated at psychrophilic (<20°C), mesophilic (25°C–40°C), or thermophilic (45°C–60°C) temperature ranges, with the optimum temperatures for the mesophilic and thermophilic processes at about 37°C and 55°C, respectively (Abbasi et al., 2012; Filer et al., 2019; Mata-Alvarez, 2003).

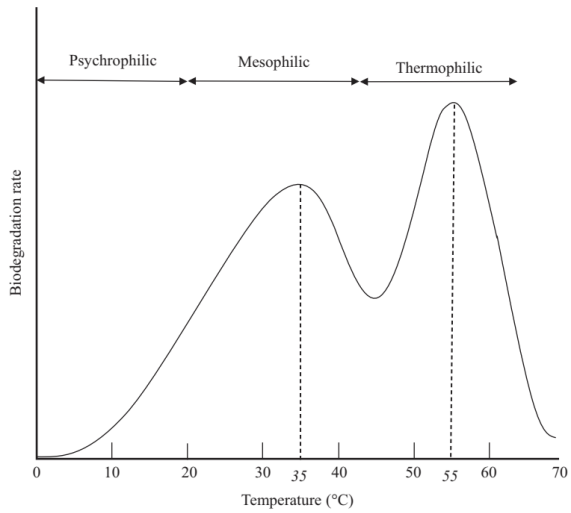

Figure 1.17: Temperature ranges for anaerobic treatment processes (Mata-Alvarez, 2003)

While AD technology is principally feasible under almost all climatic conditions, at low temperatures (mean temperature below 15 °C) the digestion process does not work satisfactorily. In cool climatic conditions either a heating system has to be installed or a larger digester has to be built to increase retention time. Also, large temperature variations such as those between day and night, or seasonal variations can adversely affect the performance of an

AD system. As such, digesters that are built underground help to minimize these changes by using the temperature buffer capacity of the soil.

The operation of a digester in the mesophilic range is more stable, as these microbial communities can tolerate greater changes in the environmental parameter and consume less energy. On the downside, however, the mesophilic microorganisms are slower and thus a longer retention time in the digester is needed to maximise biogas yield.

1.4.3.6. Solids and hydraulic retention times

The Solid Retention Time (SRT) refers to the average dwelling time of microorganisms within the system or reactor. SRT depends on microbial growth rate and the rate of removal of excess microbial biomass from the treatment system. The former is affected by the nature of the constituent organic compounds. Methanogenic bacteria have significantly slower growth rates than other microbial groups associated with anaerobic processes. Temperature also plays a vital role in the biodegradation rate, and consequently in the microbial regeneration time and SRT. Hydraulic retention time (HRT) is defined as the theoretical amount of time that the wastewater being treated is resident within the treatment system or reactor. For completely mixed suspended growth systems without biomass recycling, HRT is the same as SRT. Recommended HRT for wastes treated in a mesophilic digester range from 10 to 40 days. Lower retention times down to a few days only, are required in digesters operated in the thermophilic range.

1.4.3.7. Organic Loading Rate (OLR)

The organic loading rate (OLR) describes the relationship between the treatment rate of the organic matter and the size of the treatment system or reactor. In other words, it is a measure of the biological conversion capacity of the anaerobic digestion system. It is expressed as the weight of organic matter in terms of COD or VS (or TS) added per volume of reactor per day. The higher the OLR a system can properly treat, the greater the cost-effectiveness of the system. High-rate systems generally cope with relatively high OLR.

Table 1.4: Average Time of Regeneration of Some Microbial Groups (Akunna, 2018; Deublein & Steinhauser, 2011)

Microorganism	Time of regeneration
Acidogenic bacteria	Less than 36 hours
Acetogenic bacteria	80 – 90 hours

Methanogenic bacteria	15 – 16 days

Table 1.4 shows the average time of regeneration of microbial groups with the methanogenic bacteria having the longest regeneration time. Studies of anaerobic treatment of biowaste in industrialized countries describe organic loading rates in the range of 4 – 8 kg VS/m^3 reactor and day, which result in VS removal in the range of 50 – 70 %. This is ideal for continuously stirred reactors. However, for non-stirred AD systems which are predominant in developing countries, an OLR below 2 kg VS/m^3 reactor and day is recommended and considered suitable (Voegeli, 2014).

1.4.3.8. Substrate pre-treatment

Most feedstocks require pre-treatment before digestion. In the case of an anaerobic digestion facility, source segregation of waste or sorting is the first waste pre-treatment measure to take. But in the case of a biogas yield experiment, usually, sorting is evident as the substrates are selected. There also exist mechanical pre-treatment measures, such as grinding, ultrasonic treatment, high-pressure homogeniser, collision plate, and lysis-centrifuge. Below are explanations of how the above-mentioned pre-treatment methods are implemented.

- **Grinding**

The reduction in particle size through grinding is for two reasons; to avoid blockage of the inlet pipe and to increase the material's total exposed surface. For a treatment facility, in a continuous reactor, a diameter of max. 5 cm is recommended. Also, the greater surface of the material exposed, the more the area that can be degraded (Schnürer and Jarvis, 2010) as many microorganisms. Size reduction technology ranges from manual mincing machines suited for small amounts, household scale, to larger manual or power-driven grinders for larger amounts at institutional scale. At the AD facility, particle size reduction can be energy and labour-intensive depending on the equipment used.

- **Ultrasonic treatment**

The pre-treatment effect of ultrasound is based on the principle of cavitation. Cavitation is a phenomenon in which spontaneous formation, growth, and subsequent collapse of micro size cavities (also known as bubbles) during the propagation of ultrasonic waves in liquid medium (Subhedar and Gogate 2016; Tey et al. 2019).

- **High-pressure homogeniser**

High pressure homogenization (HPH) pre-treatment works on the principles of turbulence, cavitation and shearing, solubilizing the sludge or enlarging its surface area for enzymatic attack, so that enzymatic hydrolysis can be efficiently enhanced and subsequently bio-gas production can be significantly improved.

1.4.3.9. Mixing

The purpose of mixing and stirring inside the digester is to blend the fresh material with digestate and thus inoculate the fresh material with microbes. Such mixing avoids temperature gradients within the digester and also prevents scum formation. Scum and foam are a result of filamentous microorganisms in the digester. Low concentrations of the substrate in AD plants lead to an increase in the growth of filamentous bacteria compared to flocculating bacteria. Scum in digesters should be avoided as it can result in blockage of the gas pipe or potentially lead to foaming over the digester. This results in the displacement of slurry into pipes, machines and devices resulting in subsequent malfunction or corrosion. Loss of bacteria is usually a minor problem as they regrow.

A constant top layer of 20 – 60 cm of foam is usually regarded as “stable” in large-scale systems and is acceptable or easy to manage. A thicker impermeable scum layer however may prevent gas release from the liquid and eventually also lead to failure of the structure. Mixing and stirring equipment, and the way it is performed, varies according to reactor type and TS content in the digester. In the three most prevalent AD technologies typical for developing countries (fixed-dome, floating dome, tube digester) no stirring is typically implemented. Removing digestate outflow (equivalent to the normal daily feeding load) and feeding this back into the digester through the inlet achieves a passive mixing process. Such a recirculation of digestate also helps to flush the inlet pipe and improves the mixing of fresh feedstock with bacteria-rich digestate.

1.4.3.10. Toxic compounds

Anaerobic processes can be inhibited by substances contained in the waste, which are toxic to microorganisms. Typical microbial inhibitors include ammonia, sulphide, long-chain fatty acids, salts, heavy metals, phenolic compounds, and xenobiotics (Akunna, 2018).

- **Sulphide toxicity**

Sulphide is produced during the hydrolysis of sulphur compounds such as sulphates, sulphite, and thiosulfate, which may be present in the waste, by the activities of sulphate-reducing bacteria. Therefore, the sulphate-reducing bacteria compete with methanogenic bacteria for the available COD. Hence, the more the concentrations of sulphur compounds in the waste, the greater the quantity of COD required for its hydrolysis and the lower the methane yield.

Hydrogen sulphide exists in aqueous solution in the forms of hydrogen sulphide (H_2S), hydrogen sulphide ion (HS^-), and sulphide ion (S^{2-}), depending on the pH, under the following equilibrium reactions shown in **equations 1.12 and 1.13.**

$$H_2S \leftrightarrow HS^- + H^+ \quad (0.12)$$

$$HS^- \leftrightarrow S^{2-} + H^- \quad (0.13)$$

Figure 1.18 shows the effect of pH on H_2S, HS^-, and S^{2-} equilibrium in a 10^{-3} molar solution. At pH of 8 and above, most of the sulfide produced remains in solution, and below pH 8, it exists mainly in unionized gaseous form, H_2S. At pH of 7, about 80 % of the sulfides are present as H_2S. H_2S is considered more toxic than the ionized forms, hence, pH is, therefore, an important parameter in determining its level of toxicity.

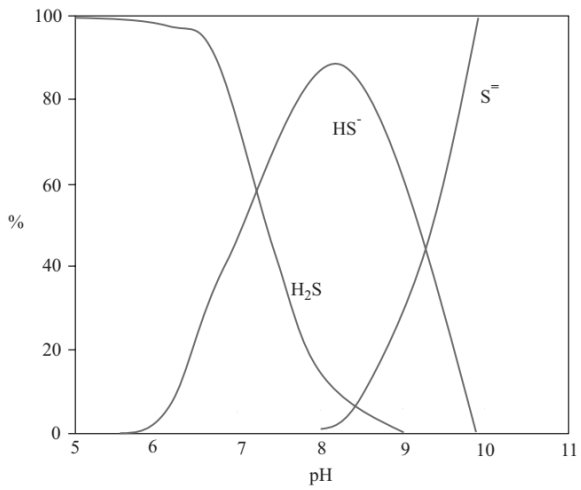

Figure 1.18: Effect of pH on hydrogen sulphide–sulphide equilibrium (10−3 molar solution, 32 mg H_2S/l) (Akunna, 2018).

Sulphide inhibition can be minimized by the following measures (Pohland 1992):

- Dilution of the influent waste or wastewater;
- Addition of iron salts into the treatment system to precipitate sulfide from the solution;

- Stripping the reactor liquid or scrubbing and recirculation of the reactor biogas;
- Biological sulfide oxidation and sulfide recovery.

Ammonia toxicity

Ammonium (NH_4) is produced by the biological conversion of protein and urea under aerobic or anaerobic conditions. Ammonia (NH_3) is a gas and toxic to microbes, animals, and humans. NH_4 is related to the toxic un-ionized ammonia (also known as free ammonia) by the pH-dependent equilibrium.

$$NH_4^+ \leftrightarrow NH_3 + H^+ \qquad (0.14)$$

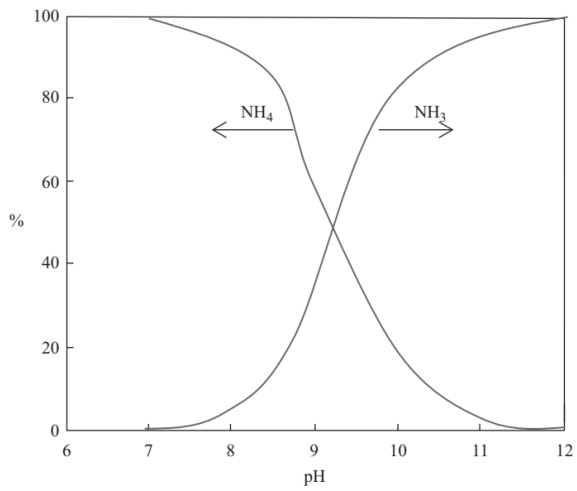

Figure 1.19: Effect of pH on ammonia–ammonium equilibrium (Akunna, 2018).

1.4.4. Biochemical methane potential

Biochemical methane potential (BMP) tests are a popular technique to determine the methane potential and biodegradability of wastewater and waste biomass. In the test, a substrate is mixed with an anaerobic bacteria culture, normally retrieved from an active digester. The bottles are then stored at a stable temperature of either 35 °C or 55 °C, and constantly mixed for a period of 30–60 days. Methane and carbon dioxide are produced during the testing period due to the anaerobic degradation of organic contents of the substrate. The methane generated from the substrate is then measured and the methane yield of the substrate which is expressed as per mass of volatile solids (VS) added or chemical oxygen demand (COD) added. **Appendix 4** shows an example of a recommended BMP set for methane yield determination.

There exist experimental protocols for conducting such experiments. An example is the German VDI 4630 (2016) standard which provides rules and specifications for tests to

determine the biogas output of organic materials and residue gas production after anaerobic digestion which serve the interpretation and optimisation of biogas plants.

1.4.5. Biogas production systems in developing countries

1.4.5.1. Biogas reactor classification

Digesters are classified according to the substrate moisture/total solid content (wet/dry digestion), the feeding mode (batch/continuous) or the operating temperatures and bacteria species (mesophilic/thermophilic), and their scale (households, community and industrial) and the number of biological processes involved (two-stage/phase), **Figure 1.20**.

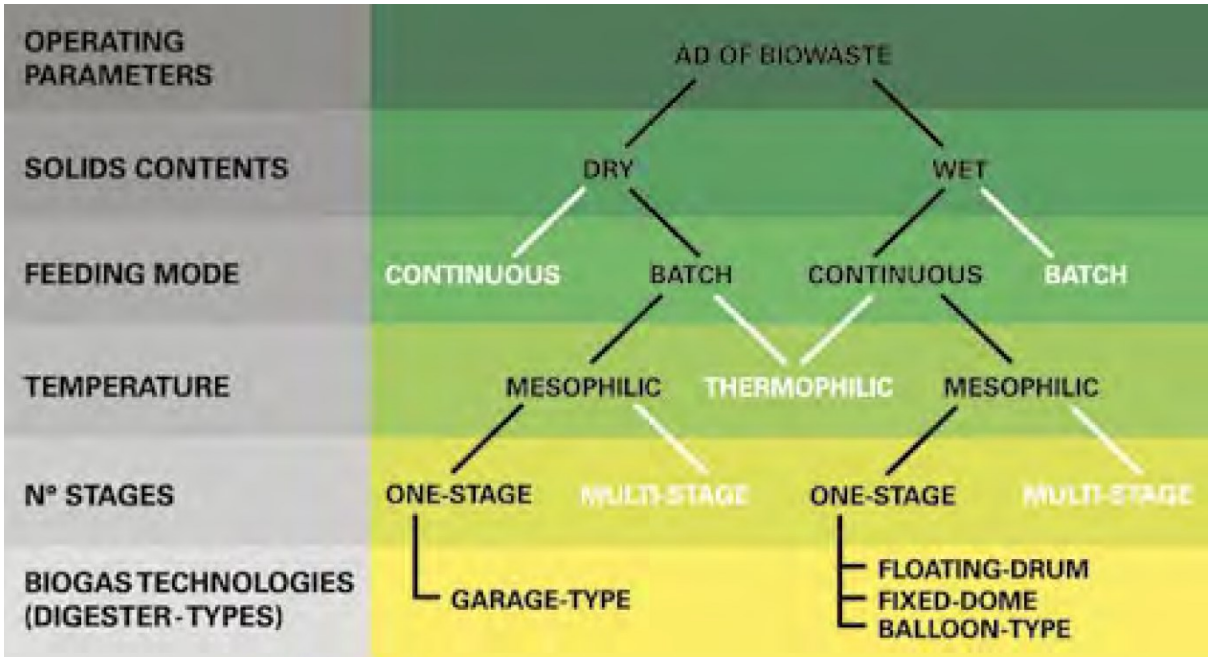

Figure 1.20: Biogas digester types considered for developing countries (Voegeli, 2014).

1.4.5.2. Fixed-dome digester

A fixed-dome plant is comprised of a closed dome shape digester with an immovable, rigid gas-holder, a feedstock inlet, and a displacement pit also named the compensation tank. A schematic diagram is shown in **Figure 1.21**. The gas produced in the digester is stored in the upper part of the reactor. With a closed outlet gas valve, increasing gas production elevates the gas pressure inside the digester thereby pushing the digestate into the compensation tank. When

the gas valve is open for gas utilization, gas pressure drops and a proportional amount of slurry flows back from the compensation tank into the digester. A schematic diagram of this type of digester in **Figure 1.21**.

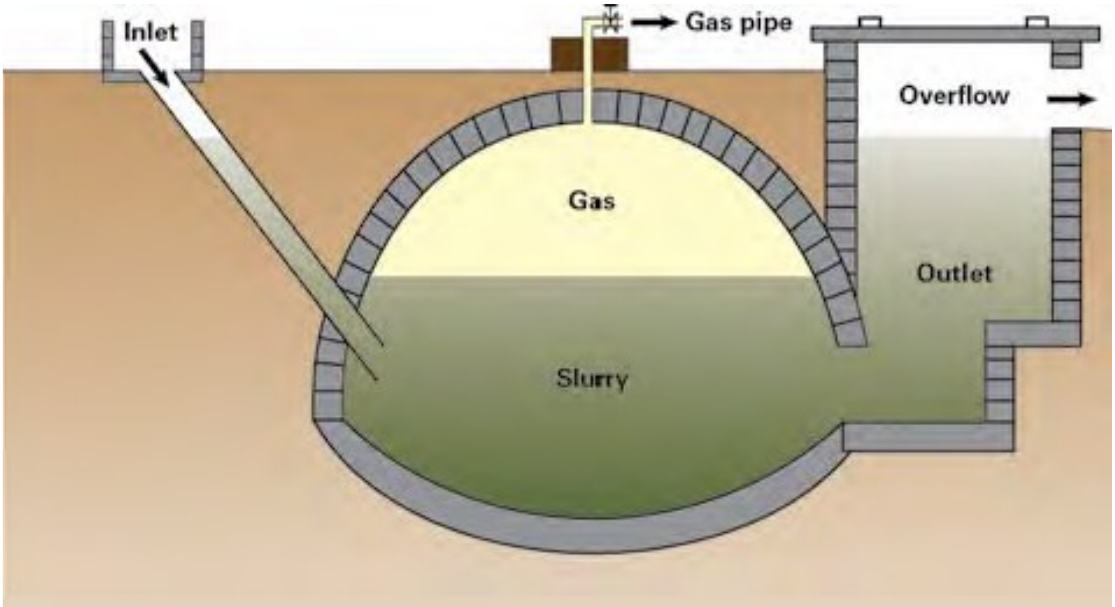

Figure 1.21: Illustration of a fixed-dome digester (Voegeli, 2014).

1.4.5.3. Floating-drum digester

A floating-drum biogas plant consists of a cylindrical digester and a movable, floating gasholder (drum). The digester is generally constructed underground whereas the floating gasholder is above ground. Smaller household-scale systems may also be fully above ground. The digester section of the reactor is usually constructed with bricks, concrete or quarry-stone masonry and then plastered. The gas holder is typically made of metal and is coated with oil paints, synthetic paints or bitumen paints to protect it against corrosion. An example of such digester is seen in **Figure 1.22**.

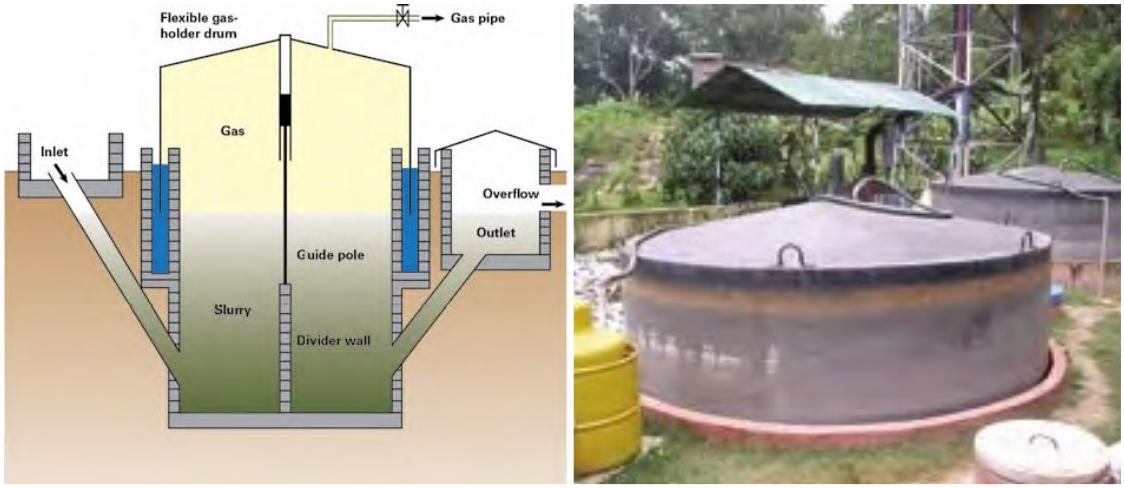

Figure 1.22: Scheme of the floating-drum digester (left), floating-drum digester for market waste in India (right) (Voegeli, 2014).

1.4.5.4. Tubular digester

A tubular biogas plant consists of a longitudinal-shaped heat-sealed, weather-resistant plastic or rubber bag (balloon) that serves as a digester and gas holder in one. The gas is stored in the upper part of the balloon. The inlet and outlet are attached directly to the skin of the balloon. As a result of the longitudinal shape, no short-circuiting occurs, but since tubular digesters typically have no stirring device, active mixing is limited and digestate flows through the reactor in a plug-flow manner. Gas pressure can be increased by placing weights on the balloon while taking care not to damage it. **Figure 1.23** shows a schematic representation of a typical tubular digester.

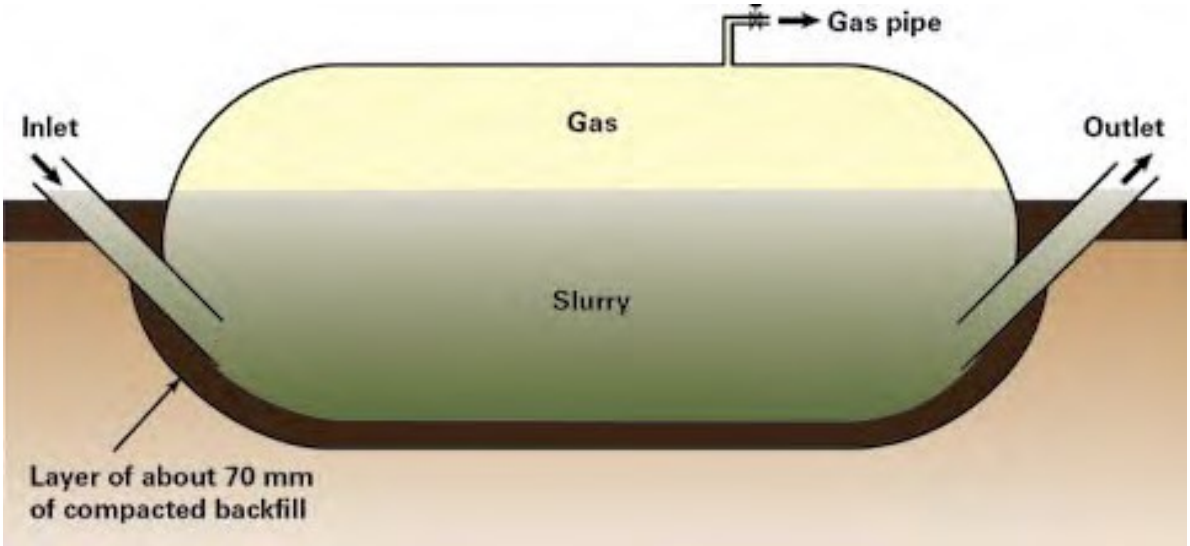

Figure 1.23: Scheme of balloon digester (Voegeli, 2014)

1.4.5.5. Some biogas plants in Africa

Table 1.5 contains information on biogas plants running in Africa.

Table 1.5: Biogas plants in Africa (Voegeli, 2014)

Location	Digester type	Digester volume (m^3)	Feedstock (waste type)	Daily load (kg/d)	Specific gas production (m3/kg VS d)
Dar es Salaam, Tanzania	Floating drum	0.85	Kitchen waste and market waste	3 (+18 L H_2O)	0.64
Der es salaam, Tanzania	Floating drum	3.4	Canteen waste	8 (+60 L H_2O)	0.45
Lesotho	Fixed-dome	6 - 19	Human feces, kitchen waste, pig and chicken manure	diverse	n/d

n/d = no data

Africa's first grid-connected biogas plant started supplying power in 2017 at Tropical Power Kenya Ltd. The Gorge Farm Energy Park anaerobic digester in Kenya consumes an annual 50,000 tons of organic waste sourced from a neighboring 800-hectare farm owned by VegPro Group, one of Tropical's investment partners, **Appendix 5**, (Voice of America, 2017).

1.5. RESPONSE SURFACE METHODOLOGY

Ther response surface methodology (RSM) is a key element of our methodology, it is the method which permits us to find the maximum or minimum response based on data obtained

from a series of biochemical methane potential (BMP) test, **objective 2** of our research. Therefore, it is important to describe what it is and its usefulness.

RSM is a widely used mathematical and statistical method for modeling and analyzing a process in which the response of interest is affected by various variables and the objective of this method is to optimize the response. The parameters that affect the process are called independent variables, while the responses are called dependent variables. The main goals of a RSM study are to understand the topography of the response surface including the local maximum, local minimum and ridge lines and find the region where the most appropriate response occurs. The RSM investigates an appropriate approximation relationship between input and output variables and identify the optimal operating conditions for a system under study or a region of the factor field that satisfies the operating requirements (Aydar, 2018).

Box-Behnken designs (BBD) and central composite design (CCD) are two main experimental designs used in response surface methodology. In the CCD, there are three sets of points; the center points, the "star" or axial points and the corner points, which make it possible to estimate the curvature of the response surface after the screening step has been carried out. **Equation 1.15** is used in the case where two factors are to be fitted to one response.

$$y = \beta_0 + \sum_{i=1}^{q} \beta_i x_i + \sum_{i=1}^{q} \beta_{ii} x_i^2 + \sum_{i<j} \beta_{ij} x_i x_j + \varepsilon \qquad (1.1)$$

Where: y – Dependent variable or estimated response;

β_0 – overall mean response or intercept constant;

β_i – regression model coefficients;

x_i – independent variable.

In this mathematical model, the main effects to the dependent value y are x_1 and x_2 terms. The interactions are indicated by $x_1 x_2$ term and their quadratic components by x_1^2 and x_2^2 terms.

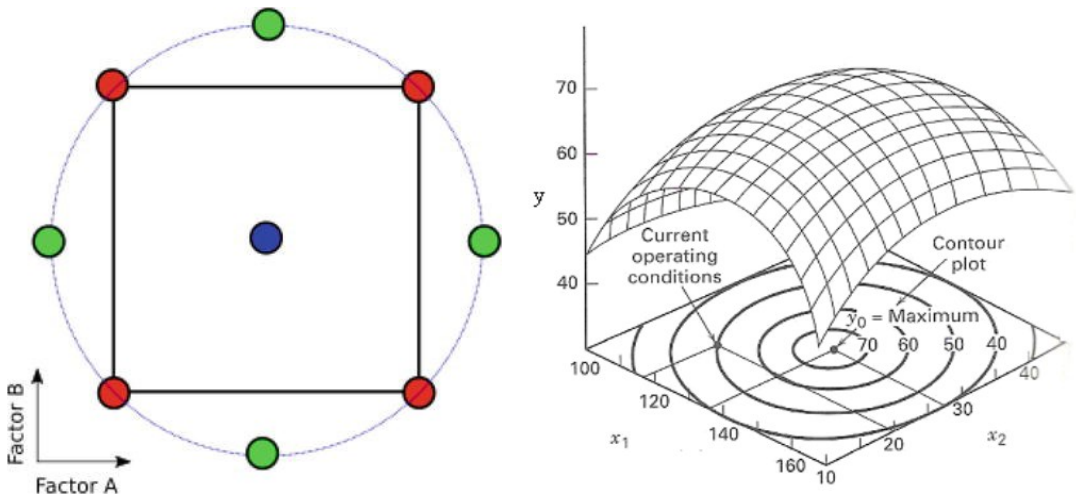

Figure 1.24: Example of a central composite with face-centered points (Bradley Nuran, 2018).

The levels of the corner points are ±1 while the levels of the axial points are ± α > 1. In case we use the Face-centered Central Composite Design (FCCD), the value of α = ±1 resulting in the axial points being located on the faces of the experimental domain, **Figure 1.24**. To evaluate the adequacy and precision of the results, an Analysis of Variance (ANOVA) in done.

Many researchers throughout the literature attempted to optimize biogas yield from various waste and feedstock (municipal solid waste, kitchen waste, agricultural waste and even food waste. The methods used by these scientists include a random variation of the parameters influencing biogas yield. Research on the production of biogas from waste of unique characteristics in co-digestion with inoculums such as cow dung (manure), pig manure, and even human faeces is increasing being done. Some of these researches used RSM, which was already been used for the optimization of chemical reactions, to achieve maximum yield. Unfortunately, no research has been carried out on the possible optimization of biogas yield from pineapple, watermelon and banana waste using RSM. The reason why our study uses this method to achieve the maximum biogas yields.

CHAPTER 2 . MATERIAL AND METHODS

Before coming up to the materials and the methods used, we are going to introduce the various software used throughout our work.

2.1. SOFTWARE USED

2.1.1. Microsoft Word (MS Word)

Microsoft word is a word processing software developed by Microsoft. It is a didactic software that helped us write our thesis. With this software we were able to edit and compile data for the general and orderly presentation of information, applying styles to text, headings and captions. The software also facilitates the grammar and vocabulary of written text enhancing the readability and the understanding of the information throughout our thesis.

In addition to that, the references were done through the Mendeley add-in in Microsoft Word for proper organisation of references in our thesis. The version used here was 2016.

2.1.2. Microsoft Excel (MS Excel)

Microsoft Excel is a spreadsheet software also developed by Microsoft. This software was one of the core software that helped with the analysis of the collected data. After analysis of this data, graphs were drawn on the software for information presented on our thesis. The version used here was 2016.

2.1.3. Microsoft Visio

Microsoft Visio is a diagramming and vector graphics application which is also part of the Microsoft Office Family. With this software, complex ideas were represented visually through flowcharts. The version used here was 2016.

2.1.4. Autodesk AutoCAD

AutoCAD is software that was developed by the company Autodesk. In the work, it was used to draw some of the 2D illustrations to convey to the reader a better understanding and flow. The version used in this work is that of 2020.

2.1.5. Google Sketchup Pro

Sketchup is a three-dimension (3D) design software developed by Trimble Inc. and owned by Google. Some of the figures that were not found on the internet, especially the experimental

design setup was drawn in 3D in SketchUp pro and sent to SketchUp layout for 2D representation before inserting in MS Word. The version used here was 2021.

2.1.6. MATLAB

MATLAB, an abbreviation of "Matrix Laboratory" is a proprietary multi-paradigm programming language and numeric computing environment developed by MathWorks. Matrix manipulations were done on this software together with the integrated Curve fitting tool to perform calculations. The version used here was the R2019a.

2.1.7. Minitab statistical software

Minitab statistical software, from its name, is a software that helps perform statistical analysis of data and has good visualisation tools. The version used here was 2022.

2.1.8. QGIS

QGIS is an open-source geographical information system software used for viewing, editing, printing and analysing geospatial data.

2.2. MATERIALS

2.2.1. Global Positioning System (GPS)

The GPS is a satellite positioning system, which determines the geographical coordinates of any point on the surface of the globe. Coordinates of important sites and infrastructures were collected using the GPS app "*Mobile Topographer*". These coordinates are automatically projected into UTM coordinate system and ready for use in QGIS.

2.2.2. Physical and chemical analysis (materials and reagents)

Physical and chemical analyses were performed on the various organic waste to be used as substrates; pineapple peelings (*Ananas comosus* botanic variety, comosus (Linnaeus) Merrill), watermelon rind (*Citrullus lanatus*), Banana peelings (*Musa acuminata* and *Musa balbisiana*), and cow-dung.

In physical analysis, we have the density of the substrate. And as chemical analysis, we have: measurement of pH value, proximate analysis and ultimate analysis. Apart from the substrate, physical analysis was also carried out on the sawdust material used through granulometric characterisation. Below are the materials necessary for the different analyses and the biochemical methane potential batch test.

2.2.2.1. Proximate analysis

The proximate analysis is a way to determine the distribution of products when the samples are heated under specified conditions. More precisely, it consists of the determination of ash content, moisture content, total solids, volatile solids, and fixed carbon on an as-received basis. Below are the material requirements for the analysis.

- Plastic bags;
- A drying oven that operates at ~105 °C;
- A muffle furnace that operates at ~550 °C;
- A desiccator;
- A pair of oven gloves;
- Laboratory latex gloves;
- Four (04) ceramic crucibles;
- A knife;
- An analytical balance with an appreciation of 0.001g;
- Air dried organic matter.

2.2.2.2. Ultimate analysis

The ultimate analysis is typically the quantification of Carbon (C), Hydrogen (H), Nitrogen (N), Oxygen (O), and Sulphur (S) in a sample. But in this work, we are going to experimentally determine the Carbon (**Table 2.1**) and Nitrogen (**Table 2.2**) content of our samples which is necessary for the evaluation of the Carbon Nitrogen ratio.

Table 2.1: Walkley and Black Method materials and reagents

Material	Reagents
- Analytical balance with an appreciation of 0.0001 g for measuring the masses of substrates; - Burette 50ml, with an appreciation of ± 0.02 ml for the titrant solution; - A 0 to 5 ml micropipette to record 10 mL, to be used with the potassium dichromate solution;	- Deionized water/distilled water; - Potassium Dichromate Standard, $K_2Cr_2O_7$, 1 M; - Sulfuric Acid, Concentrated, 98%; - Phosphoric Acid (also known as Orthophosphoric acid), 98 %;

- A measuring cylinder, capable of measuring 20.0 ml, to be used with concentrated sulfuric acid; - Four (04) Erlenmeyer flask, 500ml. - Magnetic stirrer/agitator and bar;	- Titrant (Ferrous Sulphate (FeSO4)) solution.

Table 2.2: Kjeldahl Method materials and reagents

Materials	Reagents
- Erlenmeyer Flask; - Burette; - Digestion tubes; - Air dried organic matter.	- Potassium Sulphate tablets (2 per digestion tube); - Concentrated sulphuric Acid; - Prepared 35 % (w/v) NaOH for each digestion tube; - Prepared 4.0 % (w/v) Boric acid; - Prepared 0.1M HCl; - Methyl orange;

2.2.3. Biochemical methane potential test

The materials within the following points below are required per experimentation.

- A glass bottle of extra fresco (reactor) of 300 mL;
- A medical infusion set;
- A syringe of capacity 60 mL;
- The weighted wet organic matter/substrate;
- Distilled water between 50mL to 200mL.
- A black plastic bag.

The materials needed for all experimentations.

- A bucket of base area > 0.09m^2;
- A knife;
- Silicon sealant in tube, brand name *Simbock Products*;
- Aluminium caulking gun, brand name *TOTAL*;

- Epoxy AB gum in tube, brand name *TCM Hardener and Resin*;
- A nail;
- A pair of laboratory latex gloves;
- PVC pegafort sealant.
- A painting masking tape.
- A graduated beaker;
- An analytical balance of precision 0.0001g;
- The knife mill, brand name *Retsch GM 200*;
- Sawdust.

2.3. DESIGN OF EXPERIMENT (DOE)

2.3.1. Objective

The objective of our Design of Experiment (DOE) was to understand how independent variables in an anaerobic digestion process of food waste affect the dependent variable (biogas yield) and optimise the process. In addition to that, we had as objective to compare the yield of our substrates; pineapple peelings, watermelon and banana peelings when mixed together. The flowchart, **Figure 2.1**, shows how the major steps used in this research.

Figure 2.1: Experimental design flowchart

2.3.2. Definition of variables

Independent variables:	Temperature, Total Solids (TS), retention time, carbon-to-nitrogen ratio (C/N), pre-treatment, pH and stirring.
Dependent variable:	Biogas yield

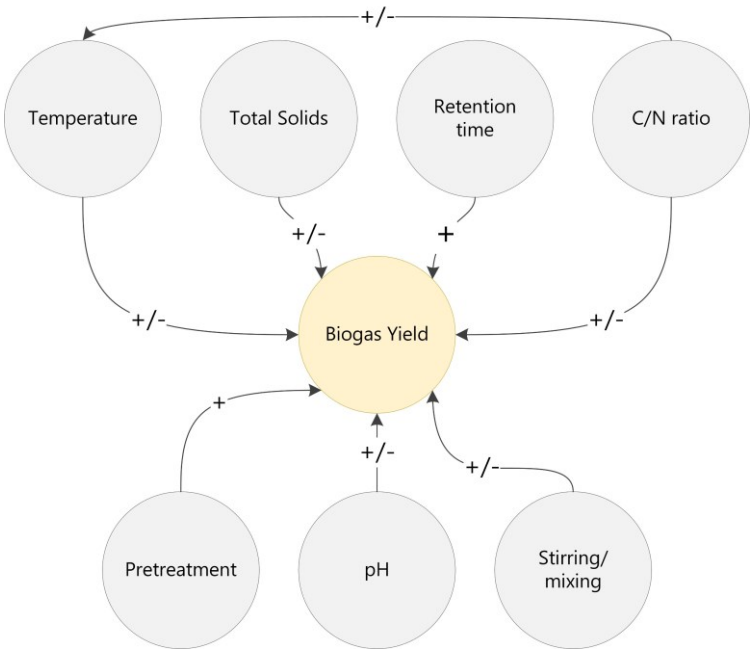

Figure 2.2: Independent and dependent variables of an anaerobic digestion process

Figure 2.2 indicates the relationship between the variables. The arrows with the +/- sign can influence the biogas yield both negatively and positively while that with only + signs can only affect the biogas yield positively if increased.

2.3.3. Batch experiment operating conditions

When attempting to optimise biogas yield, all parameters that can possibly influence biogas yield must be taken into consideration. The ranges of the independent factors used in this research were set using local realities as follows:

2.3.3.1. Temperature

The temperature was kept at mesophilic range (25°C – 40°C). To ensure this, all the digesters were submerged in buckets filled with sawdust. The advantage is the insulation effect brought to the batch assays ensuring the yields obtained can be reproducible in any geographical setting. Also, this condition simulating most digester technologies in developing countries like the fixed-dome digester. In this condition, the temperature was assumed to be self-regulated by microbial activity.

2.3.3.2. Stirring

In the absence of possible means to stir the digester content with an electronic stirrer, manual shaking was used at a frequency of twice every 24 hours, one in the morning and the other in the evening. The reactor content was swirled making rapid rotations of the buckets, in which the reactors were. Mixing was a very important aspect because it helped to homogenise the content, to avoid agglutination and to provide a path for the delocalised gas bubbles to escape and their volume measured. A form helped to keep track and ensure shaking was done as planned.

2.3.3.3. Pre-treatment

As shown above, 2.5.2. , a physical pre-treatment was employed, reducing the particle size to <1cm larger, therefore increasing surface area and breaking down the lignocellulosic links.

2.3.3.4. Incubation time

Due to time constraints, the incubation time was fixed to maximum 30 days for all experimentations.

2.3.3.5. pH

Technically we were unable to control the pH with the progress of the reaction. The buffering capacity and dilution potential of toxic compounds in the feed was assumed to be ensured through co-digestion with cow dung (Neshat et al., 2017).

2.3.3.6. Inoculum pre-incubation

The inoculum was pre-incubated for a period of 5 days to render the anaerobes active at the start of the anaerobic co-digestion process. This was done by sealing cow dung in a big plastic bag. The inoculum brought in microbial diversity in the feed.

2.3.4. Parameters under investigation

Haven brought the previous conditions to as close as possible to optimum, the TS and C/N of the reaction vessels remained the critical and controllable variables that were optimised in our work. The C/N optimised through anaerobic co-digestion with cow-dung while the TS was varied through dilution with distilled water.

2.3.5. Blank batch assays

Biochemical Methane Potential (BMP) tests require a blank and control. The blank was filled with the inoculum, the medium (water), but no substrate to provide the background to biogas and methane generation from the organic material in the inoculum. Another blank set consisting of substrates waste only and the medium was launched to serve as base and compare with the co-digestion and optimized parameters. The control assesses the accuracy of the BMP test using a substrate with a known theoretical methane yield. The control containers usually are filled with inoculum and the control substrate. The control assays were not launch because of lack of an experiment in the literature review with similar operational conditions.

To calculate the theoretical reference methane yield value for the selected control substrate, the Boyle's formula was used for substrates with the help of chemical composition (carbon, hydrogen, oxygen, nitrogen and Sulphur) gotten from literature, section 2.8. While the blank tests are the baseline, the theoretical methane potential corresponds to the maximum attainable production, therefore lower and upper boundaries.

The blank was performed in triplicates for reproducibility of the tests and statistical analysis.

2.3.5.1. Blank parameters

For the blank test, three (03) reactors contained the substrates; pineapple peelings, watermelon rind and banana peelings, mixed with distilled water. Then, cow dung was mixed equally with distilled water. All the reactor contained a waste to water ratio of 1:1.

Data on the daily volume of biogas produced was recorded.

2.3.5.2. Calculations

Given the ratio of waste to water to be a:b, then to get the quantity of waste necessary to feed the batch reactor and the volume of water required, we use the **equation 2.1** and **2.2**;

$$V_w = \frac{b}{a+b}\ x\ V_f \qquad (2.1)$$

$$M_{substrate} = \rho_{substrate}\ x\ \frac{a}{a+b}\ x\ V_f \qquad (2.2)$$

Where:

V_w is the volume of added water;
$M_{substrate}$ is the mass of the substrate;

$\rho_{substrate}$ is the density of the substrate;
V_f is the final volume of the content.

The substrate density was determined prior to the experiment, as explained in section 2.6.4.

2.3.6. Response Surface Methodology - Central Composite Design (CCD)

To find the uncoded value of α, **equation 2.3** was used.

$$uncoded\ value\ of\ \alpha = (coded\ value\ x\ L) + C \quad (2.3)$$

Where: L – length expressed in real units between center points and +1 value of factor;
C – center point value expressed in real units.

Based on previous sets of experimentations done before the start of the CCD, the values of low, center and high levels for the C/N ratio and TS were chosen amongst them. As such, the already existing gap between levels from some of the previous experimentations served to complete **Table 2.3** prior to the CCD.

Table 2.3: Factor level values

	Pineapple peelings (PP)		**Watermelon rind (WR)**		**Banana peelings (BP)**	
Level of factor	C/N ratio	TS in %	C/N ratio	TS in %	C/N ratio	TS in %
-1 (low) = - α	36.68	4.46	35.46	2.26	36.65	2.93
0 (center)	39.50	7.21	36.74	4.99	39.58	5.55
+1 (high) = + α	42.32	9.96	38.02	7.73	42.51	8.18

Appendix 6, were drawn using AutoCAD software version 2020. They illustrate the key elements of the CCD. For every design, we have two (02) factors and each factor has three (03) levels (low, center and high). As for the center point, in the design it has been replicated four (04) times. Each factor level is been encoded from its uncoded value (A and B) into a coded value (x_1 and x_2) that will be utilized in the design analysis. The total number of batch experiments to carry out in the CCD was gotten using **equation 2.4**.

$$N = k^2 + 2k + n \quad (2.4)$$

Where: N – actual number of experiments;
k – number of different factors which were incorporated within the study;

n – number of repetitions of the center points.

In the case of our study, N equaled 13 since k = 2, and n = 5.

A CCD tables were drawn contributing to the planning of the BMP experimentation phase, **Table 2.4**.

Table 2.4: Central composite design table for digestion of pineapple peelings (PP), watermelon rind (WR) and banana peelings (BP)

		Coded		**Real PP**		**Real WR**		**Real BP**	
				C/N	TS (%)	C/N	TS (%)	C/N	TS (%)
Obs	Run	x_1	x_2	A	B	A	B	A	B
1	2	1	-1	42.32	4.46	38.02	2.26	42.51	2.93
2	9	0	0	39.50	7.21	36.74	4.99	39.58	5.55
3	12	0	0	39.50	7.21	36.74	4.99	39.58	5.55
4	10	0	0	39.50	7.21	36.74	4.99	39.58	5.55
5	8	0	1	39.50	9.96	36.74	7.73	39.58	8.18
6	4	1	1	42.32	9.96	38.02	7.73	42.51	8.18
7	13	0	0	39.50	7.21	36.74	4.99	39.58	5.55
8	5	-1	0	36.68	7.21	35.46	4.99	36.65	5.55
9	11	0	0	39.50	7.21	36.74	4.99	39.58	5.55
10	3	-1	1	36.68	9.96	35.46	7.73	36.65	8.18
11	1	-1	-1	36.68	4.46	35.46	2.26	36.65	2.93
12	6	1	0	42.32	7.21	38.02	4.99	42.51	5.55
13	7	0	-1	39.50	4.46	36.74	2.26	39.58	2.93

Obs = Observation

The C/N ratio displayed on **Table 2.4**, is the final ratio after mixing the substrate with the inoculum in the cow dung to substrate ratio of 3:1 (low), 1:1 (center) and 1:3 for (high). While the TS is the result of diluting the biomass with water in different substrate to water ratios to attain the required TS level of the diagram.

To obtain the C/N value after mixing of the substrate and inoculum using the ratios for the low, center and high, we used **equation 2.5** (Municipal Solid Waste Management, 2018).

$$C/N_f = \frac{(M_{CD} x TS_{CD} x C_{CD}) + (M_{substrate} x TS_{substrate} x C_{substrate})}{(M_{CD} x TS_{CD} x N_{CD}) + (M_{substrate} x TS_{substrate} x N_{substrate})} \quad (2.5)$$

Where: $M_{CD}, M_{substrate}$ – Mass of cow dung and substrate respectively on wet basis (g);
$TS_{CD}, TS_{substrate}$ – Total Solids of cow dung and substrate (%);
$C_{CD}, C_{substrate}$ – Percentage concentration of Carbon in cow dung and substrate;
$N_{CD}, N_{substrate}$ - Percentage concentration of Nitrogen in cow dung and substrate;
C/N_f – final Carbon to Nitrogen ratio after mixture of substrate with cow dung.

The percentages of Carbon and Nitrogen used in **equation 2.5** are the results from the proximate and ultimate analysis in section 2.6, analytical methods.

To get the final TS after mixture, **equation 2.6** was used;

$$TS_f = \frac{Dry\ mass}{Total\ mass} * 100 = \frac{(M_{CD} * TS_{CD}) + (M_{substrate} * TS_{substrate})}{M_{CD} + M_{substrate} + (V_w * \rho_w)} * 100 \quad (2.6)$$

Where: V_w – Volume of distilled water in feed (ml)
ρ_w – density of water, 1 g/ml

With the **equations 2.5** and **2.6**, the masses of cow dung, substrates and the volume of water in the feed corresponding to the various points of the FCCD were obtained using the iteration algorithm of the solver tool in Microsoft Excel.

2.3.6.1. Second-order model fitting

After the identification of C/N value and TS as the factors to optimize, a second-order model was fitted to relate these factors to the biogas yield using the central composite design (equation 1.15). The software used to compute the response surface and the associated statistical analysis is Minitab software.

Analysis of variance (ANOVA) was done in order to develop the model. And so was the F test, Lack of fitness, adjusted and predicted R^2 value and adequate precision (S/N > 4) computed. A comparison of the predicted and actual values was done and the model 2D contours and 3D surface were generated.

2.4. SAMPLE COLLECTION

All waste were collected in plastic bags each time they were needed, so no preservation was necessary. Following the supply chain in Cameroon, here are the possible markets in Yaounde where waste was collected in their fresh state;

- Mokolo market;
- Mendong market;
- Accacia Market;
- Etoudi market.

Pineapple waste (peelings) and watermelon waste (rind/exocarp) were collected in their fresh state (wet and undecayed) at wholesaler points at the Mendong market, **Figure 2.3** and **2.4**, located in Yaounde VI. The banana wastes (unripe banana peelings) were equally collected at the Accacia market, precisely where women cook food to sell to the sellers and buyers at the market. The cow-dung from early excretion of cows was collected at the Yaounde slaughter house located at Etoudi district, Yaounde 1. Then, the dung was kept closed in two closed 5L bottles (anaerobic conditions) for a period of 5 days to activate anaerobic digestion microbes. **Figure 2.5** gives a map of the sampling sites for the food waste in Yaounde.

Figure 2.3: Pineapple and watermelon fruit market and waste (A) and cow slaughterhouse at Etoudi (B)

Figure 2.4: Fresh fruit waste at pineapple and watermelon selling points in the Mendong market

To avoid diseases caused by microbes, a pair of gloves was worn throughout the collection and manipulation process. These wastes were brought immediately to the laboratory for analysis and BMP test when needed.

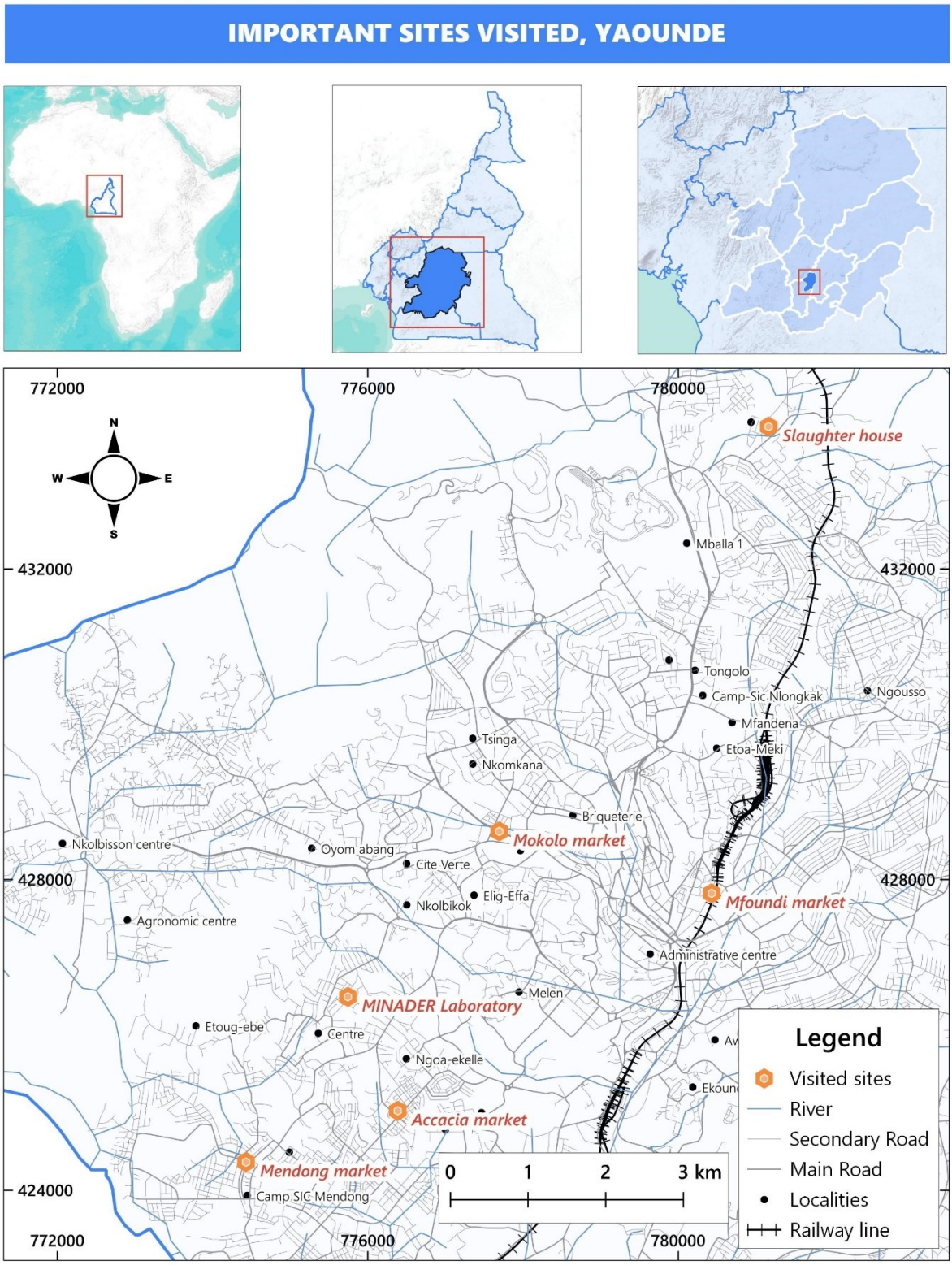

Figure 2.5: Map of important sites visited for waste collection and research study activities

2.5. PREPARATION OF SAMPLES AND PRETREATMENT

All the analysis and treatment were done at the National Laboratory for Diagnosis and Analysis of Agricultural Products and Inputs of the Ministry of Agriculture and Rural Development (MINADER) located at Etoug-ebe district, Yaounde VI.

2.5.1. Proximate analysis and ultimate analysis

For proximate analysis, fresh samples of pineapple peelings, watermelon rind, banana peelings and cow-dung were chopped into small pieces and placed into crucibles of different sizes (for identification of substrates during the analysis), before been analysed for Total Solids (TS), Ash content and Volatile Solids (VS) (**Figure 2.6**).

Figure 2.6: Waste samples prepared for proximate analysis

Meanwhile for ultimate analysis, to use the Walkley and Black method (carbon) and the Kjedahl methods (nitrogen) the waste materials had to be dried to facilitate the analysis. For rapid air drying, the waste material was cut into small pieces of about 2cm large and placed on cardboard and dried in the laboratory at room temperature (to avoid nitrogen volatilisation) for 2 weeks, **Figure 2.7**. After the sample had dried, pounded and sieved with a sieve of 2mm grid, the sample were kept in containers ready for analytical tests, **Figure 2.8**.

Figure 2.7: Cutting up of substrates for air-drying

Figure 2.8: Samples after being air-dried, pounded and sieved

After the drying process, the samples were ground in ceramic crucibles till all the samples became powdery. Then the powder was passed through a 2 mm sieve plate and the powdered particles of less than 2 mm rough size was used for analysis.

2.5.2. Biochemical methane potential

As agreed on section 2.3.3 of design of experiment, the wastes collected were pre-treated by physical means using a laboratory knife milling machine. The fresh substrates were first cut down into smaller pieces of roughly 3 cm large. The cut substrates were further reduced to smaller pieces of approximately 0.5 cm large with the aid of the knife mill *Retsch GM 200* running at a knife rotation speed of 3,000 rpm for about 2 mins in total per substrate, **Figure 2.9**.

Figure 2.9: The knife drilling machine (a), cut waste in preparation for milling (b) and milled waste (c)

2.6. EXPERIMENTAL SETUP

2.6.1. Biochemical methane potential test

2.6.1.1. Description

The reactor (or digester) is a glass container of thickness 0.2 cm, **Figure 2.10**. For every reactor, 20% of the volume, equivalent to 60 mL, was kept for headspace, such that, the final volume V_f of the content sums up to 240 mL.

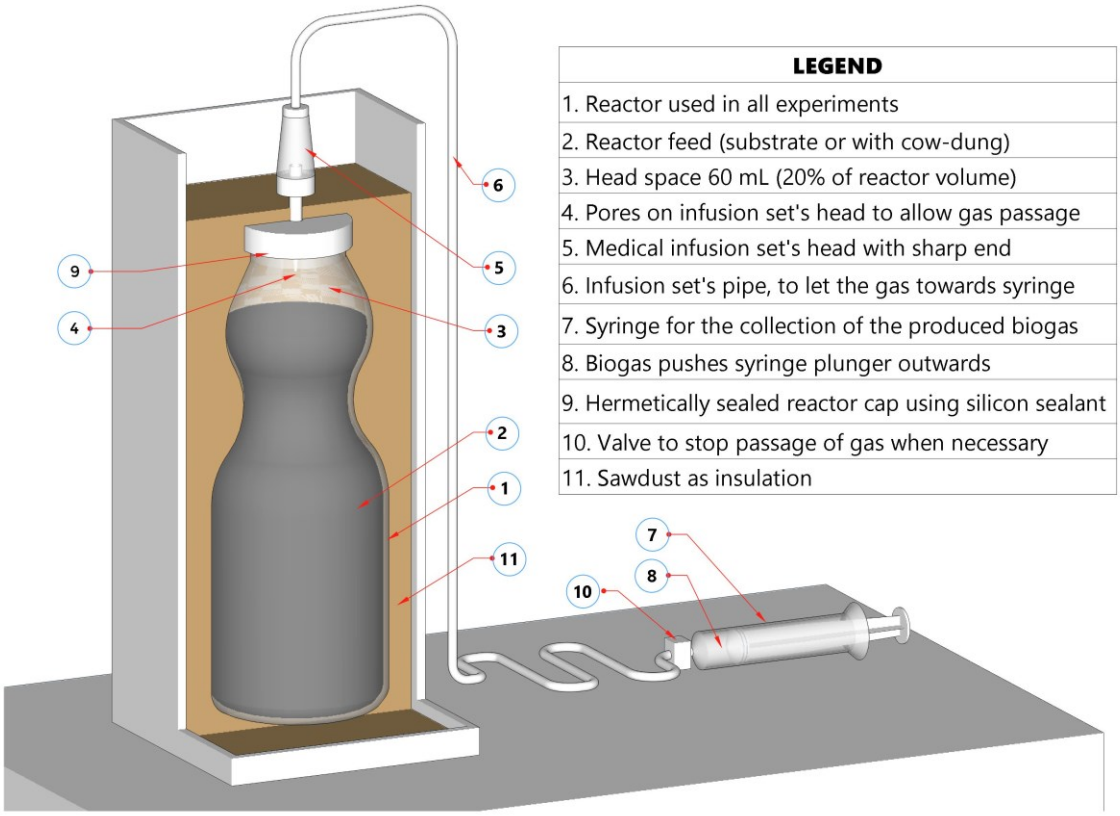

Figure 2.10: Cross section of a bioreactor setup for biochemical methane potential testing

Below are the steps for mounting the setup ready for anaerobic digestion.

- An extra fresco bottle (reactor/digester) was cleaned with soap and water, **Figure 2.11 A**;
- Pre-treatment on the substrates was done using the Retch GM knife mill, **Figure 2.11 B** and **C**;
- Using an analytical balance of precision 0.01 g, different estimated amounts of the pre-treated substrates were measured and fed into the reactor, **Figure 2.12 A** and **B**;

- The measured pre-treated substrates were used to feed the reactors using a funnel, **Figure 2.12 C**.
- Estimated volumes of distilled water using a measuring cylinder, was added to the reactor, **Figure 2.13 A**;
- A hole is burst with the aid of a nail on the lid of the reactor, the infusion set's head was passed through the hole and the epoxy gum epoxy gum was applied on it for sealing and rigidity. Then about 10 mins was allowed for the head set to dry, **Figure 2.13 B**;
- The next step was to close the reactor with its lid. The silicon sealant was used to seal the lid at the intersection point between the lid and the rest of the reactor body. The *PVC pegafort* sealant was used to seal the pressure release valve of the infusion head. Again, at least 30mins was allowed for the whole setup to dry, **Figure 2.13 C**;
- Black plastic package was rapped all over the reactor and attached with a masking tape, **Figure 2.14 A**.
- Then the bottles were placed in buckets and were filled with dried saw dust, **Figure 2.14 B**.
- The content was shaked up and down and rotated vigorously for the content to mix, homogenise and for the case with cow dung, so that the cow dung disperses into the solution;
- At last, the syringes were plugged into the other end of the infusion sets, **Figure 2.15**.

Figure 2.11: Steps of BMP assay formation

Figure 2.12: Steps of BMP assay formation

Figure 2.13: Steps of BMP assay formation

Figure 2.14: Steps of BMP assay formation

Figure 2.15: BMP assays setup

The produced gas from the biochemical reaction in the digester leaves the head space, passes through the holes of the infusion set's head, then through the infusion pipe and reaches the syringe. Once there, the gas causes the movement of the syringe plunger backwards enabling the recording of the quantity of gas produced daily.

2.6.1.2. BMP air tightness

Three zones are sealed with the use of various gums. The blue outlet at the infusion head (**Figure 2.16 E**), the space between the lid and the bottles' neck (**Figure 2.16 F**) and the hole burst to insert the infusion head into the glass bottle (**Figure 2.16 D**).

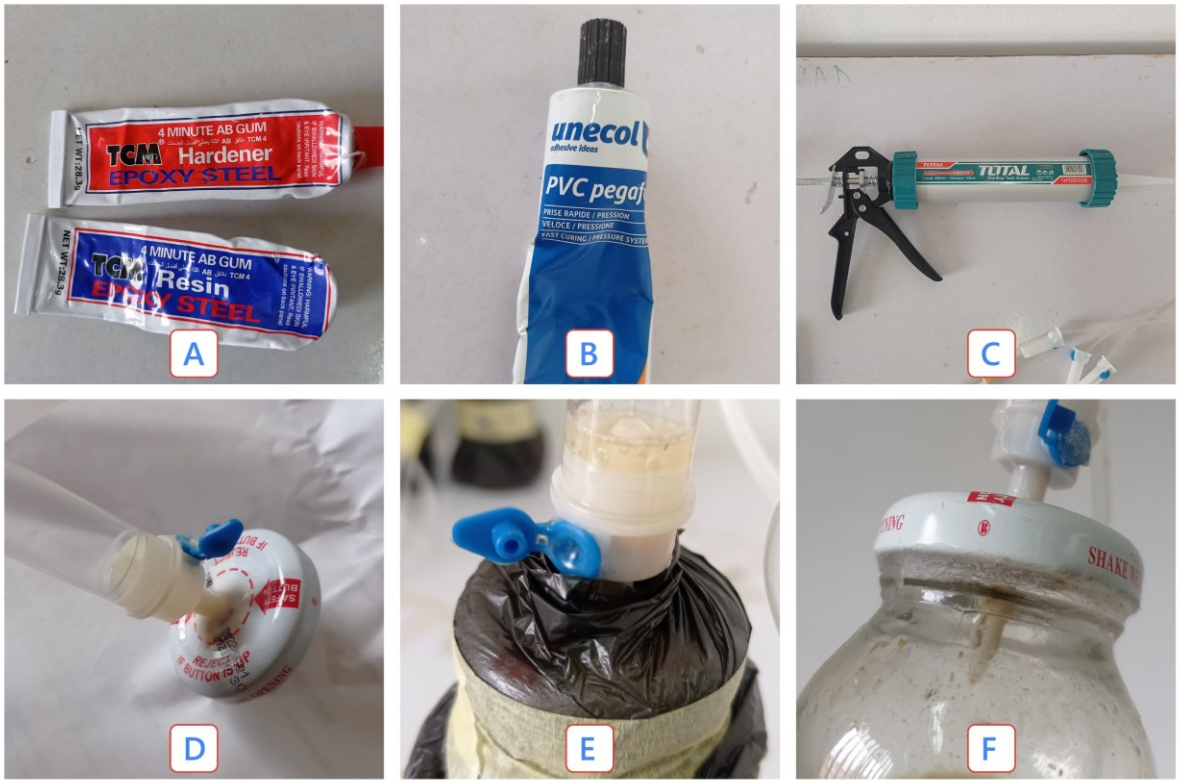

Figure 2.16: Sealing equipment and areas sealed for all batch experimentations

To check air tightness, the Ideal gas principle, $PV = nRT$ helped. If perfectly air tight, the plunger of the syringe returns to its initial point (0 mL) when dragged outwards. If the plunger doesn't return to its original position, then it might indicate that there's leakage in the system. It wasn't always sufficient to just check at the beginning, so, daily monitoring and check-up of the setup for leakage was essential. So, areas of probable leakages were inspected and repaired immediately.

2.6.1.3. Assay identification

The various assays were identified using a wall masking tape colour yellow, **Figure 2.17**. The identification for the experimentations followed the three levels of the C/N and TS were: low (L), center (C) and high (H). The identification code for the central composite design assays was as following; First letter (L, C or H) + second letter (L, C, H). Example: LL or HC. Whereas the identification code for mixtures and mono-digested substrates were simply links between their substrate's abbreviation.

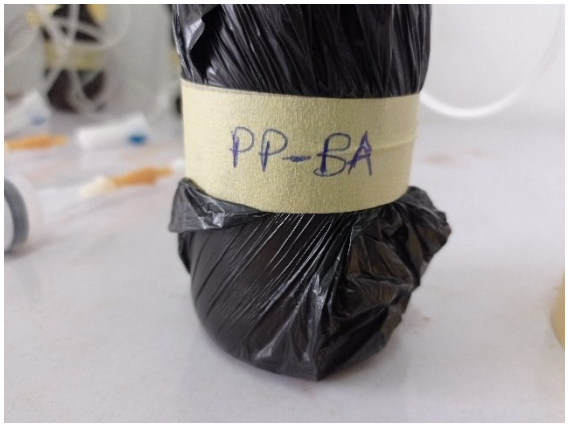

Figure 2.17: Batch experiment identification for mixed substrates

2.6.2. Biogas measurement and yield estimation

2.6.2.1. Method

Measuring the amount of biogas produced daily consisted of reading the value displayed by the syringe, **Figure 2.18**, at regular intervals. The syringes were read every morning and evening. Also, whenever the syringe reached its full possible reading (60 mL), the syringe was unplugged, emptied and plugged again while switching the valve closed.

Figure 2.18: Syringe plugged into the infusion set's end

2.6.2.2. Precautions

- The valve was positioned at the tip of the infusion set to minimize air intake when unplugging and plugging the syringe.
- Since the rate of production of biogas at the beginning of the experimentation was high, a measure undertaken was to make recordings at least 3 times a day.
- When coming in the morning and sometimes noticed that the biogas production had already exceeded the maximum 60 mL readable by the syringe, the first action was to

manually force the syringe back compressing the gas while the valve is open, close the valve, release the plunger, read the corresponding reading, then unplug, empty and plug the syringe back while the valve is still closed and unplug the valve. The gas will cause the plunger to slide back again, then read the additional reading.

The problem when applying this method is the excess pressure accumulated at each measurement that may cause failure at the level of sealant.

If a syringe plunger doesn't move, it may be due to blockage at the hole of the infusion set because of the mixing process. So sometimes it was necessary to force some air into the system to unblocking.

2.6.2.3. Data recording and Anaerobic Digestion efficiency (or biogas yield estimation)

A printed form permitted to record all information. The form was organised in such a way that, at each moment, data on the date, time of recording, value at each syringe together with the code was recorded. Every time data recording was made, a diagnosis of assays was made checking whether the sealants had no leakages.

The data recorded through the form was later inserted in the Excel file which had been prepared for automation of calculations of biogas yield of all the experimental assays. In order to calculate the biogas yield for each experiment, **equation 2.7** was used taking into account the total volatile solids contributed by each substrate and/or cow dung in **equation 2.8**.

$$Biogas\ yield\ (mL/g\ V) = \frac{Cumulated\ volume\ of\ biogas\ (ml)}{Total\ Volatile\ Solids\ (g)} \qquad (2.7)$$

$$Total\ Volatile\ Solids\ (g) = VS_1(\%)\ x\ M_1 + VS_2(\%)\ x\ M_2 + VS_3(\%)\ x\ M_3 \qquad (2.8)$$

Where: VS_i – Volatile solids content of substrate feeded (%)

M_y – Mass of substrate y feeded (g)

2.6.3. Methane production estimation

In the absence of a gas chromatograph, the methane yield was estimated (**equation 2.9**) assuming that the minimum yield as a fraction of the biogas yield is 60% (Akunna, 2018; Filer et al., 2019; Voegeli, 2014).

$$min\ Methane\ yield\ (mL/g\ VS) = 0.6\ x\ biogas\ yield\ (mL/g\ VS) \quad (2.9)$$

2.7. ANALYTICAL METHODS

2.7.1. Proximate Analysis

2.7.1.1. Procedure for proximate analysis

The analysis of total solids (TS), ash and Volatile solids (VS) were done following standard methods (APHA, 2015) in duplicates for all four samples.

First, the four (04) crucibles were placed in a muffle furnace (**Figure 2.19 B**) at 550 °C for 15 minutes;

- Using oven gloves, the crucibles were cooled in a desiccator (**Figure 2.19 C**) and weighted (P);
- Given quantities of the four (04) fresh/wet substrates were placed into the crucibles and again, the loaded crucibles were weighed (C + S wet, Q);
- The weighed Crucible + Substrate were placed in an oven (**Figure 2.19 A**) at 105 °C for 24 hours;
- The crucibles were then removed from the oven, placed into a desiccator for cooling. Once cooled, the crucible and its content were weighed, C + S dried, 105 °C, (R);
- Then, the weighed crucibles were placed in a muffle furnace and ignited to 550 °C for 1 hour;
- Finally, the crucibles were removed from the furnace and weighed, C + Ash, 550 °C, S.

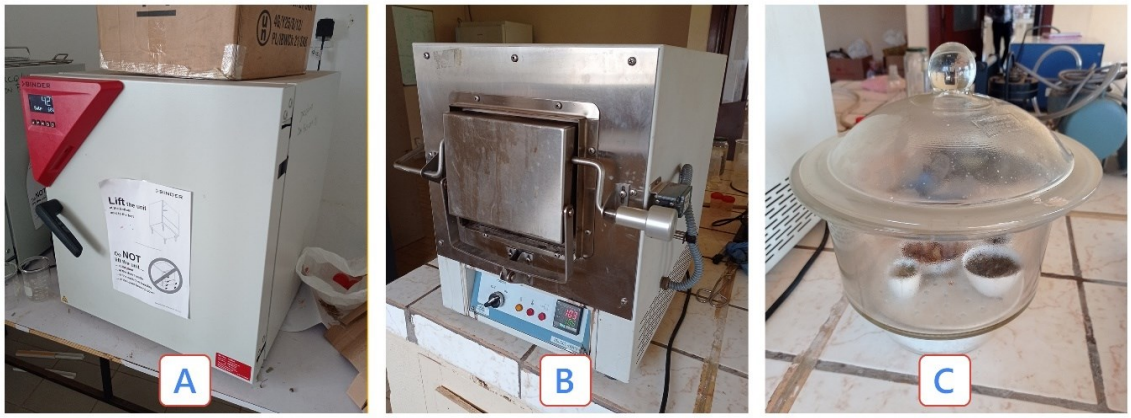

Figure 2.19: Oven (capacity 120 °C) (A), muffle furnace (capacity 600 °C) (B) and desiccator (C)

2.7.1.2. Calculations

The results of the proximate analysis were computed using the **equation 2.10, 2.11** and **2.12**.

$$TS\ [g/kg\ wet] = \frac{R-P}{Q-P}\ x\ 1000\ \ |\ \ TS\ [\%\ wet] = \frac{R-P}{Q-P}\ x\ 100 \qquad (2.10)$$

$$Ash\ [g/kg\ wet] = \frac{S-P}{Q-P}\ x\ 1000\ \ |\ \ Ash\ [\%\ wet] = \frac{S-P}{Q-P}\ x\ 100 \qquad (2.11)$$

$$VS\ [g/kg\ wet\ ] = TS - Ash\ \ |\ \ VS\ [\%\ wet] = TS\ [\%] - Ash\ [\%] \qquad (2.12)$$

Where:

P = weight of the crucible in grams

Q = weight of the crucible + wet sample in grams

R = weight of crucible + dried sample at 105 °C for 24 hours in grams

S = weight of the crucible + ash at 550 °C in grams.

2.7.2. Ultimate Analysis – determination of Carbon content

The Walkley and Black Method was used for the measurement of the Total Organic Content of each substrate.

2.7.2.1. Concept

The determination of organic carbon is based on the Walkley & Black chromic acid wet oxidation method. Oxidizable organic carbon in the organic material is oxidised by 1 M potassium dichromate ($K_2Cr_2O_7$) solution in concentrated sulfuric acid. The heat of the reaction raises the temperature which is sufficient to induce substantial oxidation.

$$2Cr_2O_7^{2-} + 3C^0 + 16H^+ \leftrightarrow 4Cr^{3+} + 3CO_2 + 8H_2O$$

The $Cr_2O_7^{2-}$ reduced during the reaction with organic material is proportional to the oxidisable organic Carbon present in the sample. The organic carbon can then be estimated by measuring the remaining unreduced dichromate by back-titration with ferrous sulphate or ammonium ferrous sulphate using diphenylamine as an indicator.

$$6Fe^{2+} + Cr_2O_7^{2-} + 14H^+ \leftrightarrow 2Cr^{3+} + 6Fe^{3+} + 7H_2O$$

2.7.2.2. Procedure

- The samples were weighted for the analysis: 0.0110 g for cow dung, 0.0146 for banana peelings, 0.0152g for watermelon rind and 0.1700 g for pineapple peelings. Then each weighted sample was placed into an Erlenmeyer flask.
- 10mL of 1 M $K_2Cr_2O_7$ was added into the flask and swirled gently to disperse the sample in the solution.
- Then with care, 20mL of concentrated H_2SO_4 was added, directing the steam produced away from the experimenter. The reaction was exothermic so was carried out with the flask submerged into water for cooling and avoiding the flask to break.
- Immediately after the addition, the flask was gently swirled again until the sample and the reagents were mixed, then more vigorously for a total of 1 min.
- The flask was then allowed to stand on an insulated sheet for 30 minutes.
- Next, 200mL of water was added to the flask.
- Then, 10mL of 98% H_3PO_4 added.
- The indicator used was barium diphenylamine sulfonate (10 droplets) and the solution was titrated with 0.5 M $FeSO_4$ solution on top of a magnetic agitator.
- After the end point was reached, the percentage of total carbon was calculated.

Figure 2.20: Addition of diphenylamine droplets to the test solutions (A) and Titration of solution with $FeSO_4$ (B)

2.7.2.3. Calculations

The **equations 2.13** to **2.16** are the steps which permitted the come up with the final equation for the estimation of the carbon content of the samples. **Equation 2.16** being the final equation that helped to estimate the quantity of organic carbon per gram of sample.

Concentration of $FeSO_4.7H_2O$:

$$M_F = \frac{M_K \, x \, V_K}{V_F} \qquad (2.13)$$

Where: $\boldsymbol{M_F}$ – molar concentration of iron sulphate

M_K – molar concentration of potassium dichromate

$V_{F,C}$ – volume of iron sulphate added to the control vessel

V_K – volume of potassium dichromate

Number of mEq and mg of organic carbon (OC) oxidated by potassium dichromate:

$$10\ mEq - \left(\frac{10}{V_f} n \, x \, V_{F,S} \, ml\right) = \frac{10(V_{F,C} - V_{F,S})}{V_{F,C}}\ mEq \qquad (2.14)$$

$$\frac{10(V_{F,C} - V_{F,S})}{V_{F,C}} mEq \ x \ \frac{3\ mg\ OC}{mEq} = \frac{30(V_{F,C} - V_{F,S})}{V_{F,C}}\ mg\ OC \qquad (2.15)$$

Where: $V_{F,S}$ – Volume of iron sulphate added to the sample vessel

P – Sample weight (g)

Concentration of OC in mg/g:

$$\frac{30(V_{F,C} - b)}{V_{F,C}}\ mg\ OC \ x \ \frac{4}{3} \ x \ \frac{1}{P\ g\ of\ substrate} = \frac{40(V_{F,C} - V_{F,S})}{V_{F,C}\ x\ P} = mg\frac{OC}{g} of\ sample \qquad (2.16)$$

2.7.3. Ultimate analysis – determination of nitrogen content

2.7.3.1. Concept

Nitrogen content by the Kjeldahl Method. This method is used to determine the nitrogen content of organic and inorganic samples and it involves three major steps; Digestion, distillation and titration.

- Digestion

The aim of the digestion procedure is to break all nitrogen bonds in the sample and convert all of the organically bonded nitrogen into ammonium ions (NH4+). Organic carbon and hydrogen forms Carbon dioxide and water.

$$\text{Sample (protein -}\mathbf{N}) + H_2SO_4 \rightarrow (\mathbf{N}H_4)_2SO_4 + CO_2 + H_2O$$

After digestion is completed, the sample is allowed to cool to room temperature, then diluted with water and transferred to the distillation unit.

- Distillation

During the distillation step, the ammonium ions (NH_4^+) are converted into ammonia (NH_3) by adding alkali (NaOH). The ammonia (NH_3) is transferred into the receiver vessel by means of steam distillation.

$(NH_4)_2SO_4 + 2NaOH \rightarrow 2NH_3$ (gas) $+ Na_2SO_4 + 2H_2O$

The receiving vessel for the distillate is filled with an absorbing solution in order to capture the dissolved ammonia gas.

- Common absorbing solutions involve aqueous boric acid [$B(OH)_3$] of 2-4% concentration. The ammonia is quantitatively captured by the boric acid solution forming solvated ammonium ions.

$B(OH)_3 + NH_3 + H_2O \rightarrow NH_4^+ + B(OH)_4^-$

- Titration

The concentration of the captured ammonium ions can be determined using two types of titrations:

When using the boric acid solution as the absorbing solution, an acid-base titration is performed using standard solutions of sulfuric acid or hydrochloric acid and a mixture of indicators. Depending on the amount of ammonium ions present, concentrations in the range of 0.01 M to 0.5 M are used. Alternatively, the end point can be determined potentiometrically with a pH-electrode. This titration is called direct titration.

$B(OH)_4^- + HX \rightarrow X^- + B(OH)_3 + H_2O$

2.7.3.2. Procedure

- To 2 g of air-dried and ground sample was added 2 tablets of potassium sulphate and 20 mL of concentrated H_2SO_4.
- Then the digestion stage: the mixture was heated for 30 minutes at ~ 350 ºC.
- Afterwards the solution was cooled down to about 50 ºC and diluted with 20 mL distilled water.
- Then the distillation stage: the digested samples was placed in digestion tubes to the distilling unit and 10 mL of 35% (w/v) NaOH was added. The sample was distilled until 100mL of distillate were collected in 25 mL of 4% (w/v) boric acid.

- Finally, the titration stage: 3 drops indicator were added to the flask and titrated with 0.1M HCl.

2.7.4. Estimation of the density of substrate

The Archimedes' Principle which states that when an object is submerge in water (or any fluid), the force it experiences is equal to the mass of the water displaced times gravity. The water displacement method was used to determine the densities of the substrates and was done in triplicates. Using **equation 2.17** the densities of pineapple peelings, watermelon rind, banana peeling and cow dung;

$$\rho_S(g/ml) = \frac{m_S}{V_f - V_i} \qquad (2.17)$$

Where: ρ_S – density of substrate or cow dung (g/ml)
m_S – mass of substrate or cow dung (g)
V_i – initial volume before submerging the substrate in measuring cylinder (ml)
V_f – final volume before submerging the substrate in measuring cylinder (ml)

2.8. THEORETICAL BIOCHEMICAL METHANE POTENTIAL

2.8.1. Method

With knowledge of the chemical composition of a waste the quantity of methane can be predicted from stoichiometric formula developed by Buswell and Hatfield in 1936 (Achinas & Euverink, 2016), **equation 2.18**.

$$C_xH_yO_z + \left(x - \frac{y}{4} - \frac{z}{2}\right)H_2O \rightarrow \left(\frac{x}{2} + \frac{y}{8} - \frac{z}{4}\right)CH_4 + \left(\frac{x}{2} - \frac{y}{8} + \frac{z}{4}\right)CO_2 \qquad (2.18)$$

Boyle's modified chemical reaction (**equation 2.19**) of Buswell and Mueller (1952) and included nitrogen and sulfur to obtain the fraction of ammonia and hydrogen sulfide in the produced biogas, (Achinas & Euverink, 2016):

$$C_aH_bO_cN_dS_e + \left(a - \frac{b}{4} - \frac{c}{2} + \frac{3d}{4} + \frac{e}{2}\right)H_2O \rightarrow \left(\frac{a}{2} + \frac{b}{8} - \frac{c}{4} - \frac{3d}{8} - \frac{e}{4}\right)CH_4 + \left(\frac{a}{2} - \frac{b}{8} + \frac{c}{4} + \frac{3d}{8} + \frac{e}{4}\right)CO_2 + dNH_3 + eH_2S \qquad (2.19)$$

Where;

$$a = \frac{SR_C}{A_C} = \frac{SR_C}{12.0107} \qquad b = \frac{SR_H}{A_H} = \frac{SR_H}{1.0079} \qquad c = \frac{SR_O}{A_O} = \frac{SR_O}{15.999}$$

$$d = \frac{SR_N}{A_N} = \frac{SR_N}{14.0067} \qquad e = \frac{SR_S}{A_S} = \frac{SR_S}{32.065}$$

SR = Stoichiometric ratio with respect to $C_aH_bO_cN_dS_e$.

The values of the C and N (in grams) will be gotten through the Carbon content analysis by Walkley and black method, while the Nitrogen content will be gotten from the results of the Kjedahl analysis. The other elements; H, O and S will be gotten from literature review.

Hence to get the Theoretical/Predicted biochemical potential of the substrate, **equation 2.20** is computed (Achinas & Euverink, 2016);

$$TBMP\ (mL\ CH_4 gVS^{-1}) = \frac{22.4\ x\left(\frac{a}{2}+\frac{b}{8}-\frac{c}{4}-\frac{3d}{8}-\frac{e}{4}\right)}{12.017a+1.0079b+15.999c+14.0067d+32.065e} \qquad (2.20)$$

Assumptions related to the formula are;

- Constant temperature and perfect mixing;
- Ideal bacterial condition, meaning full digestion;
- Input waste consists of only C, H, O, N and S;
- Products of the reaction include only CH_4, CO_2, NH_3 and H_2S;
- No accumulation of ashes.

2.8.2. Collection of secondary data

In the absence of an elementary analyser, experiments as mentioned in sections, 2.6.2 and 2.7.3. were carried out to obtain only the Carbon and the Nitrogen content. Data about the other elements was collected through a search in the internet. The collected data served in the estimation of the theoretical biogas yield.

2.9. KINETIC MODELLING

2.9.1. Concept

For the kinetic model, the first-order model and modified Gompertz equation was used for all the BMP test using a simple regression method. Considering that all the substrates are rich in cellulose and hemicellulose, therefore not readily biodegradable, the approximation of hydrolysis as the rate-limiting step appears to be realistic (Girotto et al., 2021).

The first-order model, **equation 2.21**,

$$G(t) = G_0(1 - e^{-kt}) \qquad (2.21)$$

Where: G(t) is the cumulative biogas yield at time t (d), (m^3/t VS),
G_0 is the biogas potential of the substrate (m^3/t VS),
K is biogas production rate constant (d^{-1}), (first order disintegration rate constant).

The Gompertz model, **equation 2.22**,

$$G(t) = G_0 \left(e^{-e^{\frac{e*R_{max}}{G_0}(\lambda - t)+1}} \right) \quad (2.22)$$

Where: $G(t)$ is the cumulative biogas yield at time t (d), (m^3/t VS),

R_{max} is the maximum biogas production rate (m^3/t VS/d),

λ is the lag phase (d), the time needed by micro-organism to adapt to the new substrate and begin exponential growth.

e is the exp(1) = 2.7183.

The software MATLAB R2019a was used for the analysis. The software's curve fitting tool helped to compute the non-linear fitting, minimising the value of the Residual Sum of Squares (RSS) and predict the values of G_0, R_{max} and λ. Since G_0, was also gotten through the stoichiometric equation for methane production in 2.7 above, a comparison with the curve fitting value was observed.

2.9.2. Procedure

The following are the steps that was used to generate the curve fitting of an experiment. The procedure was repeated for all the experiments.

- The MATLAB software was opened and variables were created for all data. The vector variable "day" was created for data containing information about the number of days. Then, using the assay identification notation for the set and experiments as mentioned in 2.5.1.3, data was stored in variables named accordingly;
- The custom equation was selected in the field for model equation selection and the first order equation [G*(1-exp(-k*x))] was inserted for the first calculation round while the modified Gompertz equation [G*exp(-exp((Rmax*exp(1)*(lambda-x)/G)+1))] was used for the second round. Where x is the replacement variable for the variable day;
- After MATLAB had identified the various variables in the equation, we defined the starting point, minimum value and maximum values of the variables G, R_{max} and lambda for the case of Gompertz and variable k for the case of first order equation, **Table 2.5**;
- After the definition of boundary of variables and starting point, the fit button was pressed for fitting curve computation.

- Then, back on the MATLAB workspace, the *plot, fplot* and the function creation function helped to create all the graphs for visual appreciation of the fits.

Table 2.5: Fit options in MATLAB's curve fitting tool

Variable	Start Point	Lower boundary	Upper boundary
k	0.02	0.01	Inf
G	100	0	Inf
Rmax	10	0	Inf
lambda	0.02	0.01	Inf

As results, together with the graph showing the fitted curve and the experimental data points, we have the values of the goodness of fit: Residual Sum of Squares (RSS), R-square, Adjusted R-square and the Root Mean Squared Error (RMSE).

CHAPTER 3 . RESULTS AND DISCUSSION

This chapter has four (04) main parts; the chemical and physical description of the substrates and inoculum, the estimated theoretical methane yield and the BMP test results. These results aim at helping us understand how cow dung as an inoculum enhances the anaerobic digestion of the substrates in both the kinetics (first-order and modified Gompertz model) and the biogas yield (second-order model, RSM).

3.1. PHYSICAL AND CHEMICAL CHARACTERISTICS OF THE SUBSTRATES AND INOCULUM

The proximate characterisation of the substrates and the inoculum is shown in **Table 3.1** while in **Table 3.2** are the densities of the substrates. The analysis showed that Pineapple peelings (PP) have total solids (TS) of 149.78 g/kg, ash content of 24.56 g/kg and volatile solids (VS) of 125.21 g/kg with an average density of 1.013 g/ml. Watermelon rind (WR) was constituted of total solids of 69.56 g/kg, ash content of 15.75 g/kg and volatile solids of 53.81 g/kg with an average density of 0.850 g/ml. The Banana peelings (BP) were made of total solids of 114.34 g/kg, ash weight of 9.87 g/kg and volatile solids of 104.48 g/kg with an average density of 0.817 g/ml. The physical constituents of the inoculum (cow dung (CD)) have total solids of 202.25 g/kg, ash weight of 72.10 g/kg and volatile solids of 130.15 g/kg with an average density of 0.835 g/ml.

Table 3.1: Results of the proximate analysis of the substrates

Crucible ID	Crucible (g) (P)	C + S (wet) (g) (Q)	C + S (dried) (g) (R)	C + Ash (g) (550 °C) (S)	TS g/kg wet (T)	Ash g/kg wet (U)	VS g/kg (T – U)
PP 1	22.61 ±0.13	38.89 ±11.88	25.04 ±1.85	23.02 ±0.42	149.78 ±2.14	24.56 ±0.19	125.22 ±2.33
WR 1	12.34 ±0.03	22.12 ±1.98	13.02 ±0.11	12.49 ±0.01	69.56 ±0.37	15.75 ±0.05	53.81 ±0.33
BP 1	12.38 ±0.01	19.38 ±1.06	13.18 ±0.13	12.45 ±0.01	114.35 ±0.63	9.87 ±0.08	104.48 ±0.7
CD 1	16.02 ±0.01	24.55 ±0.72	17.74 ±0.15	16.63 ±0.06	202.26 ±0.17	72.11 ±0.06	130.15 ±0.12

Table 3.1 shows that WR has the lowest TS, so, the highest moisture content. It also has the lowest amount of organic material. Then we have BP and PP which follows the trend up to CD with the lowest moisture content and the highest organics content. These results can be acceptable as it is generally known of fruits to contain more water content than the majority of organic materials. The values of TS and VS are similar to previous research works (Achinas et al., 2019; Aragaw et al., 2013)

Table 3.2, indicates that most substrates and inoculum, except for pineapple peel, are less dense than water (1 g/ml). As a result, most of the substrate elements was moved upwards by water, resulting in a lower water layer and an upper substrate layer. Thus, this reinforces the need to agitate at an adequate frequency.

Table 3.2: Density of substrates and cow dung

Sample ID	Density (g/ml)
PP	1.013 ± 0.102
WR	0.850 ± 0.156
BP	0.817 ± 0.052
CD	0.835 ± 0.107

The partly performed ultimate analysis in **Table 3.3**, revealed that even though the inoculum has the highest amount of organic material, it possesses the lowest Carbon/Nitrogen (C/N) ratio compared to the substrates. In descending order, the C/N ratio of Banana peelings (BP), Pineapple peeling (PP) and Watermelon rind (WR) were 53.73, 51.19 and 46.43 respectively. The trend in C/N appears to be right, as many researchers say that cow dung has a low C/N ratio (Zareei & Khodaei, 2017). The values for PP, BP and WR are in phase with previous research works (Aili Hamzah et al., 2020).

Table 3.3: Partly performed ultimate analysis' results

Element/Substrate	PP	WR	BP	CD
Carbon	52.21	52.47	60.18	63.47
Nitrogen	1.02	1.13	1.12	1.83
C/N ratio	**51.19**	**46.43**	**53.73**	**34.68**

3.2. THEORETICAL BIOGAS POTENTIAL ESTIMATION

From the physicochemical parameters of the substrates and inoculum, using Boyle's modified chemical reaction and formula, the maximum possible methane yield (methane potential) of the substrates and inoculum was estimated. The data used to compute these potentials was obtained from scientific articles (ECN & TNO, 1998; Fajobi et al., 2022; Kabenge et al., 2018), **Table 3.4**.

Table 3.4: Theoretical Biochemical Methane Potential (TBMP) of substrates and inoculum

Substrate	PP	WR	BP	CD
Carbon	47.30	N/D	35.65	43.08
Hydrogen	6.03	N/D	6.19	7.87
Oxygen	40.93	N/D	45.94	47.06
Nitrogen	1.13	N/D	1.94	1.53
Sulphur	0.21	N/D	0.002	0.46
C/N ratio	**41.86**	**N/D**	**18.38**	**28.16**
Reference	(ECN & TNO, 1998)	N/D	(Kabenge et al., 2018)	(Fajobi et al., 2022)
TBMP (mL CH_4/g VS)	**479.27**	**N/D**	**369.99**	**445.66**

N/D: No data found.

Not much information is available on the ultimate analysis of the substrates. But at least elementary composition for PP, BP and CD were found. **Table 3.4** suggest that rather than CD being the lowest in C/N, BP has the lowest. Firstly, the gap between C/N value gotten from ultimate analysis (**Table 3.3**) is large as all values from literature are lower. Secondly, despite the variation in the values of C/N, the expected methane yield (TBMP) does not differ a lot (PP and CD). This might be explained by the fact that the amount of available nitrogen in CD and BP balances with the corresponding amount of carbon in such a way that the stoichiometric equation balances and equalise with the TBMP of PP.

3.3. ANAEROBIC DIGESTION - BLANK ASSAYS

These assays are the first set of assays launched for baseline establishment and comparison with the yield of co-digestion assays. The order of presentation is as follows; the BMP results followed by the kinetic analysis of the BMP assays.

3.3.1. BMP experiments

As specified in section 2.4.3, the blank assays (samples without the inoculum) were subjected to initial parameters; temperature insulation with saw dust, manual shaking of two times a day, knife milling to a particle size of less than 1cm large, no pH regulation and a waste to water ratio of 1:1.

From **Table 3.5** and **Figure 3.1**, the BMP shows that the CD produces the highest biogas yield of 49.3 mL/g VS. PP equally gave a reasonably high biogas yield of 25 mL/g VS. Meanwhile, BP and WR showed the worst performance with biogas yields of 5.7 mL/g VS and 6.6 mL/g VS respectively.

Table 3.5: BMP results of blank assays

Substrate	F/W Ratio a (Feedstock)	F/W Ratio b (Water)	Substrate density (g/mL)	Water (mL)	Substrate mass (g)	VS content (g)	Biogas yield (mL/g VS)
PP	1	1	1.013	120.0	121.57	15.02	25.4
BP	1	1	0.817	120.0	98.04	10.19	5.7
WR	1	1	0.850	120.0	101.97	5.51	6.6
CD	1	1	0.834	120.0	100.14	13.02	49.3

According to the literature, the pH of PP is between 3.24 and 3.84 (Roha, 2013), that of WR is 5.39 (Zabala & Goles, 2021) while for BP is 9.91 (Stephen, 2016). Indicating that pineapple peelings are acidic, the watermelon rind is equally acidic but half as acidic as the pineapple peelings and the banana peelings are basic but not too far from neutral pH. Given that the anaerobic digestion performs better in the neutral pH zone of 6.5 – 7.8 (Hartmann & Ahring, 2006), the WR followed by BP mono-digestion should have yielded better amongst the substrates. Instead, **Table 3.5** reveals an opposite behaviour with the less conducive pineapple peelings producing the best yield and the more conducive WR and BP displaying the worst performance.

Results from **Table 3.5** also gives another important information, the biodegradability of the substrates. Except for PP, the other substrates despite their high values of TBMP, their real biogas yield is very small. Yet, CD which already possessed anaerobes after incubation for a period of 5 days, observed a constant increase in biogas production, **Figure 3.1**.

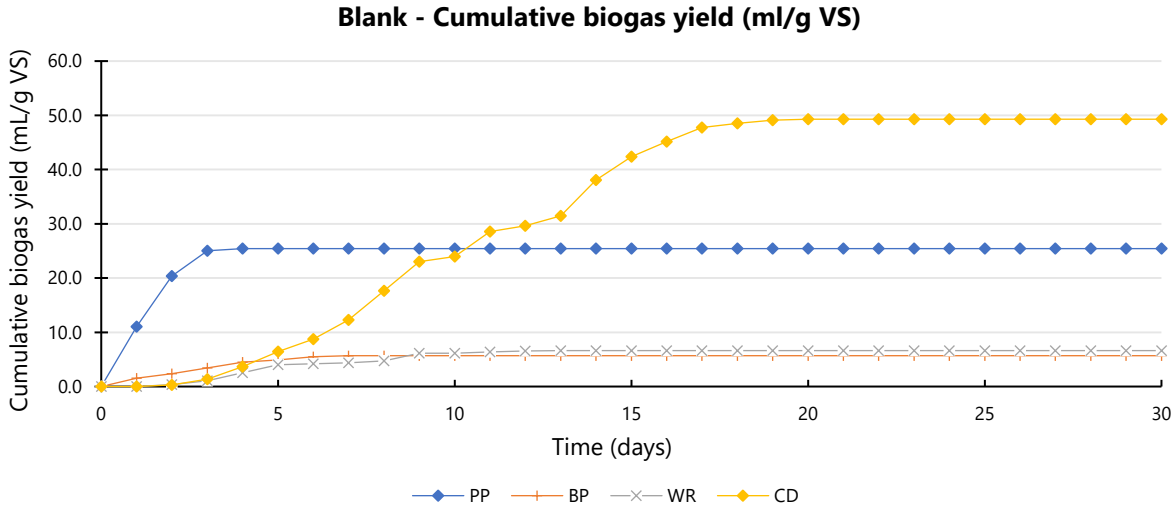

Figure 3.1: Cumulative biogas yield for BMP batch experimentations of the blank assays

PP reached its maximum yield the earliest meanwhile CD reached its maximum yield on day 20, **Figure 3.1**.

3.3.2. Kinetic modelling results

The first-order model coefficients Go and k obtained through fitting with a difference between predicted and measured biogas yield ranging from 46.27% to 0.71%. The first-order model allowed getting the hydrolysis constants k (rate-determining step) for the substrates. Cow dung has the lowest value of 0.05 d^{-1}, as the hydrolysis phase takes the longest time. Then followed by watermelon and banana peels with 0.15 d^{-1} and 0.35 d^{-1} respectively. The highest hydrolysis constant was gotten from pineapple peelings, showing that the biochemical reaction in the pineapple feed is the fastest.

Table 3.6: Kinetic model of the blank assays

	First-order model			Modified Gompertz model			
Sample	G_0 (mL/gVS)	K (d^{-1})	R^2	G_0 (mL/gVS)	λ(d)	Rmax (mL/gVS/d)	R^2
PP	25.22	0.7532	0.9843	25.12	0.2373	13.89	0.9985
WR	7.096	0.1513	0.9368	6.727	1.6790	1.004	0.9884
BP	5.768	0.3513	0.9810	5.721	0.1077	1.288	0.9925
CD	72.11	0.0455	0.9215	49.3	4.218	4.437	0.9917

In **Table 3.6**, λ and R_{max} parameters were estimated using the modified Gompertz model. The lag phase period is mainly influenced by the initial concentration of microorganisms,

substances stimulating the growth of bacteria, and acclimatisation of the inoculum to the substrate (Girotto et al., 2021). In the present batch experiment for the blanks, no acclimation procedure was included. A short λ was observed for BP and PP with 0.11 d and 0.24 d respectively. The longest duration for bacteria acclimatisation was noted at CD with a λ equals 4.218, since it had already been incubated under anaerobic conditions for a period of 5 days. The maximum biogas production rate R_{max} was highest in PP with 13.89 mL/g VS/d. The values of R^2 were calculated as statistical indicators proving the optimal correlation of both models to the case of study.

Figure 3.2 and **Figure 3.3** are the graphs of the fitted models.

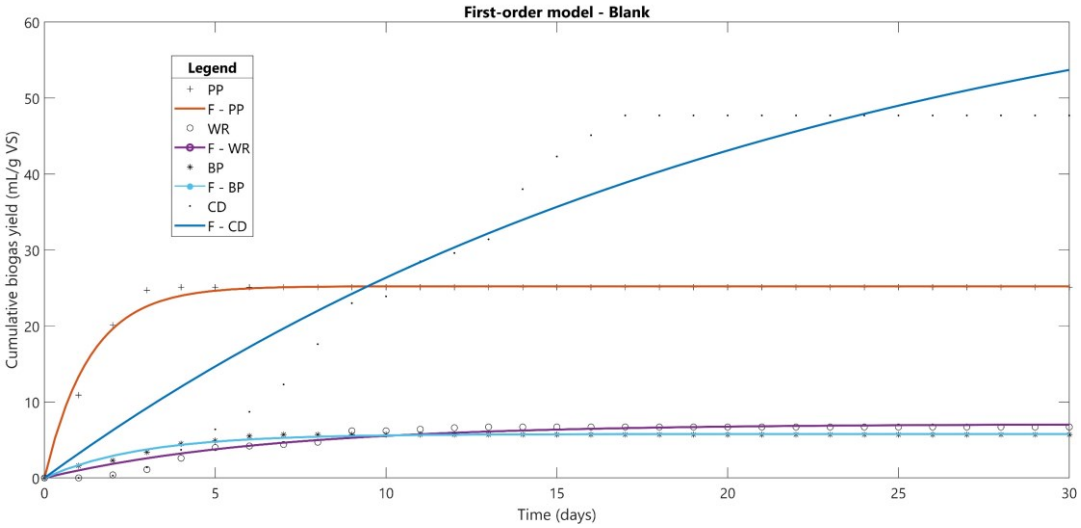

Figure 3.2: First-order model for blanks

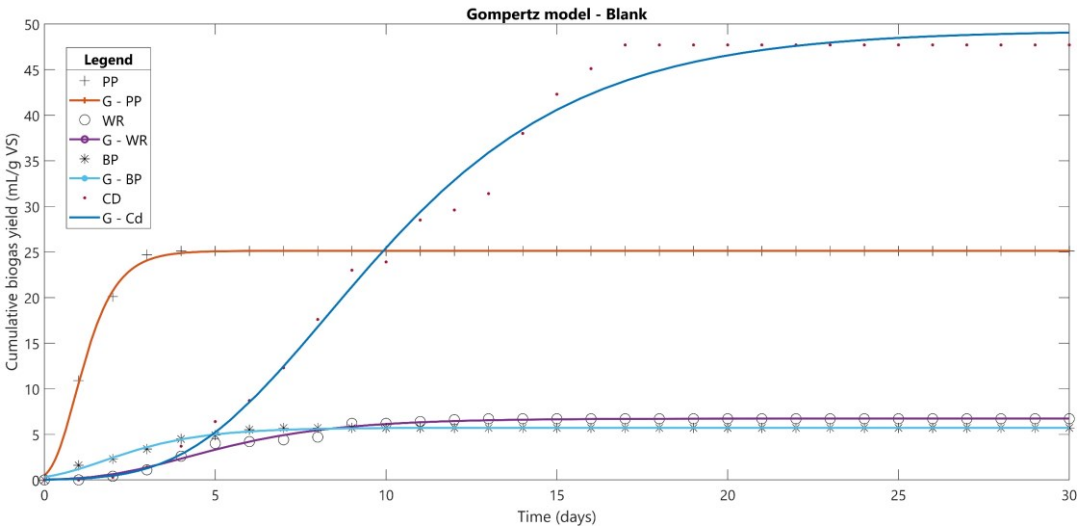

Figure 3.3: Gompertz model for blanks

After the blanks has been studied, the optimization process of the substrates in the co-digestion followed. The results are presented in the following sections.

3.4. ANAEROBIC CO-DIGESTION WITH COW DUNG

As in section 3.3 results of the biogas yield of all three (03) substrates are presented, followed by kinetic modelling. In addition to that, we have the results of the response surface methodology used for optimisation using Face-centered Central Composite Design (FCCD).

3.4.1. BMP batch experiments' results

Appendix 8, **Appendix 9** and **Appendix 10** present the volumes of water, mass of cow dung and mass of substrates which together constituted the feed in all co-digestion experiments. Also, as required in a CCD, the value of independent variables A (C/N ratio) and B (TS), that is, the two factors investigated, were displayed with their corresponding cumulative biogas produced and biogas yield. Our response in this case was biogas yield.

3.4.1.1. Pineapple peeling (PP) in co-digestion with cow dung

Thirteen (13) experimental runs were generated at different operating conditions of C/N and TS. The operation conditions were the same as in the blank with the only difference being the inoculum in co-digestion with the substrates. **Appendix 8** show the results of the batch experimentation set for pineapple peelings. From the results, the feed containing the high level (H) of C/N and the center level (C) of TS produced the highest yield, 74.8 ml/g VS. Another configuration as high as that of HC was LC. This point is completely at opposite ends of the CCD cube denoting a possibility of good biogas produced both in I/S ratio of 3:1 and that of 1:3 with the TS varying around the center level. The lowest yield was gotten from CH configuration with 45.4 ml/g VS.

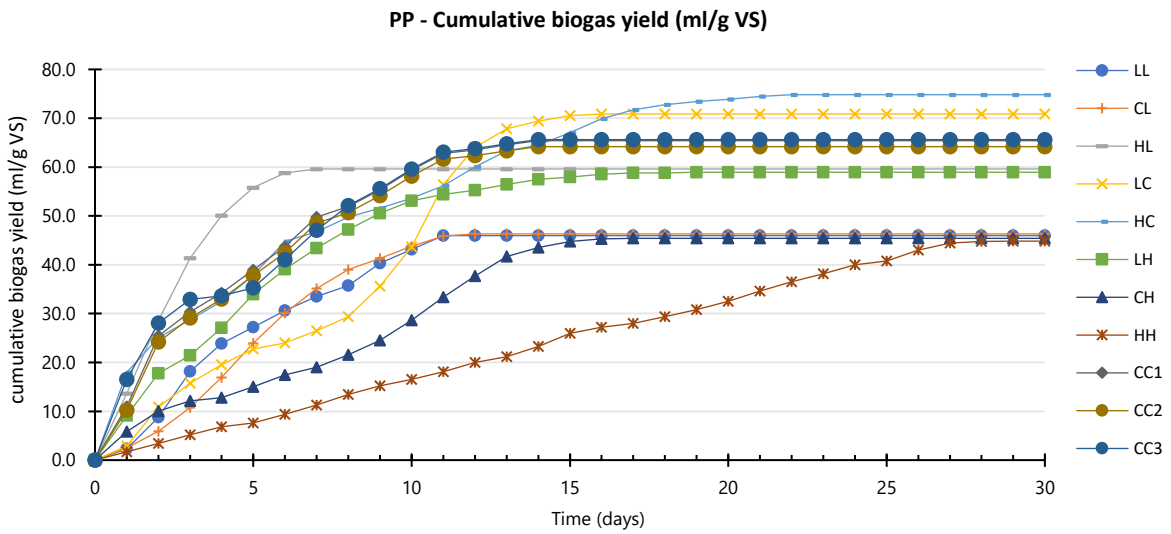

Figure 3.4: Cumulative biogas yield from pineapple peelings

Figure 3.4 shows the equivalent biogas yield on VS basis of the cumulative biogas produced. Noting that the VS here is the total VS obtained from the individual calculated VS of cow dung and the substrate. Another observation that can be made is that the co-digestion of PP with CD has increased the yield from 25.4 mL/g VS to a minimum yield of 45.4 mL/g VS and a maximum yield of 74.8 mL/g VS. Corresponding to a 78.74% and a 194.49% increase respectively.

3.4.1.2. Watermelon rind (WR) in co-digestion with cow dung

Appendix 9 is similar to **Appendix 8** and displays the same kind of data. For watermelon rind, the highest biogas yield was observed at LH, 100.6 mL/g VS while the lowest biogas yield at CL, 59.6 mL/g VS.

From **Figure 3.5**, as in the case of PP, it is clearly seen that the digestion situation is different from the blanks of both WR and CD. There is a 104.06% increase in biogas yield from the highest biogas yield obtained under 30 days retention time and the highest biogas yield from co-digested watermelon and cow dung.

Not only has the yield improved but also the initial slopes have turn to be improved as well.

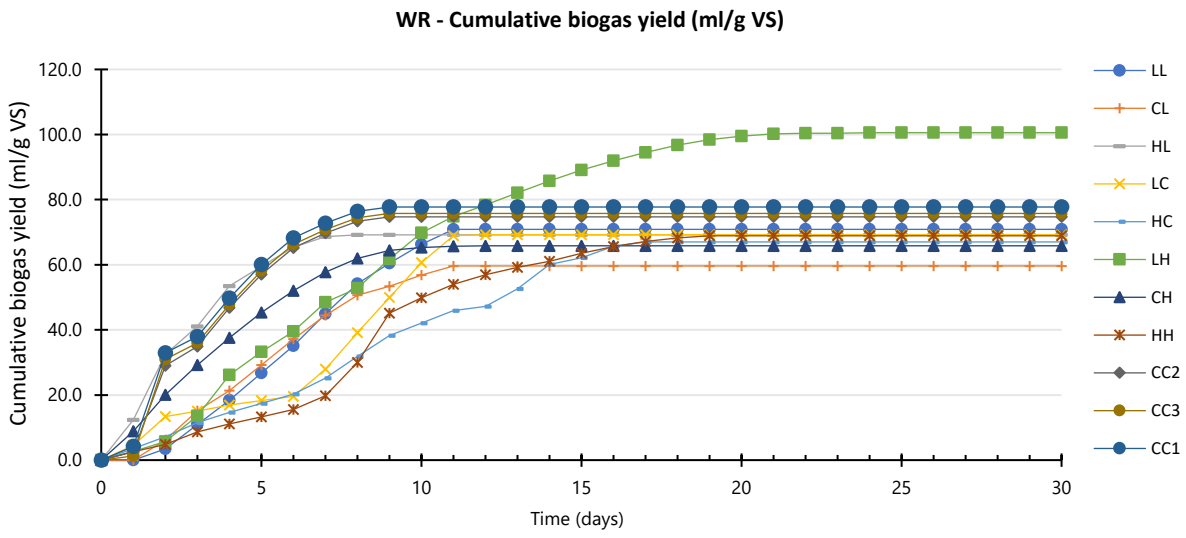

Figure 3.5: Cumulative biogas yield from watermelon rind

3.4.1.3. Banana peelings (BP) in co-digestion with cow dung

For the batch experiment of the banana peelings (**Appendix 10**), the highest biogas yield was at LH with a biogas yield of 99.1 ml/g VS. The lowest biogas yield was obtained from LL and HH with a biogas yield of 65.1 ml/g VS. Then a visual representation of the production of biogas for all the BMP setups concerning BP is shown in **Figure 3.6**.

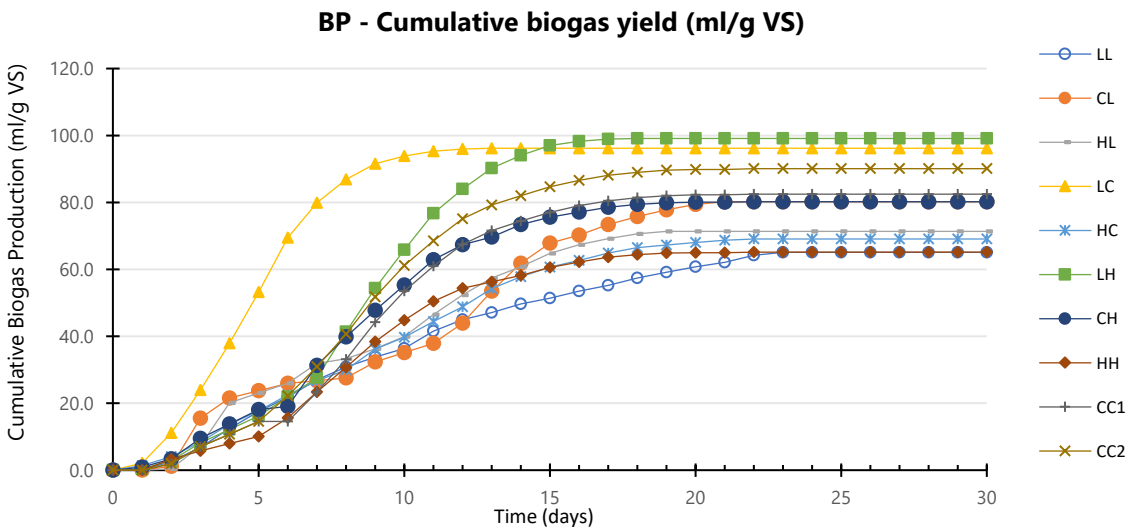

Figure 3.6: Cumulative biogas yield from banana peelings

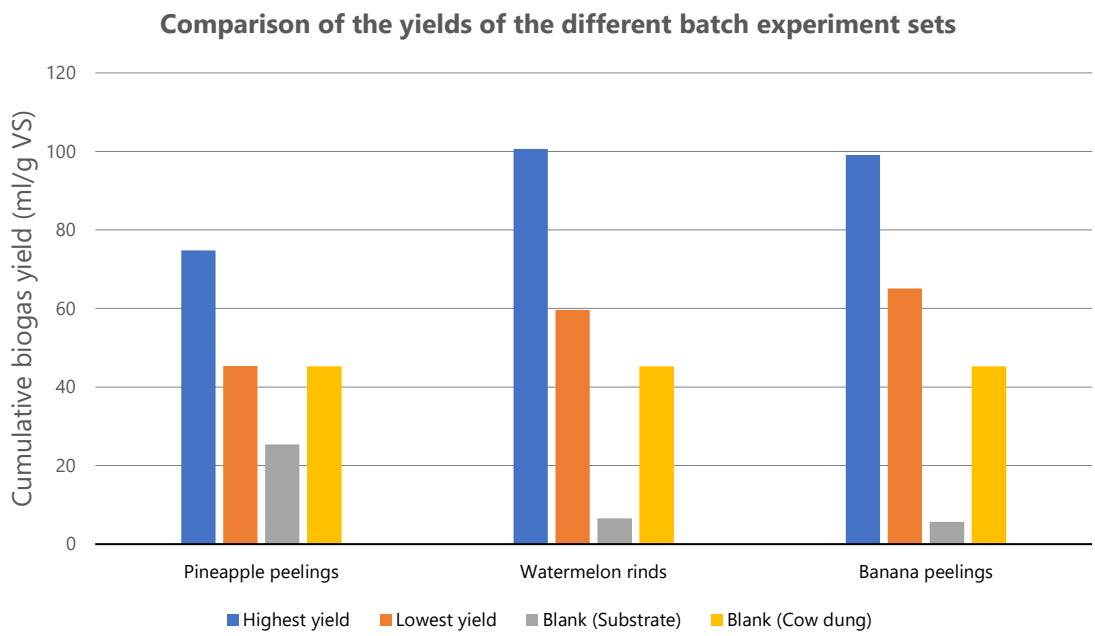

Figure 3.7: Comparison of batch experiments in co-digestion against the blanks.

From **Figure 3.7**, we see that the co-digestion yields are higher than their corresponding substrates under mono-digestion. In every given substrate case, the yield was always higher than the yield produced from cow dung blank. Watermelon rind and banana peelings gave the highest biogas yields in co-digestion.

3.4.2. Kinetic modelling

3.4.2.1. Introduction

The MATLAB software helped to obtain the kinetic coefficients of both the first-order model (Go and k) and the modified Gompertz model (Go, λ and R_{max}) as earlier seen for the blank experiments.

3.4.2.2. Pineapple peelings (PP)

The Gompertz model fits better the experimental points than the first-order model and this can be appreciated by observing the fitting curves on

Figure 3.8 and **Figure 3.9**. Nevertheless, the first-order model once again permits us to compare the rate-determining step's rate, k. The greater the value of k, the faster hydrolysis takes place (IB Chem, 2021). From **Table 3.7**, we see that the slowest biochemical reaction is that of HH with 0.007 d^{-1} and the fastest reaction is from HL with 0.3986 d^{-1}.

Table 3.7: Kinetic modelling of pineapple peelings batch experimentations

Pineapple peelings							
PP	First-Order Model			Modified Gompertz Model			
Sample	G_0 (mL/gVS)	K (d^{-1})	R^2	G_0 (mL/gVS)	λ(d)	Rmax ($mLCH_4$/gVS/d)	R^2
PP-LL	47.68	0.1820	0.9731	46.27	0.5318	6.194	0.9911
PP-LC	83.09	0.0868	0.9268	73.64	1.8570	6.366	0.9684
PP-LH	60.61	0.1795	0.9906	59.05	0.00001	6.939	0.9960
PP-CL	48.68	0.1640	0.9471	46.61	1.5600	7.197	0.9984
PP-CC1	66.85	0.1994	0.9901	65.50	0.00001	8.341	0.9828
PP-CC2	65.17	0.1988	0.9984	64.89	0.00001	8.261	0.9839
PP-CC3	65.36	0.1989	0.9927	65.12	0.00001	8.352	0.9811
PP-CH	52.20	0.0912	0.9457	47.41	0.7544	3.578	0.9741
PP-HL	60.21	0.3986	0.9814	59.70	0.2849	16.680	0.9984
PP-HC	77.31	0.1361	0.9836	74.12	0.00004	6.781	0.9588
PP-HH	252.2	0.0070	0.9968	56.54	1.5630	1.876	0.9961

Looking at the Gompertz model, the assays at the CC levels have lowest lag time with the lowest lag time gotten from experiment CC (0.00001 day, almost immediately). The highest lag time was obtained from experiment LC with 1.857 days (approximately 45 hours). Across C/N level, the results revealed no clear pattern for the value of the lag time as lag time ranking varies.

Figure 3.8 and **Figure 3.9** are the graphical representations of the fitting models using first-order model and the modified Gompertz model.

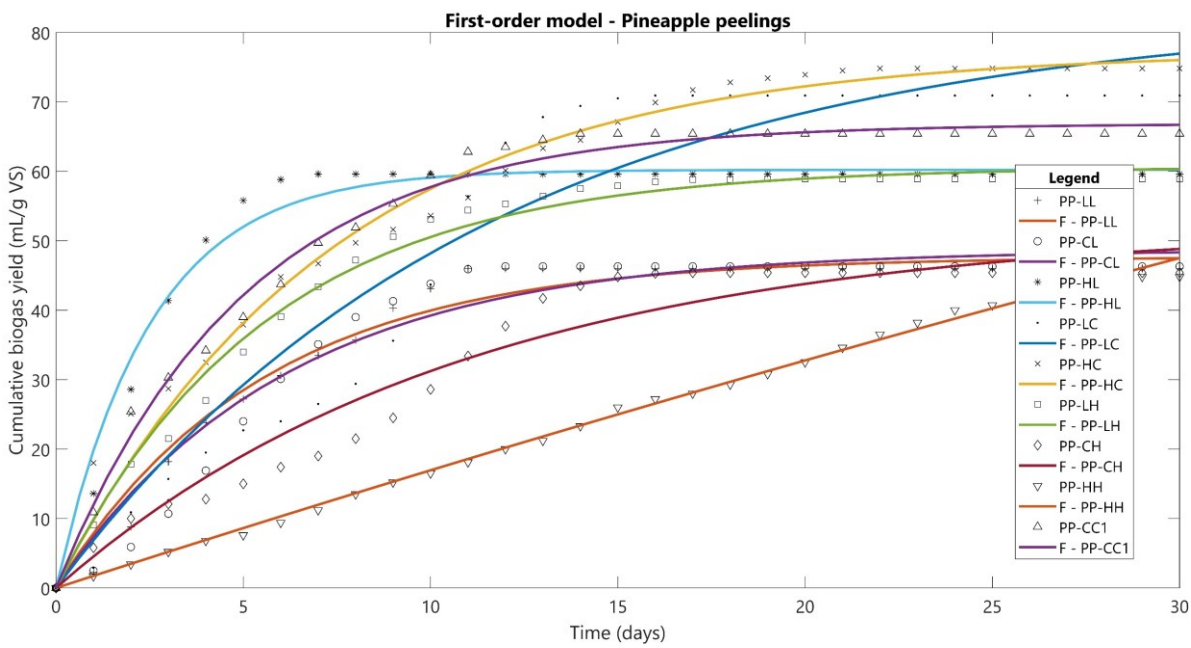

Figure 3.8: First-order model fitting curves for pineapple peelings

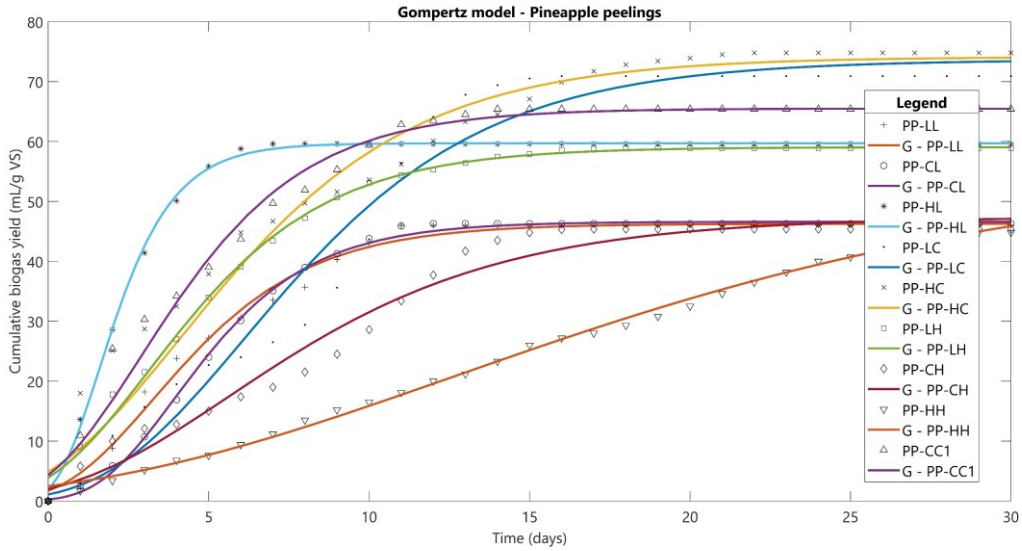

Figure 3.9: Gompertz model fitting curves for pineapple peelings

3.4.2.3. Watermelon rind (WR)

The difference between the first-order fits and the experimentation data ranges from 153.69 % to 3.91 %. The Gompertz model resulted to a better fitting of the data with the difference ranging from 121.71 % to 6.00 %, visually observable on **Figure 3.10** and **Figure 3.11**. **Table 3.8**, reports on the fitted coefficients of the first-order (G_o and k) and the modified Gompertz model (G_o, λ and R_{max}). The slowest reaction gotten from HH with 0.074 d^{-1} and the fastest reaction from HL with 0.3442 d^{-1}.

Table 3.8: Kinetic modelling of watermelon rind batch experimentations

Watermelon rind							
WR	First-Order Model			Modified Gompertz Model			
Sample	G_0 (mL/gVS)	K (d^{-1})	R^2	G_0 (mL/gVS)	λ(d)	Rmax ($mLCH_4$/gVS/d)	R^2
WR-LL	76.68	0.1328	0.9197	71.62	2.4940	11.05	0.9956
WR-LC	77.42	0.1084	0.9008	70.88	2.6460	8.517	0.9640
WR-LH	116.6	0.0846	0.9731	101.90	1.4570	8.53	0.9978
WR-CL	62.85	0.1606	0.9412	60.03	1.6930	9.393	0.9971
WR-CC1	79.12	0.2750	0.9683	77.90	0.4796	15.73	0.9894
WR-CC2	79.24	0.2745	0.9685	77.76	0.4788	15.68	0.9859
WR-CC3	79.22	0.2722	0.9679	77.45	0.4792	15.41	0.9882
WR-CH	67.30	0.2364	0.9784	66.11	0.3762	10.94	0.9971

WR-HL	70.04	0.3442	0.9817	69.33	0.2567	16.40	0.9959
WR-HC	82.00	0.0734	0.9533	69.48	1.9590	5.557	0.9906
WR-HH	84.59	0.0740	0.9237	69.80	3.4960	7.58	0.9903

The variation in value of k doesn't also show a clear pattern across the C/N ratios.

Following the values of lag time, λ, the lowest lag time is gotten from experiment HL with 0.26 day approximately 6 hours and the highest lag time was from HH with 3.496 days (approximately 83.9 hours). **Figure 3.10** and **Figure 3.11** display graphically the fitted models with respect to the experimental data obtained. It can be observed that the Gompertz model curves fits better the data.

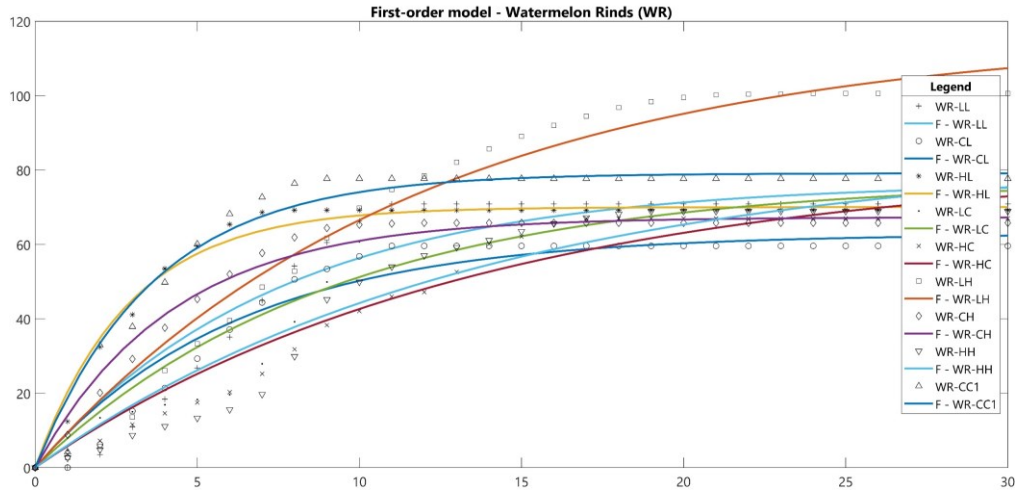

Figure 3.10: First-order model fitting curves for watermelon rind

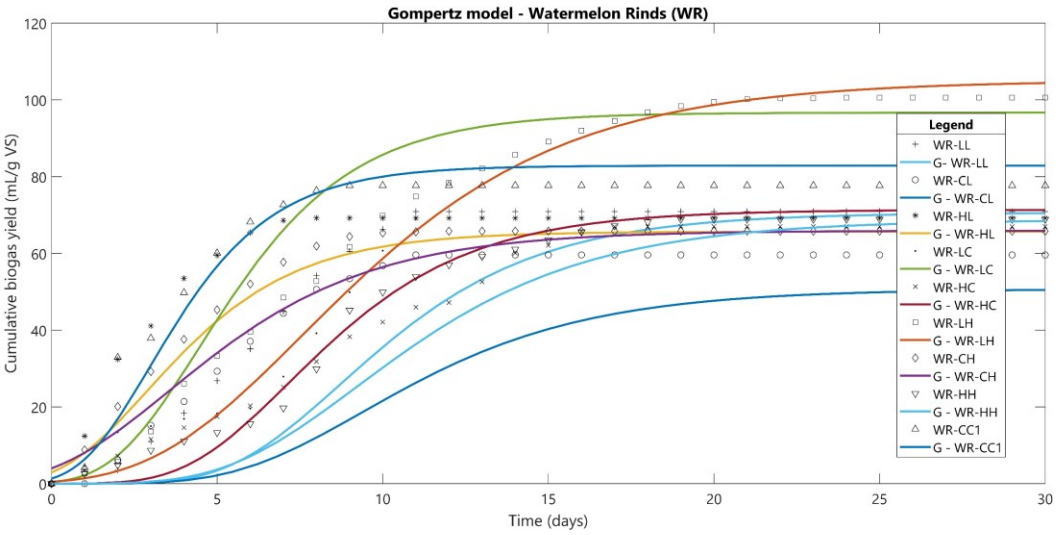

Figure 3.11: Modified Gompertz model fitting curves for watermelon rind

3.4.2.4. Banana peelings (BP)

The difference between the first-order fits and the experimentation data ranges from 171.75 % to 20.13 %. The Gompertz model resulted to a better fitting of the data with the difference ranging from 119.31 % to 1.82 %, visually observable on **Figure 3.12** and **Figure 3.13**. **Table 3.9**, reports on the fitted coefficients of the first-order (G_o and k) and the modified Gompertz model (G_o, λ and R_{max}). The slowest reaction gotten from CL with 0.0471 d^{-1} and the fastest reaction from LC with 0.1789 d^{-1}.

Table 3.9: Kinetic modelling of banana peelings batch experimentations

Banana peelings							
BP	First-Order Model			Modified Gompertz Model			
Sample	G_0 (mL/gVS)	K (d^{-1})	R^2	G_0 (mL/gVS)	λ(d)	Rmax ($mLCH_4$/gVS/d)	R^2
BP-LL	84.65	0.0542	0.9748	64.38	1.955	4.442	0.9956
BP-LC	100.5	0.1789	0.9366	96.65	1.745	17.61	0.9988
BP-LH	124.9	0.0702	0.9048	100.8	4.327	12.42	0.9937
BP-CL	117.2	0.0471	0.9502	86.58	1.868	5.185	0.9738
BP-CC1	112.5	0.0709	0.9214	91.16	3.791	10.33	0.9982
BP-CC2	111.4	0.0711	0.9275	91.23	3.796	10.30	0.9975
BP-CC3	111.8	0.0701	0.9226	90.95	3.789	10.29	0.9980
BP-CH	89.88	0.0718	0.9253	73.46	3.492	7.845	0.9965
BP-HL	87.84	0.0717	0.9575	73.83	1.816	5.728	0.9874
BP-HC	87.9	0.0648	0.9632	71.33	2.105	5.453	0.9965
BP-HH	87.74	0.0761	0.9285	72.93	3.416	8.066	0.9975

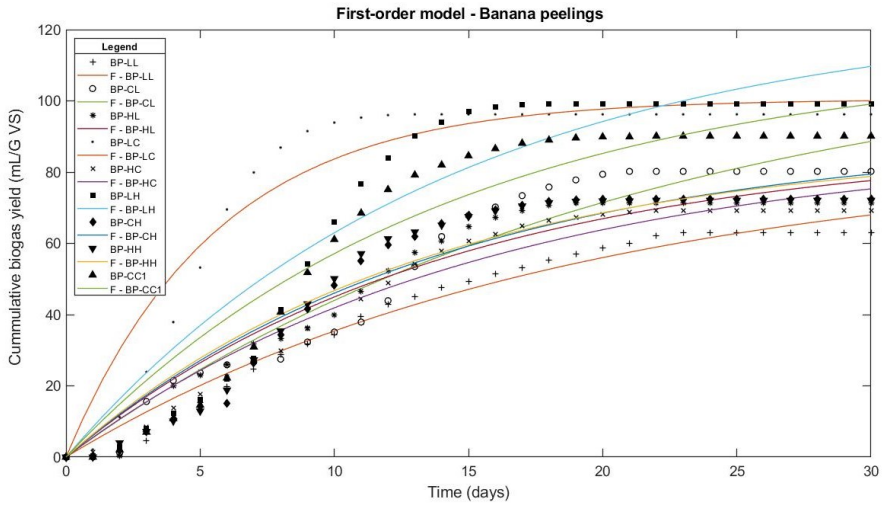

Figure 3.12: First-order model fitting curves for banana peelings

The rate coefficient, k, appears to be the lowest in the center level of C/N ratio.

Following the values of lag time, λ, the lowest lag time is gotten from experiment LC with 1.748 days and the highest lag time was from LH with 4.327 days. **Figure 3.12** and **Figure 3.13** displays graphically the fitting models with respect to the experimental data obtained. It can be observed that the Gompertz model curves fits better the data.

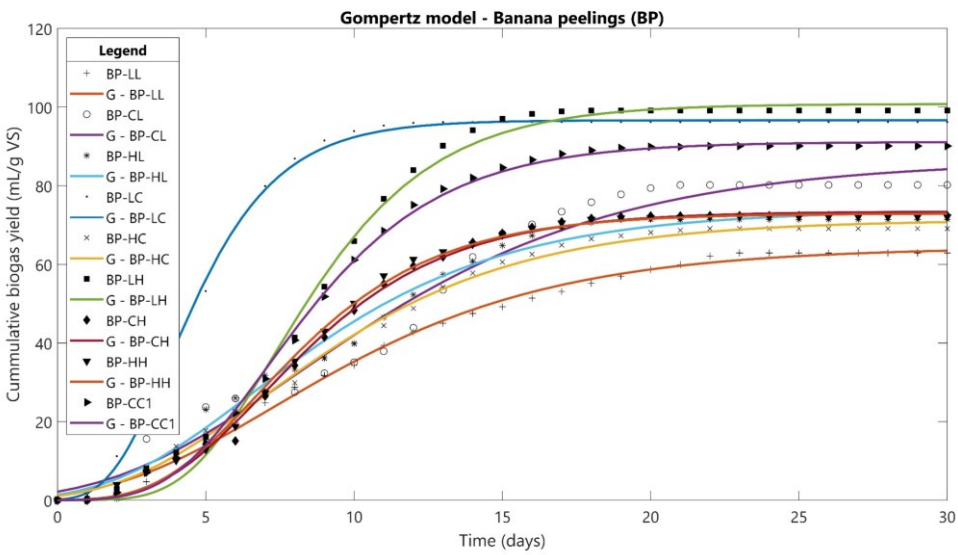

Figure 3.13: Modified Gompertz model fitting curves for banana peelings

Kinetic modelling was used successfully in this section to model the co-digestion of PP, WR and BP with CD. The modified Gompertz model described the data better than the first order equation. It is interesting to note that, the presence of cow dung tends to lower the value of k for PP, a higher value of WR and a lower value of BP compared to the conditions without the substrates.

3.4.3. RSM – Face-centered Central Composite Design (FCCD)

The results of the quadratic model fitness parameters, the results of the Analysis of Variance (ANOVA), the regression equations, the contours and surface plots and the fits and pareto chart of standardized effects.

3.4.3.1. Models' fitness parameters and Analysis of Variance (ANOVA)

From **Table 3.10**, the results shows that the final quadratic model fitting through the value of the coefficient of determination (R^2) explains 99.14 %, 90.46 % and 92.28 % of the pineapple

peelings, watermelon rind and banana peelings co-digestion with cow dung respectively. This signified that the three (03) quadratic models accurately fit the experimental data and can be used to determine the optimum parameters for all the experimentation sets.

Table 3.10: Model fitness parameters

Model summary				
Substrate	S	R-sq	R-sq (adj)	R-sq (pred)
PP	0.9660	99.50 %	99.14 %	95.08 %
WR	4.6802	90.46 %	83.65 %	19.77 %
BP	4.2983	92.28 %	86.76 %	22.22 %

Minitab attempts to fit a series of models to the data (first-order or linear, first-order with interaction or square, and the second-order or two-way interaction). ANOVA tables for the second order equation used in modelling are presented in **Table 3.11**, **3.12** and **3.13**.

Table 3.11: ANOVA results for co-digestion of PP with cow dung

Analysis of Variance – Pineapple peelings (PP)					
Source	DF	Adj SS	Adj MS	F-Value	P-Value
Model	5	1302.75	260.55	279.19	0.000
Linear	2	300.11	150.06	160.79	0.000
C/N	1	128.94	128.94	138.16	0.000
TS [%]	1	171.15	171.15	183.39	0.000
Square	2	1107.07	553.53	593.13	0.000
C/N*C/N	1	134.43	134.43	144.05	0.000
TS*TS	1	1105.72	1105.72	1184.82	0.000
2-Way Interaction	1	192.55	192.55	206.33	0.000
C/N*TS	1	192.55	192.55	206.33	0.000
Error	7	6.53	0.93		
Lack-of-Fit	3	6.53	2.18	*	*
Pure Error	4	0.00	0.00		
Total	12	1309.29			

Table 3.12: ANOVA results for the co-digestion of WR with cow dung

Analysis of Variance – Watermelon rinds (WR)					
Source	DF	Adj SS	Adj MS	F-Value	P-Value
Model	5	1453.94	290.789	13.26	0.002
Linear	2	640.17	320.087	14.60	0.003
C/N	1	313.39	313.389	14.29	0.007
TS [%]	1	326.74	326.737	14.90	0.006
Square	2	355.62	177.810	8.11	0.015
C/N*C/N	1	228.64	228.642	10.43	0.014
TS*TS	1	261.76	261.763	11.94	0.011
2-Way Interaction	1	224.06	224.056	10.22	0.015
C/N*TS	1	224.06	224.056	10.22	0.015

Error	7	153.50	21.929		
Lack-of-Fit	3	153.50	51.167	*	*
Pure Error	4	0.00	0.000		
Total	12	1607.45			

Table 3.13: ANOVA results for the co-digestion of BP with cow dung

Analysis of Variance – Banana peelings (BP)					
Source	DF	Adj SS	Adj MS	F-Value	P-Value
Model	5	1544.61	308.923	16.58	0.001
Linear	2	674.22	337.112	18.09	0.002
C/N	1	76.09	76.095	4.08	0.043
TS [%]	1	584.58	584.581	31.37	0.001
Square	2	510.75	255.375	13.70	0.004
C/N*C/N	1	109.42	109.423	5.87	0.046
TS*TS	1	211.34	211.341	11.34	0.012
2-Way Interaction	1	409.73	409.728	21.99	0.002
C/N*TS	1	409.73	409.728	21.99	0.002
Error	7	130.45	18.636		
Lack-of-Fit	3	130.45	43.484	*	*
Pure Error	4	0.00	0.000		
Total	12	1675.06			

Table 3.11, **3.12** and **3.13** presents the results of the Analysis of Variance (ANOVA) of co-digestion experiments. The model is significant with a p-value < 0.0001. Generally, p-values less than 0.0500 mean that the represented terms are significant, while the p-value of a model term greater than 0.05 indicates insignificance.

For PP, C/N, TS, C/N*TS, C/N*C/N, TS*TS are significant model terms **Table 3.11**. The values of R^2, Adjusted R^2, and Predicted R^2 are close to 100%, an indication that the experimental results obtained are reliable and consistent. The regression equation in terms of real factors is developed to establish a mathematical relationship between the response of anaerobic digestion (biogas yield) and two independent process (C/N and TS) variables as represented in **equation 3.1**.

$$Biogas\ yield_{PP} = \mathrm{f(CN, TS)} = 1035 - 62.64\,CN + 73.23TS + 0.88CN * CN - 2.64TS * TS - 0.89CN * TS \quad (3.1)$$

For WR, C/N, TS, C/N*TS, C/N*C/N, TS*TS are significant model terms as well with p-values ranging from 0.001 to 0.015, **Table 3.12**. The regression equation in terms of real factors was developed and represented in **equation 3.2**.

$$Biogas\ yield_{WR} = \mathrm{f(CN, TS)} = 7427 - 405CN + 93.7TS + 5.55CN * CN - 1.30TS * TS - 2.14CN * TS \quad (3.2)$$

For BP, C/N, TS, C/N*TS, C/N*C/N, TS*TS are significant model terms as well with p-values ranging from 0.001 to 0.045, **Table 3.13**. The regression equation in terms of uncoded factors was developed and represented in **equation 3.3**.

$$Biogas\ Yield_{BP} = \mathrm{f(CN, TS)} = -1275 + 62.3C/N + 68.0TS - 0.73C/N * C/N - 1.27TS * TS - 1.32C/N * TS \quad (3.3)$$

3.4.3.2. Factor values for maximum biogas yield

The response optimizer tool of Minitab was used to maximize biogas yield using the second-order models for substrates' co-digestion obtained in section 3.4.3.1. .

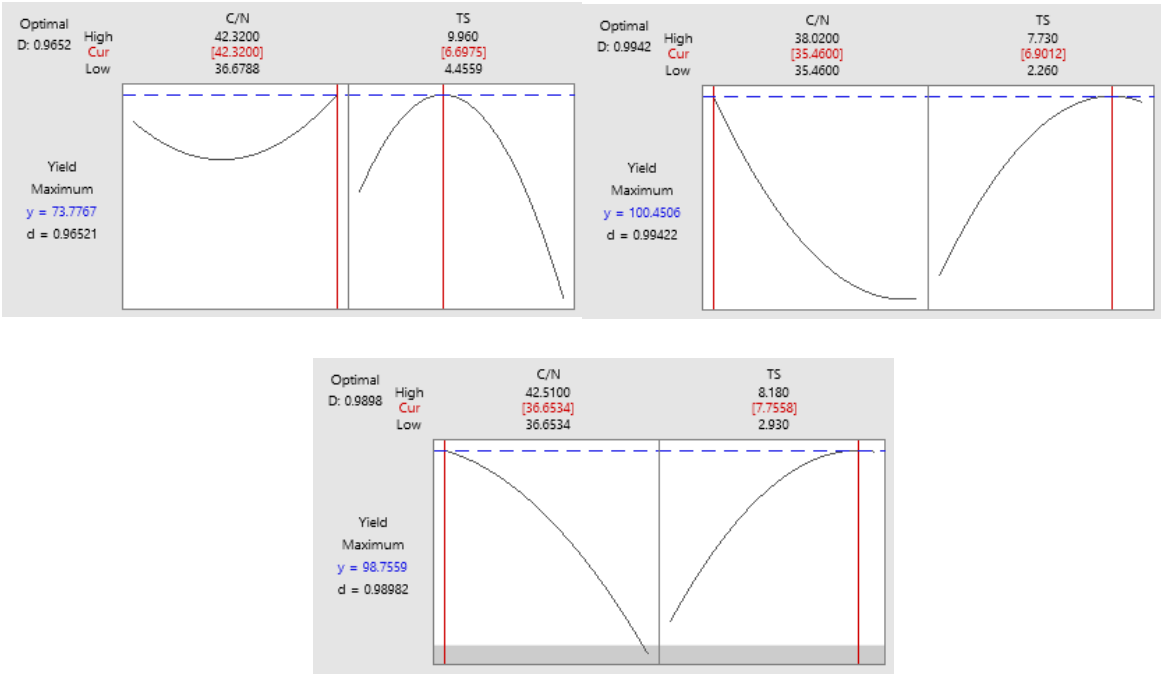

Figure 3.14: Response optimization; PP (top-left), WR (top-right) and BP (bottom-center)

In **Figure 3.14**, curvature is obtained for TS (%) for the three CCD of substrates. While, for C/N curvature is not attained but lies at the extreme end of the experimented levels. In a nutshell, the parameters C/N and TS were optimized under initial conditions, **Table 3.14**;

Table 3.14: Initial parameters for co-digestion batch experiments

Temperature: mesophilic range (25°C – 40°C)	Pretreatment: Knife milling to particle size under 1cm (physical/mechanical treatment).
Agitation or stirring: two times every 24h.	
No pH regulation.	Retention time – 30 days

The objective of the optimization was to maximize the biogas yield given the constraints set in **Table 3.14**. The final optimum parameters for all substrates are presented on **Table 3.15** and **Figure 3.14**. The optimization function $f(C/N, TS)$ was translated thanks to the excel solver add-in which permitted to iterate in the equations of final C/N and final TS (**equations 2.5** and **2.6**). Such that the optimum parameters become easier to implement into the function $f(I, S, W)$, where I is the Inoculum mass ratio from final C/N **equation 2.5**, S the Substrate mass ratio from final C/N and W the Water mass ratio from final TS **equation 2.6**.

Table 3.15: Optimum parameters of C/N and TS (%) for all the substrates

	Pineapple peelings (PP)	Watermelon rind (WR)	Banana peelings (BP)
C/N	42.3200	35.4600	36.6534
TS (%)	6.6975	6.9012	7.7558
Yield (ml/g VS)	73.7767	100.4506	98.7559
I/S ratio	1:2.087 (0.479)	1:0.333 (3.000)	1:0.333 (3.000)
F/W ratio	1:1.490 (0.671)	1:1.450 (0.690)	1:1.325 (0.755)
I : S : W	**1.00 : 2.09 : 4.06**	**3.00 : 1.00 : 5.80**	**3.00 : 1.00 : 5.30**

Where I = Inoculum, S = Substrate and W = Water ratio.

In line with the results obtained for the mono-digestion of the substrates, section 3.3. The necessary amount of cow dung required to enhance the biogas yield of pineapple waste is lesser in PP than in WR and BP as the required amount of inoculum necessary for the digestion of these substrates are higher.

3.4.3.3. Contour and surface plots

Contour plots are a way to show a three-dimensional surface like the response surface. On the contour plot, the independent variables are found on either the x or the y-axis (real or coded), while the dependent variable is classified into levels and shown as contours. It permits us to visually appreciate the behaviour of the response as the independent variables are varied.

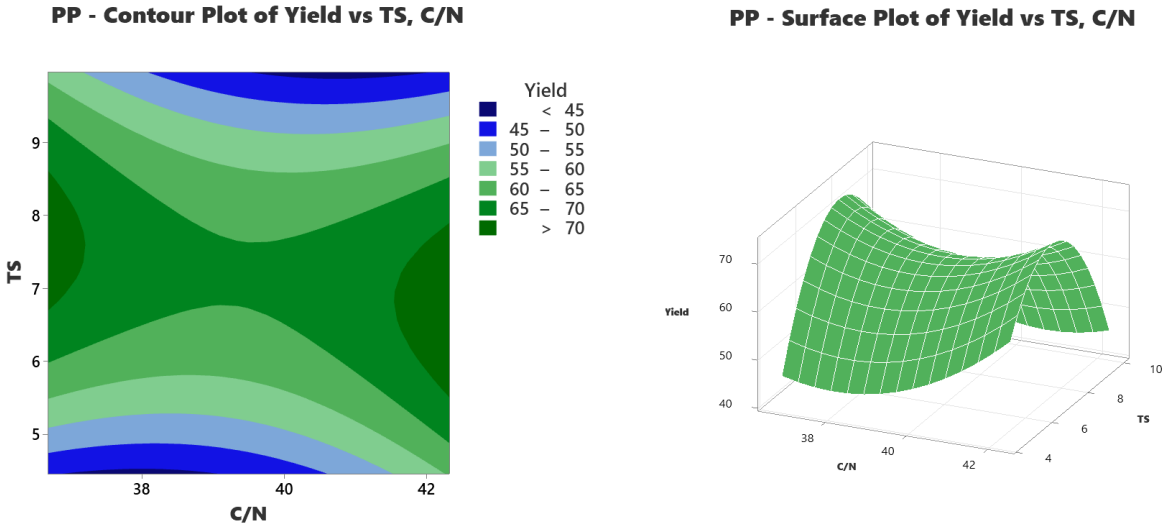

Figure 3.15: Contour and surface plots of Pineapple peelings' (PP) anaerobic digestion

The contour plot and surface plot for pineapple peelings in **Figure 3.15** shows that high biogas yield was generated at both the lowest C/N with TS close to 7 % (left) and highest C/N with close to 6 % (right). Biogas yield increases to a maximum value as the variables increase and then decrease to lower values.

Figure 3.16 displays the contour and surface plots for watermelon rind. The plots shows that maximum yields are achieved at lower levels of C/N and close to the TS value of 7%. The surface also diminishes through a steep slope and later on enlarges as we go from the left to the right, showing that another high value of biogas yield can possibly be achieved as we increase the C/N value.

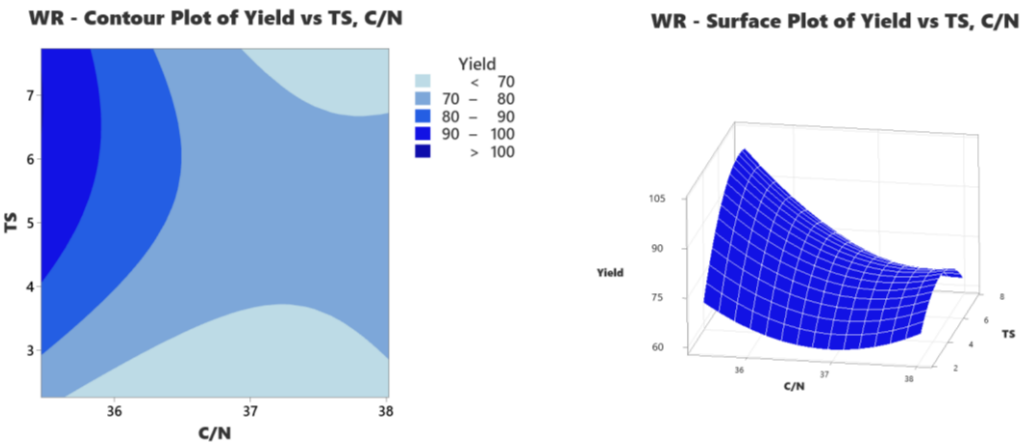

Figure 3.16: Contour and surface plots of Watermelon rind's (WR) anaerobic digestion

For banana peelings, the contour and surface plots in **Figure 3.17** shows that the parameters of C/N and TS producing the highest yields are towards low-level C/N and high-level TS. Unlike PP and WR, the contour plot of BP, **Figure 3.17**, does not present any other high yields.

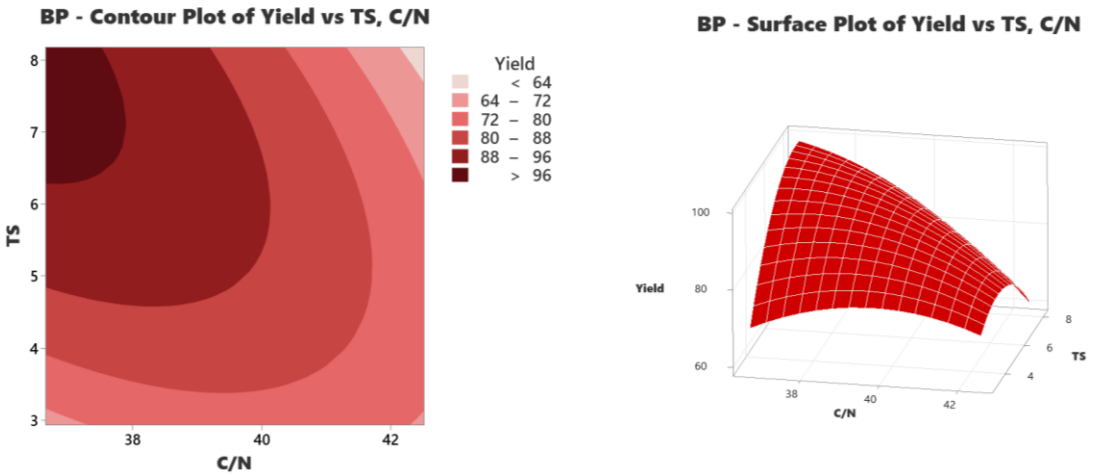

Figure 3.17: Contour and surface plots of Banana peelings' (BP) anaerobic digestion

3.4.3.4. Fits and Pareto chart of standardized effects

The plot of predicted against the actual value of biogas yield for co-digestion of PP, WR and CD are depicted in **Figure 3.18**, **Figure 3.19** and **Figure 3.20**. All the data points are either on or close to the line of fitness. This further supports the high R^2 obtained for these models.

The Pareto chart shows the absolute values of the standardized effects from the largest effect to the smallest effect. The standardized effects are t-statistics that test the null hypothesis that the effect is 0. The chart also plots a reference line to indicate which effects are statistically significant. The reference line for statistical significance depends on the significance level (denoted by α or alpha). The chart is used to determine the magnitude and the importance of the effects. On the Pareto chart, bars that cross the reference line are statistically significant.

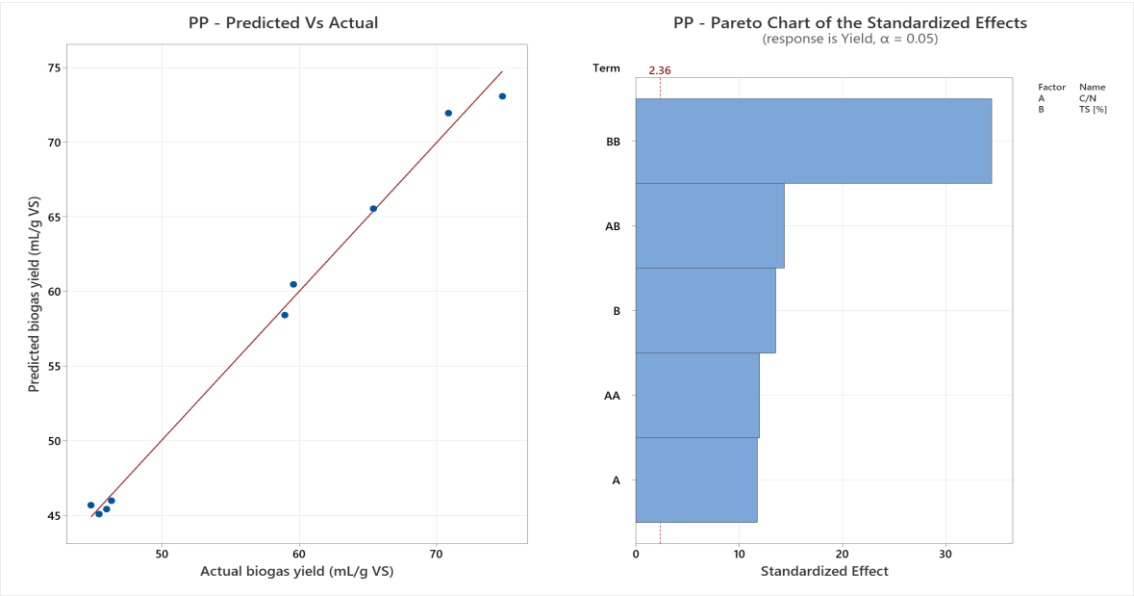

Figure 3.18: The plot of predicted vs actual yield (left) and the Pareto chart of standardized effects (right) of PP's co-digestion

In the Pareto chart in **Figure 3.18** for PP, the bars that represent factors BB, AB, B, AA and A in order of magnitude cross the reference line that is at 2.36. These factors are statistically significant at the 0.05 level with the current model terms.

In the Pareto chart in **Figure 3.19** for WR, the bars that represent factors A, BB, AA, AB and B in order of magnitude cross the reference line that is at 2.365. These factors are also statistically significant at the 0.05 level with the current model terms.

In the Pareto chart in **Figure 3.20** for WR, the bars that represent factors A, AB, BB, B and B in order of magnitude cross the reference line that is at 2.365. These factors are also statistically significant at the 0.05 level with the current model terms.

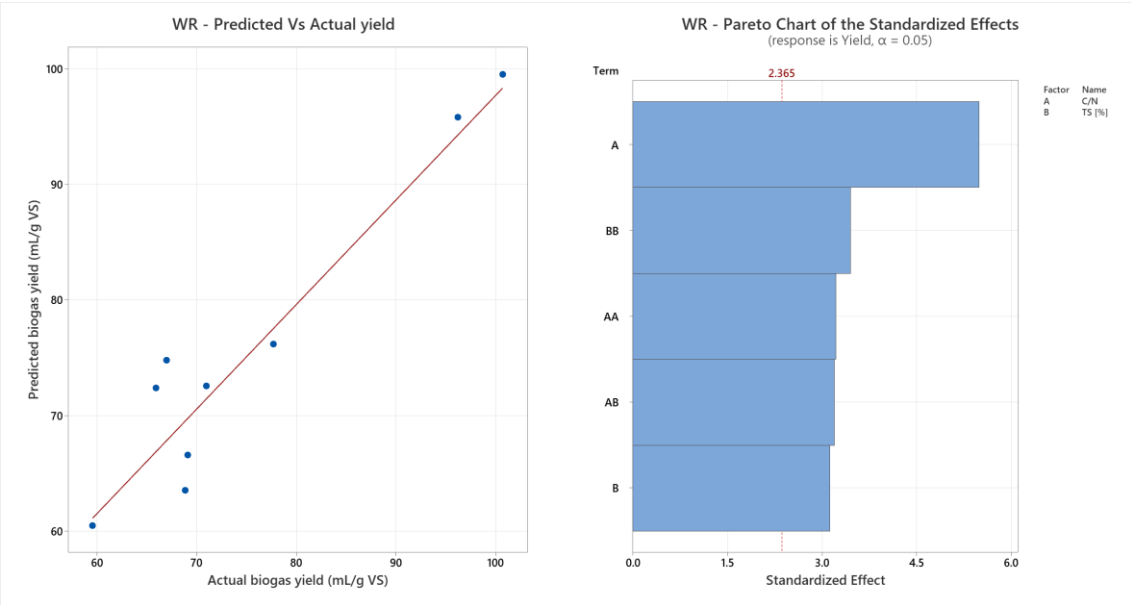

Figure 3.19: The plot of predicted vs actual yield (left) and the Pareto chart of standardized effects (right) of WR's co-digestion

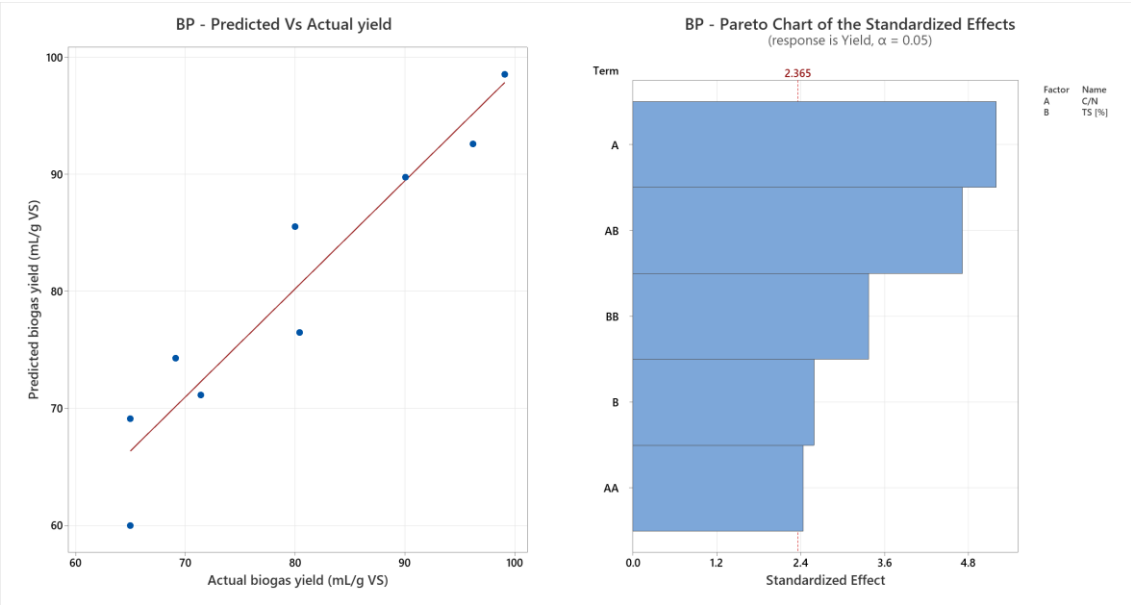

Figure 3.20: The plot of predicted vs actual yield (left) and the Pareto chart of standardized effects (right) of BP's co-digestion

The Minitab software was used to fit a second-order model for the cogeneration departments with a good coefficient of determination. The coefficients for the quadratic equation were determined and thanks to this, the optimiser tool of Minitab found the parameter values for

optimum response (biogas yield). The contour and surface plots were generated by this same software permitting the graphical appreciation of the variation of biogas yield as the parameters are varied. Other statistical evaluations like the pareto charts permitted to determine which terms of the quadratic model are significant as well as their order of significance.

3.5. ANAEROBIC DIGESTION OF MIXTURES OF SUBSTRATES

3.5.1. Introduction

This section permitted the fulfilment of **objective 2** of our research work. It begins by showing the results of the BMP experiments carried on with the mixture of substrates, and concludes with the kinetic study of the experiments.

3.5.2. BMP batch experiments' results

The BMP batch experimentations carried out with the mixed substrates was conducted under the same conditions stated previously in section 3.3.1. So, just as the blank assays, the feed here constituted just of the substrates mixed together in a substrate1 to substrate2 ratio of 1:1. The mixtures was then mixed with water in an overall ratio of total substrate to water of 1:1.

From the results presented on **Table 3.16**, the highest yield is that of PP – BP with 25.5 ml/g VS while the lowest yields is from WR – BP with 5.1 ml/g VS. Concerning the mixtures including WR and BP, they tend to produce a similar low yield as when they were in mono-digestion, **Table 3.5**. The only combination that produced a yield as high as that produced by PP in mono-digestion is the mixture PP – BP with a biogas yield of 25.5 mL/g VS. Other combinations that produced comparatively high yields were all those associated with PP. Which might signify that, the mixture of substrates does not increase the biogas yield but rather, decreases it.

Table 3.16: BMP results of the mixture set

Mixture								
Substrate	Mass 1	Mass 2	Mass 3	Water (mL)	Mass1's VS	Mass2's VS	Mass3's VS	Biogas yield (mL/g VS)
PP - BP	54.9	54.9	0.0	120	6.8	5.7	0.00	25.5
WR - BP	50.0	50.0	0.0	120	2.7	5.2	0.00	5.1
PP - WR	55.9	55.9	0.0	120	6.9	3.0	0.00	11.3
WR - BP - PP	35.7	35.7	35.7	120	1.9	3.7	4.41	18.7

Most of the substrates stopped producing biogas latest at day 5. This situation is similar to the mono-digestion of the substates in **Figure 3.1**. On this same figure, the biogas generated from cow dung continued to be produced up till day 19. This reinforces the idea that, cow dung helps to stabilise the production of biogas. **Figure 3.21** shows the cumulative biogas yield on VS basis of the BMP experiments of the mixtures of substrates.

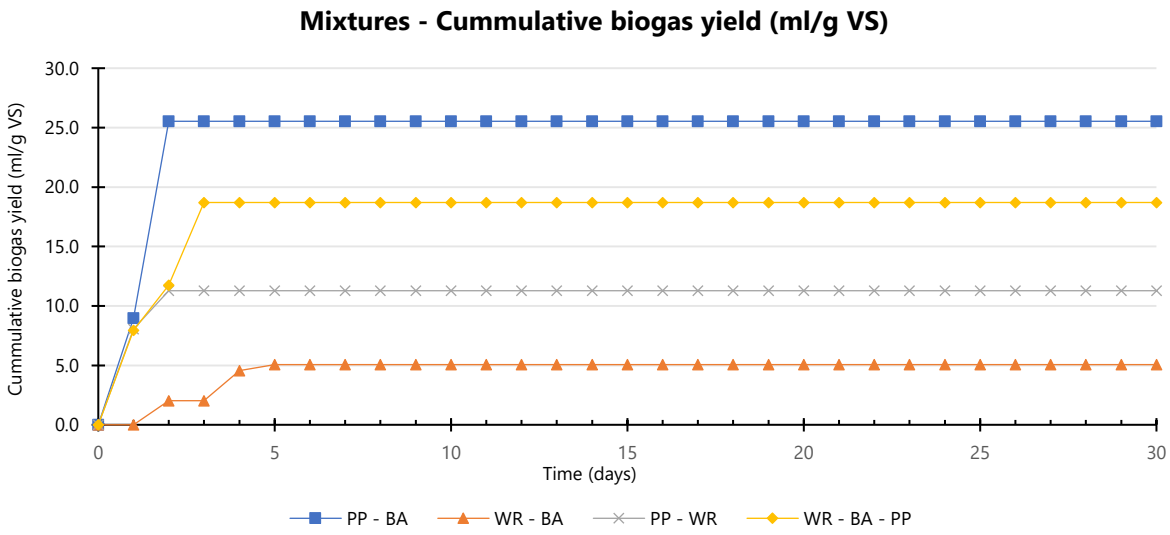

Figure 3.21: Cumulative biogas yield from BMP batch experimentations of mixtures of substrates

3.5.3. Kinetic modelling results

From **Table 3.17**, the fastest digestion occurred in assay PP – WR with rate constant k of 1.375 d^{-1} while the lowest was from WR – BP with k of 0.3223 d^{-1}.

Table 3.17: Kinetic model of the mixture of substrates assays

Mixture of substrates							
	First-Order Model			Modified Gompertz Model			
Sample	G_0 (mL/gVS)	K (d^{-1})	R^2	G_0 (mL/gVS)	λ(d)	Rmax ($mLCH_4$/gVS/d)	R^2
PP - BP	25.45	0.8315	0.9335	25.3	0.8939	83.90	1.0000
WR - BP	5.20	0.3223	0.9024	5.125	1.1820	1.67	0.9714
PP - WR	11.22	1.3750	0.9948	11.2	0.7218	30.94	1.0000
WR - BP - PP	18.71	0.6517	0.9708	18.65	0.1403	7.99	0.9815

Comparing **Table 3.6** from the mono-digestion of substrates and **Table 3.17** from co-digestion between substrates, shows that the co-digestion between substrates did not greatly influence a lot the lag time for microbial activity. On **Figure 3.22** and **Figure 3.23** are the graphs displaying the fitting curves generated by the first-order and modified Gompertz fitting.

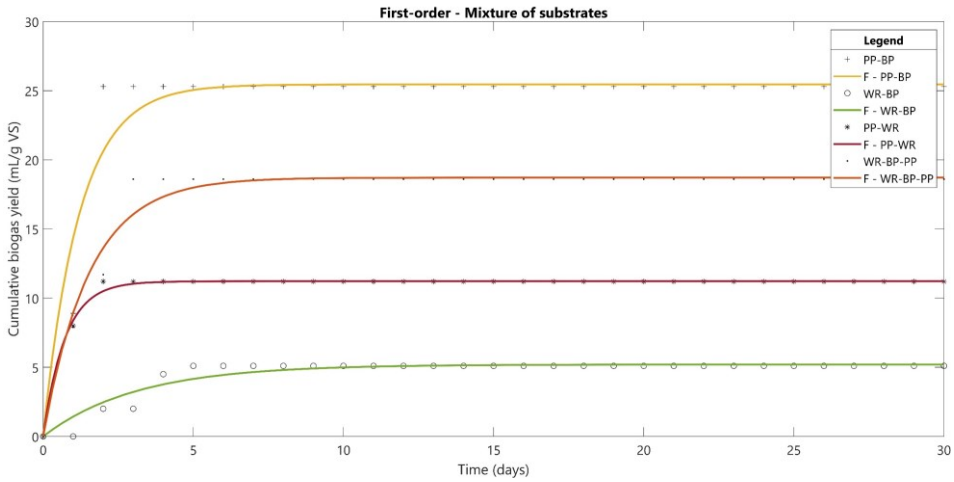

Figure 3.22: First-order kinetics model fitted curves for mixtures of substrates

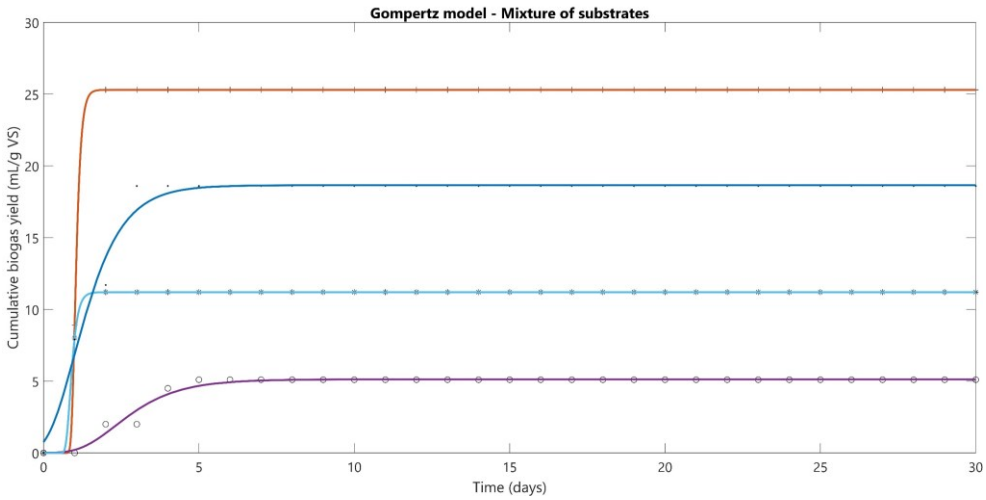

Figure 3.23: Modified Gompertz model curves fittings for mixtures of substrates

Regarding objective 2, that is, determining mixtures of substrates that give high yields of good quality biogas, we conclude that compared to mono-digestion of substrates, co-digestion between them does not generate higher yields. Nevertheless, it is important to note that most of the substrates given it mono- or co-digested produce yields up to 25.5 mL/g VS in a short incubation time of 5 days. This advantage is not negligible. Therefore, our study shows that mixtures that generate yields of biogas are PP – BP (25.5 mL/g VS), PP – WR (11.3 mL/g VS) and WR – BP – PP (18.7 mL/g VS).

3.6. BIOGAS YIELD TO ENERGY CLASSIFICATION

Considering the kinetics of the various BMP assays, a biogas facility may want to optimize the total quantity of biogas produced in the long run. Different configurations were selected looking at the different shapes (different kinetics) in **Figure 3.4** for PP, **Figure 3.5** for WR and **Figure 3.6** for BP. Using the second-order equation obtained from the RSM study, we generated with the help of Minitab the 100 % biogas yield obtained at different configurations of C/N and TS. Then computed the 80 % and 50 % of that maximum yield. We calculated the corresponding time to achieve the respective percentages yield using the modified Gompertz model with the help of the goal seek tool of MS Excel. Then, the time obtained was extrapolated to 3 months, considering that the facility functions in batch mode only and reloads the digester after the given time. The energy generated in MJ/t VS/year and the electricity in kWh/t VS/year was computed. The assumption made was that, 1m3 of biogas generates 22MJ of energy or 2.14 kWh of electricity. **Table 3.18** is the result of that estimation.

Table 3.18: Biogas yield to energy classification table

	PP			WR			BP		
	CC1	**HC**	**CL**	**CC1**	**LH**	**CH**	**LC**	**LH**	**CH**
100% yield (ml/g VS)	65.54	73.09	46.03	76.23	99.51	72.45	92.57	98.54	85.57
t (day)	26	21	14	9	23	17	10	19	28
3 months yield (ml/g VS)	260.17	346.59	321.48	762.30	162.03	409.32	833.13	484.78	276.48
Energy (MJ/t VS)	5,723.74	7,624.98	7,072.56	16,770.60	3,564.66	9,005.04	18,328.86	10,665.16	6,082.56
Electricity (kWh/t VS year)	2,227.06	2,966.81	2,751.87	6,525.29	1,386.98	3,503.78	7,131.59	4,149.72	2,366.67
Rank	**3**	**1**	**2**	**1**	**3**	**2**	**1**	**2**	**3**
80% yield (ml/g VS)	52.43	58.47	36.82	60.98	79.61	57.96	74.06	78.83	68.46
t (day)	7	10	7	5	12	7	6	12	16
3 months yield (ml/g VS)	675.75	526.23	472.41	1,097.64	596.02	748.75	1,110.90	573.16	391.01
Energy (MJ/t VS)	14,866.50	11,577.06	10,393.02	24,148.08	13,112.44	16,472.50	24,439.80	12,609.52	8,602.22
Electricity (kWh/t VS year)	5,784.42	4,504.53	4,043.83	9,395.80	5,101.93	6,409.30	9,509.30	4,906.25	3,347.05
Rank	**1**	**2**	**3**	**1**	**3**	**2**	**1**	**2**	**3**
50% yield (ml/g VS)	32.77	29.24	23.02	38.12	49.76	36.23	46.29	49.27	42.79
t (day)	4	4	5	3	7	4	4	8	9
3 months yield (ml/g VS)	737.75	657.47	414.36	1,143.60	635.87	814.91	1,027.19	542.24	427.90
Energy (MJ/t VS)	16,230.50	14,464.34	9,115.92	25,159.20	13,989.14	17,928.02	22,598.18	11,929.28	9,413.80
Electricity (kWh/t VS year)	6,315.14	5,627.94	3,546.92	9,789.22	5,443.05	6,975.63	8,792.75	4,641.57	3,662.82
Rank	**1**	**2**	**3**	**1**	**3**	**2**	**1**	**2**	**3**

With this example of three selections from each substrate, **Table 3.18**, for the case of PP, the configuration HC has the highest yield (73.09 ml/g VS) when incubated for a period of 21 days. This can provide 2,966.81 kWh/t VS year. Another configuration still relative to PP is CC1 which provides instead 6,315.14 kWh/t VS year in incubated rather at interval of 4 days. If we decide on the amount of incubation intervals, it is possible to obtain the best configuration that produces the best yield with the help of this classification table.

Selecting less duration in tales a less than 100% VS removal. Biogas facilities may then include other reactors that will take in the remain material for further digestion before the digestate can be used for agricultural purposes.

GENERAL CONCLUSION AND PERSPECTIVES

The main objective was to produce and quantify the biogas produced from food waste. Specifically, to determine the optimum operating conditions of the parameters that could be used for the anaerobic digestion of pineapple peelings, watermelon rinds and banana peelings. Also, the second objective was to determine which mixtures of substrates produces the high biogas of good quality.

To meet this objective, the specific objectives were identified: Biochemical methane potential (BMP) assays were carried out while varying C/N and TS parameters were investigated. Data from biogas production were collected and two modelling tools were used to explore the biogas production process. The first-order and modified Gompertz model for the digestion kinetic studies on four (04) blank assays and four (04) mixture preparations of the substrates and the face-centred central composite design (FCCD) of 39 (13 x 3) co-digestion experiments to predict the optimal response.

The optimal Inoculum to Substrate to Water (I:S:W) ratio for co-digestion of pineapple peelings (PP) with cow dung (CD) was 1:2.09:4.06 and the corresponding biogas yield was 73.78 ml/g on volatile solids (VS) basis. For watermelon rind (WR), the I:S:W ratio equalled 3:1:5.8 and the corresponding biogas yield was 100.45 ml/g VS. Finally, for banana peelings (BP), the I:S:W ratio equalled 3:1:5.3 and the corresponding biogas yield was 98.75 ml/g VS. The digestion in mixtures of substrates produced good but lesser biogas yield than with co-digestion with cow dung; PP – BP (25.5 ml/g VS), PP – WR (11.3 ml/g VS), WR - BP (5.1 ml/g VS) and WR – BP – PP (18.7 ml/g VS).

It is therefore very clear that using inoculum like cow dung in an anaerobic process enhances biogas yield and is a very important factor to consider in biogas production from waste.

In addition to these results, the kinetic study of the co-digestion processes enabled the elaboration of a biogas yield guide destined at guiding the users of this research work on the possibility of selecting yields different from the optimal yield obtained on a long run basis.

Limitations

- The reliability of the corresponding values of C/N and TS needed depends on the accuracy of the ultimate analysis done (Walkley and black method and Kjeldahl method).

- The reliability of the biogas yield produced also depends on how good the BMP setup was air-tight.
- Lab-scale reactors can't simulate at 100 % the situation of a large scale biodigester or a digester facility. The impact is more felt in our situation as operational parameters like the quantity of volatile acids produced, pH change, volatile solids removal and temperature wasn't monitored.
- Temperature, pH control and buffering were not made. So, it may be possible to increase further the yield if the pH was regulated to the neutral zone.
- The possible interactions between factors other than C/N and TS were not investigated. So, there exist a possibility of maintaining the parameters of C/N and TS recommended by this work, then decide to change conditions like pH or stirring rhythm and obtain either more than expected or undesirable results.
- The required amount of cow dung (inoculum) required depends on the state of the inoculum before inoculation. When the inoculum is well preserved, the biogas yield may increase significantly.

The way forward

In order to complete the present work and improve the quality of the results obtained, the following should be done:

- Provide a cost-benefit analysis using the parameters of co-digestion obtained through this work. Design a biogas plant that suits the operational parameters of this work.
- Perform co-digestion experiments with the mixture of food waste to verify if it enhances the biogas yield as well.
- Further studies on the influence of temperature maintained at 35 °C on biogas yield can be done. These studies can be carried out on large scale biodigesters.
- Research can be done on both lower and higher C/N values than the ones chosen in this works to explore possibilities of other favorable C/N conditions.
- Co-digestion candidates can be varied with for example pig manure, human feces or others to see whether they perform better than cow dung.

REFERENCES

3SMedia. (2020, October 19). Food waste initiative aims to achieve more sustainable planet. Infrastructure News. Retrieved September 12, 2022, from https://infrastructurenews.co.za/2020/10/19/food-waste-initiative-aims-to-achieve-more-sustainable-planet/

Abbasi, T., Tauseef, S. M., & Abbasi, S. A. (2012). Anaerobic digestion for global warming control and energy generation - An overview. In *Renewable and Sustainable Energy Reviews* (Vol. 16, Issue 5, pp. 3228–3242). https://doi.org/10.1016/j.rser.2012.02.046

Achinas, S., & Euverink, G. J. W. (2016). Theoretical analysis of biogas potential prediction from agricultural waste. *Resource-Efficient Technologies*, *2*(3), 143–147. https://doi.org/10.1016/j.reffit.2016.08.001

Achinas, S., Krooneman, J., & Euverink, G. J. W. (2019). Enhanced Biogas Production from the Anaerobic Batch Treatment of Banana Peels. *Engineering*, *5*(5), 970–978. https://doi.org/10.1016/j.eng.2018.11.036

Aili Hamzah, A. F., Hamzah, M. H., Ahmad Mazlan, F. N., Che Man, H., Jamali, N. S., & Siajam, S. I. (2020). Anaerobic Co-digestion of Pineapple Wastes with Cow Dung: Effect of Different Total Solid Content on Bio-methane Yield. *Advances in Agricultural and Food Research Journal*, *1*(1). https://doi.org/10.36877/aafrj.a0000109

Akunna, J. C. (2018). *Anaerobic Waste-Wastewater Treatment and Biogas Plants*.

APHA. (2015). *Standard Methods for the Examination of Water and Wastewater* (23rd ed.). https://doi.org/10.2105/SMWW.2882.216

Aragaw, T., Andargie, M., & Gessesse, A. (2013). Co-digestion of cattle manure with organic kitchen waste to increase biogas production using rumen fluid as inoculums. *International Journal of Physical Sciences Full Length Research Paper*, *8*(11), 443–450. https://doi.org/10.5897/IJPS2013.3863

Arnell, M., & et al. (2007). Operational experience of cost-effective production of biogas in Linköping, Sweden. *Integrated Porject N° 019795, Biogasmax*.

Aydar, A. Y. (2018). Utilization of Response Surface Methodology in Optimization of Extraction of Plant Materials. In *Statistical Approaches With Emphasis on Design of Experiments Applied to Chemical Processes*. InTech. https://doi.org/10.5772/intechopen.73690

Bischofsberger, W., Rosenwinkel, K.-H., Dichtl, N., Seyfried, C. F., Bohnke, B., Bsdok, J., & Schroter, T. (2005). *Anaerobtechnik* (W. Bischofsberger, K.-H. Rosenwinkel, N. Dichtl, C. F. Seyfried, B. Böhnke †, J. Bsdok, & T. Schröter, Eds.). Springer-Verlag. https://doi.org/10.1007/b137857

Bhada-Tata, P., & Hoornweg, D. (2012). What a Waste : A Global Review of Solid Waste Management. Urban Development & Local Government Unit, World Bank, 1–116.

Crtv. (2018, July 4). *Agriculture: One billion CFA F to boost Palm oil, banana and pineapple production*. https://www.crtv.cm/2018/07/agriculture-one-billion-cfa-f-to-boost-palm-oil-banana-and-pineapple-production/

Denis Achiri, T., Nsuh Konje, C., Assan Nkuh, A., Nsobinenyui, D., & Author, C. (2019). Comparative Studies on Watermelon Production in the North West and South West Regions of Cameroon: A Rural and a Peri-Urban Experience. *Issue 4 Ser. I*, *12*, 55–68. https://doi.org/10.9790/2380-1204015568

Deublein, D., & Steinhauser, A. (2011). Biogas from waste and renewable resources: an introduction. *Wiley -VCH Verlag GmbH & Co. KGaA*.

ECN, & TNO. (1998). *Phyllis 2*. https://phyllis.nl/Browse/Standard/ECN-Phyllis#dung

EPA. (2012). *Increasing Anaerobic Digester Performance with Codigestion*. www.epa.gov/agstar.

EPA. (2021, September 17). *Food Recovery Hierarchy*. https://www.epa.gov/sustainable-management-food/food-recovery-hierarchy

Fajobi, M. O., Lasode, O. A., Adeleke, A. A., Ikubanni, P. P., & Balogun, A. O. (2022). Investigation of physicochemical characteristics of selected lignocellulose biomass. *Scientific Reports*, *12*(1). https://doi.org/10.1038/s41598-022-07061-2

FAO. (1981). *Food loss prevention in perishable crops*. https://www.fao.org/3/s8620e/S8620E06.htm

Feukam Nzudie, H. L., Zhao, X., Liu, G., Tillotson, M. R., Hou, S., & Li, Y. (2021). Driving force analysis for food loss changes in Cameroon. *Journal of Cleaner Production*, *278*. https://doi.org/10.1016/j.jclepro.2020.123892

Filer, J., Ding, H. H., & Chang, S. (2019). Biochemical methane potential (BMP) assay method for anaerobic digestion research. In *Water (Switzerland)* (Vol. 11, Issue 5). MDPI AG. https://doi.org/10.3390/w11050921

Girotto, F., Alibardi, L., & Cossu, R. (2015). Food waste generation and industrial uses: A review. *Waste Management*, *45*, 32–41. https://doi.org/10.1016/j.wasman.2015.06.008

Girotto, F., Lavagnolo, M. C., Acar, G., & Piazza, L. (2021). Bio-methane production from tomato pomace: preliminary evaluation of process intensification through ultrasound pre-treatment. *Journal of Material Cycles and Waste Management*, *23*(1), 416–422. https://doi.org/10.1007/s10163-020-01122-2

Gustavsson, Jenny., Food and Agriculture Organization of the United Nations., & ASME/Pacific Rim Technical Conference and Exhibition on Integration and Packaging of MEMS, N. (2011). *Global food losses and food waste : extent, causes and prevention : study conducted for the International Congress "Save Food!" at Interpack 2011 Düsseldorf, Germany*.

Hartmann, H., & Ahring, B. K. (2006). Strategies for the anaerobic digestion of the organic fraction of municipal solid waste: an overview. *Water Science and Technology*, *53*(8), 7–22. https://doi.org/10.2166/wst.2006.231

IB Chem. (2021). *The rate constant, k*. Retrieved September 27, 2022, from https://www.ibchem.com/IB16/06.32.htm#:~:text=Significance%20of%20the%20rate%20constant%20The%20rate%20constant%2C,the%20rate%20and%20that%20the%20reaction%20is%20rapid.

IndiaMART InterMESH. (n.d.). Vermi Bed With Shade - Dual Vermibed With Shade Manufacturer from Jaipur. Disha Organic Science Tech Industries. Retrieved August 20, 2022, from https://www.dishaorganicindia.co.in/vermi-bed-with-shade.html

Invest Cameroon. (2013, October 15). Business in Cameroon. Retrieved July 16, 2022, from https://www.businessincameroon.com/?option=com_k2&view=item&id=4363:15-billion-to-produce-26000-tons-of-pineapple-in-awae&Itemid=96&tmpl=component&print=1

Kabenge, I., Omulo, G., Banadda, N., Seay, J., Zziwa, A., & Kiggundu, N. (2018). Characterization of Banana Peels Wastes as Potential Slow Pyrolysis Feedstock. *Journal of Sustainable Development*, *11*(2), 14. https://doi.org/10.5539/jsd.v11n2p14

Kojima, R., & Ishikawa, M. (2013). *Prevention and Recycling of Food Wastes in Japan: Policies and Achievements Objectives Food Waste Flows in Japan*.

K., J. (2020, April 11). Cameroun-agriculture : la production de la php (plantations du haut penja) en net recul. 237 Actu. Retrieved September 10, 2022, from https://237actu.com/cameroun-agriculture-la-production-de-la-php-palmeraies-du-haut-penja-en-net-recul

Lavagnolo, M. C. (2020). *Module12 SW Anaerobic digestion Process*.

Mahmoud, M., & El-Halwagi. (2006). Overview of optimization. In *Process Systems Engineering* (Vol. 7, pp. 285–314). https://doi.org/10.1016/S1874-5970(06)80012-3

Mata-Alvarez, J. (2003). Fundamentals of the Anaerobic Digestion Process. *Biomethanization of the Organic Fraction of Municipal Solid Wastes*, 202–209.

Mboumboue, E., & Njomo, D. (2018). Biomass resources assessment and bioenergy generation for a clean and sustainable development in Cameroon. *Biomass and Bioenergy*, *118*, 16–23. https://doi.org/10.1016/j.biombioe.2018.08.002

Municipal Solid Waste Management. (2018, October 15). *3.15 Determining C:N ratio of biowaste mixtures*. Youtube. https://www.youtube.com/watch?v=YuS_qpt935M

Nes, Wim, J., Nhete, & Tinasche, D. (2007). Biogas for a better life: an african initative. *Appropriate Technology*.

Neshat, S. A., Mohammadi, M., Najafpour, G. D., & Lahijani, P. (2017). Anaerobic co-digestion of animal manures and lignocellulosic residues as a potent approach for sustainable biogas production. In *Renewable and Sustainable Energy Reviews* (Vol. 79, pp. 308–322). Elsevier Ltd. https://doi.org/10.1016/j.rser.2017.05.137

Parawira, W. (2004). *Anaerobic Treatment of Agricultural Residues and Wastewater - Application of High-Rate Reactors, Lund, Sweden.*

Parfitt, J., Barthel, M., & MacNaughton, S. (2010). Food waste within food supply chains: Quantification and potential for change to 2050. In *Philosophical Transactions of the Royal Society B: Biological Sciences* (Vol. 365, Issue 1554, pp. 3065–3081). Royal Society. https://doi.org/10.1098/rstb.2010.0126

Renewable Energy Agency, I., Development Bank, K., & Gesellschaft für Internationale Zusammenarbeit, D. (2021). *The Renewable Energy Transition in Africa Powering Access, Resilience and Prosperity On behalf of the*.

Repak. (2019, March 13). The Circular Economy and EU Legislation | Repak. Repak. Retrieved July 16, 2022, from https://repak.ie/driving-change/circular-economy-eu-legislation/

Roha, S. (2013). Physico-chemical properties of pineapple variety N36 harvested and stored at different maturity stages. In *International Food Research Journal* (Vol. 20, Issue 1).

SIE-Cameroun. (2011). Système d'Information Energétique du Cameroun. *Ministry of Water and Energy, Yaounde*.

Singh, L., Yousuf, A., & Madhab Mahapatra. Durga. (2020). *Bioreactors: Sustainable Design and Industrial Applications in Mitigation of GHG Emissions*.

Stephen. (2016, February 5). *Alberta urban garden*. https://www.albertaurbangarden.ca/2016/02/05/fertilize-your-organic-garden-for-free-with-banana peels/#:~:text=Banana%20peels%20have%20quite%20a,can%20change%20the%20soils%20pH.

The World Bank. (2020). Access to electricity (% of population) - Cameroon | Data. Retrieved April 13, 2022, from https://data.worldbank.org/indicator/EG.ELC.ACCS.ZS?locations=CM

UCMP. (2009). *UCMP Gloassary: Ecology*. https://ucmp.berkeley.edu/glossary/gloss5ecol.html

Vergara, V., & Jammi, R. (2022, April 7). *Towards a circular economy: Addressing the waste management threat*. World Bank Group. https://ieg.worldbankgroup.org/blog/towards-circular-economy-addressing-waste-management-threat

Voegeli, Yvonne. (2014). *Anaerobic digestion of biowaste in developing countries : practical information and case studies*. Eawag-Sandec.

Voice of America. (2017). *East Africa's Largest Biogas Energy Plant Supplies Kenya's National Grid*. https://youtu.be/ff7wdwNX9sY

Ward, A. J., Hobbs, P. J., Holliman, P. J., & Jones, D. L. (2008). Optimisation of the anaerobic digestion of agricultural resources. In *Bioresource Technology* (Vol. 99, Issue 17, pp. 7928–7940). https://doi.org/10.1016/j.biortech.2008.02.044

Weiland, P. (2001). Grundlagen der Methangärung—Biologie und Substrate (Fundamentals of methane fermentation—biology and substrates). *VDI-Berichte 1620*.

Weinrich, S. 1985-, Schäfer, F., Liebetrau, J., Bochmann, G., Baier, U. 1957-, Murphy, J. D., & International Energy Agency Task Energy from Biogas. (2018). *Value of batch tests for biogas potential analysis method comparison and challenges of substrate and efficiency evaluation of biogas plants*.

Wellinger Arthur, Murphy Jerry, & Baxter David. (2013). *The Biogas Handbook Science, Production and Application*. Woodhead Publishing.

Zabala, V. B., & Goles, C. E. (2021). Watermelon Rind-Ponkan Marmalade: A Physico-chemical Analysis. *Journal of Physics: Conference Series*, *1835*(1). https://doi.org/10.1088/1742-6596/1835/1/012114

Zaman, A., & Reynolds, C. (2015). *The economic and bio-energy production potential of South Australian food waste using Anaerobic digestion*.

Zareei, S., & Khodaei, J. (2017). Modeling and optimization of biogas production from cow manure and maize straw using an adaptive neuro-fuzzy inference system. *Renewable Energy*, *114*(PB), 423–427. https://doi.org/10.1016/j.renene.2017.07.050

APPENDIX

Appendix 1: Updated IPCC classification of MSW, 2019

TABLE 2.3 (UPDATED)
MSW COMPOSITION DATA BY PERCENT – REGIONAL DEFAULTS

Region	Food waste	Garden waste	Paper /cardboard	Wood	Textiles	Nappies	Rubber /Leather	Plastic	Metal	Glass	Other
Asia											
Central Asia	30.0	1.4	24.7	2.5	3.5	0	0	8.4	0.8	5.9	23.0
Eastern Asia	40.3	0.0	20.4	2.1	1.0	0.0	0.0	6.5	2.7	4.3	22.9
South-Eastern Asia	49.9	1.0	11.2	0.8	0.4	0.0	0.0	10.2	4.2	3.7	18.6
Southern Asia	66.1	0.0	9.2	0.0	1.2	0.0	0.4	7.0	0.9	1.5	13.9
Western Asia	42.2	3.2	15.3	0.8	3.0	0.4	0.3	17.2	2.5	3.4	11.8
Africa											
Northern Africa	50.4	0.0	12.1	0.0	5.8	0.0	0.0	13.8	4.4	3.3	10.5
Eastern Africa	44.4	6.9	10.4	0.5	3.0	0.0	0.4	8.0	2.6	2.1	21.7
Middle Africa	28.4	0	8	0	1.3	0	0	7.1	1.4	1.1	52.7
Southern Africa	24.0	0.0	14.5	0.0	5.5	0.0	0.0	26.5	6.5	9.0	14.0
Western Africa	53.9	0.0	7.5	0.0	1.9	0.0	0.0	6.4	2.7	1.3	26.5

Appendix 2: Continuation of the updated IPCC classification of MSW, 2019

TABLE 2.3 (UPDATED) (CONTINUED)
MSW COMPOSITION DATA BY PERCENT – REGIONAL DEFAULTS

Region	Food waste	Garden waste	Paper/ cardboard	Wood	Textiles	Nappies	Rubber/ Leather	Plastic	Metal	Glass	Other
Europe											
Eastern Europe	31.8	2.4	17.1	2.5	3.1	0.1	0.5	4.6	0.7	1.8	35.3
Northern Europe	30.3	5.2	13.8	1.8	3.2	1.2	0.0	4.9	1.4	4.3	34.0
Southern Europe	35.8	1.4	21.4	1.2	2.8	1.1	0.2	14.1	2.0	3.5	16.7
Western Europe	33.2	2.7	17.2	2.3	5.9	3.0	0.0	20.5	1.5	1.4	12.3
America											
Central America	62.7	0.0	12.6	0.3	2.2	0.0	0.0	10.3	2.7	3.3	6.0
South America	54.1	3.3	12.4	0.0	1.7	1.9	0.6	13.7	2.0	3.0	7.2
Northern America	20.2	6.8	23.3	4.1	3.9	0	1.6	15.8	6.4	4.2	14.0
Oceania											
Australia and New Zealand	25.9	12.2	12.0	6.5	2.9	3.5	0.0	8.3	1.8	2.8	24.1

Note 1: Data are based on weight of wet waste of MSW without industrial waste at generation around year 2010.

Note 2: The region-specific values are calculated from national, partly incomplete composition data. The percentages given may therefore not add up to 100percent. Some regions may not have data for some waste types - blanks in the table represent missing data.

Note 3: Data of rest of Oceania and Caribbean are not refined

Appendix 3: Dumping site for pineapple waste at one of the processing facilities in Kangulmumira, Uganda.

Appendix 4: Automatic Methane Potential Test System (AMPTS) II. Source: https://bpcinstruments.com/vdi-4630-test-standard/

Appendix 5: Anaerobic digestion plant in Kenya, transformer site. Source: https://youtu.be/ff7wdwNX9sY

Appendix 6: Central composite design 2D diagram for the anaerobic digestion of pineapple peelings, watermelon rind and banana peelings

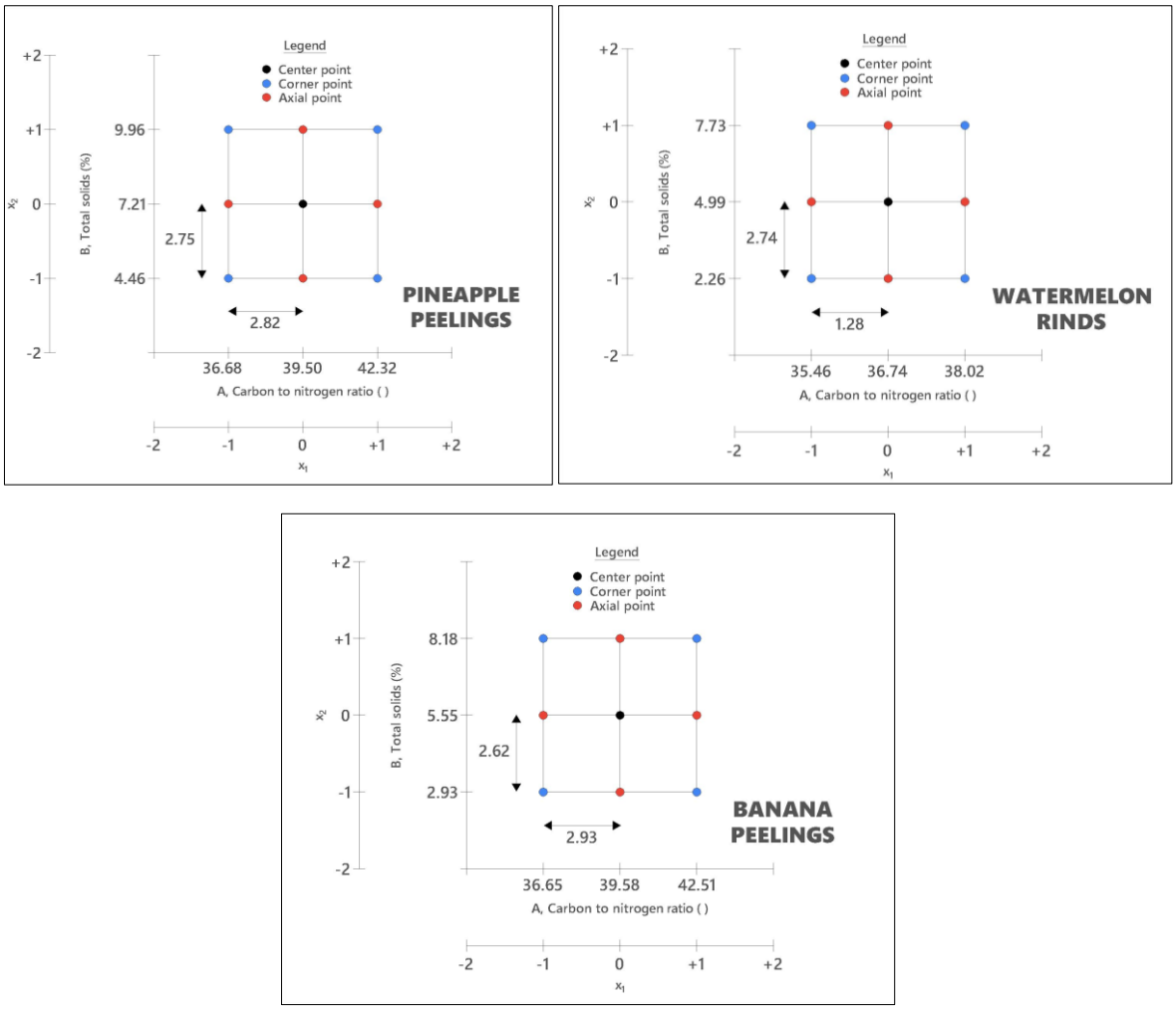

Appendix 7: Results of the analysis of the density of substrates

Trial No	Mass (g)	Volume after (mL)	Volume before (mL)	Density (g/mL)
		Pineapple peelings (PP)		
1	10.937	360	350	1.094
2	36.600	395	360	1.046
3	17.996	320	300	0.900
Average				**1.013 ± 0.102**
		Watermelon rind (WR)		
1	21.395	371	350	1.019
2	34.175	318	270	0.712
3	8.185	310	300	0.819
Average				**0.850 ± 0.156**

Banana peelings (BP)					
	1	3.859	255	250	0.772
	2	11.290	314	300	0.806
	3	5.237	306	300	0.873
Average					**0.817 ± 0.052**
Cow dung (CD)					
	1	16.574	318	300	0.921
	2	10.016	264	250	0.715
	3	15.620	288	270	0.868
Average					**0.835 ± 0.107**

Appendix 8: FCCD table of pineapple peelings

Face-centered Central Composite Design (FCCD) table of pineapple peelings								
Substrate ID	Volume of water (mL)	Mass of cow dung (g)	Mass of watermelon rind (g)	Cumulative biogas produced (mL)	Total VS content (g)	A C/N ratio	B TS (%)	Response/ Biogas yield (mL/g VS)
PP-LL	178	41.0	13.7	324	7.05	38.81	3.98	46.0
PP-CL	166	34.3	34.3	406	8.77	42.94	3.98	46.3
PP-HL	180	14.5	43.6	438	7.35	47.07	3.98	59.6
PP-LC	141	65.0	21.7	792	11.17	38.81	6.42	70.9
PP-CC1	122	54.5	54.5	910	13.91	42.94	6.42	65.4
PP-CC2	122	54.5	54.5	910	13.91	42.94	6.42	65.4
PP-CC3	122	54.5	54.5	910	13.91	42.94	6.42	65.4
PP-CH	79	74.2	74.2	860	18.94	42.94	8.85	45.4
PP-HC	88	36.7	110.2	1390	18.58	47.07	6.42	74.8
PP-LH	120	79.1	26.4	802	13.61	38.81	8.85	58.9
PP-HH	32	50.3	150.8	1140	25.42	47.07	8.85	44.8

Appendix 9: FCCD table of watermelon rind

Face-centered Central Composite Design (FCCD) table of watermelon rind								
Substrate ID	Volume of water (mL)	Mass of cow dung (g)	Mass of watermelon rind (g)	Cumulative biogas produced (mL)	Total VS content (g)	A C/N ratio	B TS (%)	Response/ Biogas yield (mL/g VS)
WR-LL	203	23.4	7.8	246	3.47	38.75	2.26	70.9
WR-CL	194	19.3	19.3	212	3.56	42.81	2.26	59.6
WR-HL	180	12.7	38.1	256	3.70	46.87	2.26	69.2
WR-LC	160	50.3	16.8	516	7.45	38.75	4.99	69.2
WR-CC1	142	41.3	41.3	590	7.59	42.81	4.99	77.7
WR-CC2	142	41.3	41.3	590	7.59	42.81	4.99	77.7
WR-CC3	142	41.3	41.3	590	7.59	42.81	4.99	77.7
WR-CH	94	61.5	61.5	745	11.32	42.81	7.71	65.8
WR-HC	114	26.7	80.1	522	7.79	46.87	4.99	67.0
WR-LH	120	75.5	25.2	1124	11.17	38.75	7.71	100.6
WR-HH	53	39.6	118.9	796	11.55	46.87	7.71	68.9

Appendix 10: FCCD table of banana peelings

Face-centered Central Composite Design (FCCD) table of banana peeling								
Substrate ID	Volume of water (mL)	Mass of cow dung (g)	Mass of banana peelings (g)	Cumulative biogas produced (mL)	Total VS content (g)	A C/N ratio	B TS (%)	Response/ Biogas yield (mL/g VS)
BP-LL	195	28.3	9.4	304	4.67	39.45	2.93	65.1
BP-CL	188	21.4	21.4	402	5.01	44.21	2.93	80.4
BP-HL	180	12.3	37.0	390	5.47	48.97	2.93	71.4
BP-LC	156	52.2	17.4	828	8.61	39.45	5.55	96.2
BP-CC1	145	39.2	39.2	828	9.19	44.21	5.55	90.1
BP-CC2	145	39.2	39.2	828	9.19	44.21	5.55	90.1
BP-CC3	145	39.2	39.2	828	9.19	44.21	5.55	90.1
BP-HC	131	22.5	67.4	688	9.96	48.97	5.55	69.1
BP-LH	120	74.7	24.9	1222	12.33	39.45	8.18	99.1
BP-CH	105	55.9	55.9	1052	13.12	44.21	8.18	80.2
BP-HH	85	31.8	95.5	920	14.12	48.97	8.18	65.1

Appendix 11: Proximate analysis of the substrates

Crucible ID	Crucible (g) (P)	C + S (wet) (g) (Q)	C + S (dried) (g) (R)	C + Ash (g) (550 °C) (S)	TS g/kg wet (T)	Ash g/kg wet (U)	VS g/kg (T – U)
Pineapple Peelings (PP)							
PP 1	22.698	47.283	26.343	23.305	148.261	24.690	123.571
PP 2	22.521	30.491	23.727	22.716	151.285	24.430	126.855
Watermelon Rind (WR)							
WR 1	12.352	20.717	12.936	12.484	69.815	15.780	54.035
WR 2	12.315	23.513	13.091	12.491	69.298	15.717	53.581
Banana Peelings (BP)							
BP 1	12.380	18.631	13.092	12.442	113.902	9.918	103.983
BP 2	12.379	20.124	13.268	12.455	114.784	9.813	104.971
Cow Dung (CD)							
CD 1	16.011	24.045	17.635	16.590	202.141	72.069	130.072
CD 2	16.015	25.053	17.844	16.667	202.368	72.140	130.228

Appendix 12: Laboratory substrate analyses' estimates

REPUBLIQUE DU CAMEROUN
Paix – Travail – Patrie
.....
MINISTERE DE L'AGRICULTURE
ET DU DEVELOPPEMENT RURAL
.....
SECRETARIAT GENERAL
.....
DIRECTION DE LA REGLEMENTATION
ET DU CONTROLE DE QUALITE DES INTRANTS ET
DES PRODUITS AGRICOLES
.....
LABORATOIRE NATIONAL D'ANALYSE
DIAGNOSTIQUE DES PRODUITS ET INTRANTS
AGRICOLES

REPUBLIC OF CAMEROON
Peace – Work – Fatherland
.....
MINISTRY OF AGRICULTURE
AND RURAL DEVELOPMENT
.....
GENERAL SECRETARIAT
.....
DEPARTMENT OF REGULATION AND
QUALITY CONTROL OF AGRICULTURAL
PRODUCTS AND INPUTS
.....
NATIONAL LABORATORY FOR
DIAGNOSISAND ANALYSIS OF
AGRICULTURALPRODUCTS AND INPUTS

N° 030 /22/D/MINADER/SG/DRCQ/LNAD/SEF Yaoundé, le 25 JUL 2022

DEVIS

DROIT : Stephane

TELEPHONE : 680 08 57 25

OBJET : Analyse de 04 échantillons de composts.

DENOMINATION(S)	ELEMENTS A ANALYSER	Qté	PRIX UNITAIRE FCFA	PRIX TOTAL FCFA
Compost	Matière organique	4	5 000	20 000
	Azote total	4	5 000	20 000
	pH	4	1 500	6 000
	Total solid	4	2 000	8 000
	Volatile solid	4	2 000	8 000
	NET A PAYER			64 000

Soit en lettres la somme de soixante quatre mille. /-

CHEF DE LABORATOIRE

Le Chef du Laboratoire
Mbom Ngala
Administration

Appendix 13: Laboratory analyses of substrates' results

REPUBLIQUE DU CAMEROUN
Paix – Travail - Patrie

MINISTERE DE L'AGRICULTURE ET DU DEVELOPPEMENT RURAL

SECRETARIAT GENERAL

DIRECTION DE LA REGLEMENTATION ET DU CONTROLE DE QUALITE DES INTRANTS ET DES PRODUITS AGRICOLES

LABORATOIRE NATIONAL D'ANALYSE DIAGNOSTIQUE DES PRODUITS ET INTRANTS AGRICOLES

SERVICE DES ENGRAIS ET FERTILISANTS

BP : 2082 messa-yaoundé/ Tél :

Minader

REPUBLIC OF CAMEROON
Peace – Work – Fatherland

MINISTRY OF AGRICULTURE AND RURAL DEVELOPMENT

GENERAL SECRETARIAT

DEPARTMENT OF REGULATION AND QUALITY CONTROL OF AGRICULTURAL PRODUCTS AND INPUTS

NATIONAL LABORATRY FOR DIAGNOSTIS AND ANALYSIS OF AGRICULTURAL PRODUCTS AND INPUTS

SERVICE OF FERTILIZERS

PO BOX : 2082 messa-yaounde/ Phone :

Yaoundé, 04 OCT 2022

RAPPORT D'ESSAI

1- IDENTITE DU CLIENT

- Client : **M. DJOUFACK LEKE Stéphane** Adresse: ND Téléphone : 680 08 57 25

2-DESCRIPTION DE L'OBJET DE L'ESSAI

- Objet de l'essai : Diagnostic de la formulation des composts
- Préleveur de(s) l'échantillon(s) : **M. DJOUFACK LEKE Stéphane**
- Nombre d'échantillons soumis: 04 (Quatre)

3-RECEPTION DES ECHANTILLONS AU LABORATOIRE ET ESSAIS

- Date de réception des échantillons :-
- Conditionnement des échantillons : -
- Prétraitement des échantillons : séchage à l'air libre

4-METHODES UTILISEES POUR LES ESSAIS SUR LES ECHANTILLONS SOUMIS

N°	Paramètres	Principe de la méthode	Référence
01	Azote total	Kjeldahl modifié	Pauwels et al (1992) : *manuel de laboratoire de pédologie.* p.19-23
02	Matière organique	Walkley et Black	Pauwels et al (1992) : *manuel de laboratoire de pédologie*
03	Matière sèche totale	Etuvage	Protocole interne
04	Matière volatile	Four	Protocole interne

5- TABLEAU RECAPITULATIF DES RESULTATS

			Code échantillon			
N°	Paramètres	Unité	Bourse de vache	D.Ananas	D. pastèque	D. banane
01	Azote total	% ou g/100 g de matière sèche	1.83	1.03	0.13	1.13
02	Carbone organique	%	63.47	52.21	52.46	60.18
03	Matière sèche totale	g/kg de matière fraiche	202.25	149.77	69.56	114.34
04	Matière volatile	g/kg de matière fraiche	130.15	125.21	53.81	104.48

UM DJON HENOCK CHARLES
CADRE CONTRACTUEL D'ADMINISTRATION

TABLE OF CONTENT

Dedication ii
Acknowledgements iii
Abstract iv
Résumé v
Summary 115
List of abbreviations and symbols vii
List of Figures ix
List of Tables xii
List of Appendixes xiii
General Introduction 1
CHAPTER 1 . LITERATURE REVIEW 3
1.1. Concepts and definitions 3
1.1.1. Anaerobic digestion 3
1.1.2. Biogas potential and biogas yield 3
1.1.3. Substrate 3
1.1.4. Co-digestion 3
1.1.5. Optimization 4
1.1.6. Food loss, food waste and the food supply chain 4
1.1.7. Renewable energy 5
1.2. Food waste generation 5
1.2.1. Sources of food loss (FL) and food waste (FW) 5
1.2.2. Food waste statistics 6
1.2.3. Environmental and social impacts of mismanaged food waste 12
1.3. Food waste recovery technologies and circular economy 14
1.3.1. Composting and vermicomposting 14
1.3.2. Incineration 15
1.3.3. Landfill treatment 16
1.3.4. Anaerobic digestion 16
1.3.5. Food recovery hierarchy and circular economy 17
1.4. Anaerobic digestion technology 19
1.4.1. Biodegradability parameters 19
1.4.2. Biochemical reactions in anaerobic digestion 20
1.4.3. Factors affecting anaerobic process efficiency 24
1.4.4. Biochemical methane potential 32
1.4.5. Biogas production systems in developing countries 33
1.5. Response surface methodology 36
CHAPTER 2 . MATERIAL AND METHODS 39
2.1. Software used 39
2.1.1. Microsoft Word (MS Word) 39
2.1.2. Microsoft Excel (MS Excel) 39

2.1.3. Microsoft Visio 39
2.1.4. Autodesk AutoCAD 39
2.1.5. Google Sketchup Pro 39
2.1.6. MATLAB 40
2.1.7. Minitab statistical software 40
2.1.8. QGIS 40
2.2. Materials 40
2.2.1. Global Positioning System (GPS) 40
2.2.2. Physical and chemical analysis (materials and reagents) 40
2.2.3. Biochemical methane potential test 42
2.3. Design of experiment (DOE) 43
2.3.1. Objective 43
2.3.2. Definition of variables 45
2.3.3. Batch experiment operating conditions 45
2.3.4. Parameters under investigation 46
2.3.5. Blank batch assays 47
2.3.6. Response Surface Methodology - Central Composite Design (CCD) 48
2.4. Sample collection 51
2.5. Preparation of samples and pretreatment 54
2.5.1. Proximate analysis and ultimate analysis 54
2.5.2. Biochemical methane potential 56
2.6. Experimental setup 57
2.6.1. Biochemical methane potential test 57
2.6.2. Biogas measurement and yield estimation 62
2.6.3. Methane production estimation 63
2.7. Analytical methods 64
2.7.1. Proximate Analysis 64
2.7.2. Ultimate Analysis – determination of Carbon content 65
2.7.3. Ultimate analysis – determination of nitrogen content 67
2.7.4. Estimation of the density of substrate 69
2.8. Theoretical biochemical methane potential 69
2.8.1. Method 69
2.8.2. Collection of secondary data 70
2.9. Kinetic modelling 70
2.9.1. Concept 70
2.9.2. Procedure 71
CHAPTER 3 . RESULTS AND DISCUSSION 73
3.1. Physical and chemical characteristics of the substrates and inoculum 73
3.2. Theoretical biogas potential estimation 75
3.3. Anaerobic digestion - blank assays 75
3.3.1. BMP experiments 76
3.3.2. Kinetic modelling results 77

3.4. Anaerobic co-digestion with cow dung 79
3.4.1. BMP batch experiments' results 79
3.4.2. Kinetic modelling 82
3.4.3. RSM – Face-centered Central Composite Design (FCCD) 87
3.5. Anaerobic digestion of mixtures of substrates 96
3.5.1. Introduction 96
3.5.2. BMP batch experiments' results 96
3.5.3. Kinetic modelling results 97
3.6. Biogas yield to energy classification 99
General conclusion and perspectives 101
References 103
Appendix 108
Table of content vi